ABSTRACT

Title of Document: **INVESTIGATION OF CHICKEN EMBYO METABOLISM AND SUBSTRATE UTILIZATION DURING LATER DEVELOPMENT**

Qiong Hu, Doctor of Philosophy, 2013

Directed By: Associate Professor, Brian J. Bequette, Department of Animal and Avian Sciences

The objective of this research was to determine metabolic adaptations and substrate utilization during chicken embryo development and to determine the influence of breeder age and egg size on embryonic growth and metabolism during development (embryonic day 11 to posthatch day 1). In Study One, for both small (n = 60, 53.2 ± 1.04 g) and large (n = 60, 69.0 ± 1.86 g) eggs from 26 versus 42 wk-old broiler breeders, glucose content in albumen decreased to negligible levels by embryonic day (e) 11 whereas mannose and fucose remained constant. Higher yolk glucose content was observed in small eggs from e17 onwards whereas proportions of yolk linoleic and linolenic acids were greater in larger eggs. Liver adenosine monophosphate protein kinase (AMPK), the central cellular energy-sensor, was higher in activity in embryos from large eggs, and AMPK activity was at its highest for both sizes of eggs on e14. These observations suggest that glucose was consumed in early development (before e11). Lower liver AMPK activity and higher yolk glucose at later stages in small eggs from young hens suggests that anaplerotic metabolism is enhanced to alleviate the relative nutrient deficiency.

In Study Two, a gas chromatography-mass spectrometry-based metabolomic profiling approach was employed to investigate effects of hen age and egg size on embryo metabolism. Principal component analysis of liver and blood metabolites showed separate clusters on both e14 and e20 from 32 and 51 wk-old hens. The separate clusters featured branched-chain amino

acid, glycine, serine and threonine metabolism. Clear separation of metabolites was not observed for embryos from small versus large eggs at any developmental age. Breeder age had a larger influence on embryo metabolism and growth. Three clusters corresponding to liver metabolites from e14, e17 and e20 embryos formed a sub-tree that merged with the cluster from posthatch day 1 chicks in the Hierarchical clustering analysis. This result confirmed that embryo metabolism adapted during later development. Embryos from 51 wk-old hens displayed predominant developmental changes in ketone, glycerolipid and glutathione metabolic pathways in the liver compared to 32 wk-old hens.

Study Three aimed to quantify gluconeogenesis, and substrate utilization and partition in e14 and e19 embryos. A constant infusion protocol (8 h) was developed for delivery of [U-^{13}C] glucose and [U-^{13}C] glycerol into the chorio-allantoic fluid. Gluconeogenesis was higher in e19 compared to e14 embryos, consistent with the need for increased liver and muscle glycogen by e19 embryos in preparation for emergence. The contribution of glucose to non-essential amino acid (NEAA) synthesis was greater in e14 *vs* e19 embryos, indicating a higher demand for amino acids for tissue growth. Glycerol contributed very little (< 5%) to gluconeogenesis; thus the remainder must be ascribed to amino acids. Relatively more of acetyl-CoA flux was derived from fatty acid metabolism in e14 embryos compared to 3-carbon pool substrates.

In summary, this thesis research established aspects of embryo metabolism and nutrient partition in developing embryos that previously were unknown. This included demonstration of a role of AMPK in development, the influence of breeder age on global embryo metabolism, and metabolic adaptations in gluconeogenesis, Krebs cycle activity and glycerol metabolism during the latter half of chicken embryo development.

INVESTIGATION OF CHICKEN EMBRYO METABOLISM AND SUBSTRATE UTILIZATION DURING LATER DEVELOPMENT

By

Qiong Hu

Dissertation submitted to the Faculty of the Graduate School of the
University of Maryland, College Park, in partial fulfillment
of the requirements for the degree of
Doctor of Philosophy
2013

Advisory Committee:
Associate Professor Brian J. Bequette, Chair
Dr. Ransom L. Baldwin
Dr. Erin E. Connor
Associate Professor Douglas A. Julin, Dean's representative
Associate Professor Jiuzhou Song
Assistant Professor Lisa A. Taneyhill

ACKNOWLEDGEMENTS

My sincere thanks to my Advisor, **Dr. Brian J. Bequette**, for your relentless encouragement, support and guidance during the last five years. Thanks for all the constant help and valuable suggestions for my career development.

Thanks to my committee members, **Drs. Ransom Baldwin, Erin Connor, Douglas Julin, Jiuzhou Song, and Lisa Taneyhill** for their valuable inputs to my work.

Special thanks to:

Dr. Lisa Taneyhill: for teaching me the fundamentals of molecular biology, specifically protein assay and Western blot, and for permitting me to use your lab resources.

Dr. Jiuzhou Song: for permitting me to use of the lab equipment.

Dr. Mark Richards: for the generous gift of ELISA kit and valuable suggestions for my research.

Mr. Bill Lee and **Ms. Maria Clements**: assistance for me to collect eggs from Perdue farm hatchery for the studies.

My Colleagues from the lab, Umang Agarwal: for being a good friend, for helping me with long hours of sample collection and selfless help and discussion on my thesis writing. **Leslie Juengst** and **Jennifer Colvin**: for being good friends and for suggestions on my presentations.

Katelyn Somers, **Kelly Bailey**, **Amy Brown**, **Mallan Willis**, **Morgan Lewis**, **Anna McGucken**: for the help of long hours of sample collection and processing.

I would like to thank my family for their unfailing love and support and my friends for their continued support and help in what I have been perusing in my life.

Table of Contents

List of Tables

List of Figures

List of Abbreviations

AMPK	adenosine monophosphate protein kinase
BW	body weight
BCAA	branched-chain amino acid
DM	dry matter
EFA	essential fatty acid
ELISA	enzyme linked immunosorbent assay
GC-MS	gas chromatography-mass spectrometry
GNG	gluconeogenesis
HCA	hierarchical clustering analysis
LC-MS	liquid chromatography-mass spectrometry
MIDA	mass isotopomer distribution analysis
NEAA	non-essential amino acid
NMR	nuclear magnetic resonance
PC	pyruvate carboxylase
PCA	principal component analysis
PDH	pyruvate dehydrogenase
PEPCK	phosphoenolpyruvate carboxykinase
PLS-DA	partial least square-discriminant analysis
PK	pyruvate kinase
RQ	respiratory quotient
VLDL	low density lipoprotein

CHAPTER 1: INTRODUCTION

The rate of embryonic growth and development is largely influenced by the initial egg size, composition of egg nutrients (yolk, albumen) and the period of incubation (Ricklefs, 1987; Wilson, 1991). Production records and field observations indicate a high mortality rate of embryos from small eggs (< 55 g), especially those from younger layers (< 30 wk). Initial egg size and nutrient composition determine substrate availability, and therefore necessitate alterations in substrate utilization and metabolic pathways during embryo development. This doctoral dissertation investigated the metabolic adaptation and substrate utilization during chicken embryo development, and determined the influence of breeder age and egg size on embryo growth and metabolism during later embryo development, i.e. from embryonic day (e) 11 of incubation to posthatch day 1.

It is well documented that egg size increases with breeder age, and chicks hatched from larger (65-70 g) eggs are heavier and have a larger residual yolk sac (Weatherup and Foster, 1980; Wilson, 1991; Lourens, et al., 2006). In addition, the ratio of yolk to albumen in large (62-67 g) eggs is greater than in smaller (52 g) eggs (Peebles et al., 2000). Studies have shown that embryos and broiler chicks from small (< 55 g) compared to large (65-70 g) eggs are associated with high mortality, poor uniformity and reduced growth performance (Noble et al., 1996; Peebles and Brake, 1987). As the nutrient environment is established once the egg is formed, the ability of the embryo to regulate patterns of substrate utilization is critical for development and emergence. Latour et al., (1996) observed lower blood glucose and tissue glycogen levels in embryos from small compared to large eggs. Moreover, the transfer of yolk lipids into the embryo towards the end of the incubation period was reduced in eggs from young compared to

old hens (Noble et al., 1986; Yafei and Noble, 1990). These phenomena of energy regulation might be linked to higher embryo mortality, reduced posthatch body weight and suboptimal growth performance in the small eggs from younger breeders.

Metabolic adaptation, especially energy partitioning, in the chicken embryo is most pronounced during later development. The yolk sac contains 45% lipids; thus lipid metabolism dominates in embryos from mid incubation until 2-3 days before hatch (Sato et al., 2006; Moran, 2007). Gluconeogenesis and glycogenesis are vital for embryo survival and early posthatch life to ensure an optimal supply of glucose. The Krebs cycle generates ATP and its metabolites are extensively linked to intermediary metabolism. The pentose phosphate pathway ensures the indispensible supply of ribose for nucleic acid synthesis, because there are very minimal amounts of nucleic acids in a freshly laid egg (Reddy et al., 1952; De Oliveira et al., 2008). However, little is known about how metabolic pathways change during later development, and the importance of various substrates utilized for energy metabolism. Moreover, sensing and regulating energy status is of particular importance in developing chicken embryos, given that the supply of energy substrates in the egg is fixed. In the past decade, 5'-adenosine monophosphate-activated protein kinase (AMPK) has been demonstrated to be a key metabolic regulator for sensing energy status changes in multiple animal and cellular systems (Kahn et al., 2005; Towler and Hardie, 2007; Lage et al., 2008). And, despite recent work characterizing the tissue distribution of AMPK and its subunits in the developing chicken embryo (Proszkowiec-Weglarz and Richards, 2009), the role of the AMPK sensing system in the developing chicken embryo is unknown.

Overall Aim of Research

The aim of this research was to characterize substrate utilization during metabolic adaptation of chicken embryos as well as the role of energy regulation mechanisms (i.e., AMPK) from the latter period of development to posthatch day 1.The main factors investigated were breeder age (old *vs* young) and egg size (small *vs* large). These factors determine egg nutrient composition (e.g., yolk, albumen, fatty acids and carbohydrates) which influences substrate utilization in developing chicken embryos.

Research Hypothesis

It was hypothesized that egg size and hen age would influence embryo development by necessitating changes in metabolic pathways that lead to differential use of energy substrates. Moreover, the regulation of key metabolic events also was expected to change during development, and as a consequence of egg component composition.

Thus, the differences in egg size will dictate the absolute amount of egg nutrients available. Further, because hen age has a large influence on the yolk to albumen ratio, we also expected that embryonic metabolism and partitioning will differ in response to the different nutrient environments.

Although many studies have been conducted to evaluate the effect of egg size on embryo growth and hatchability, there is a lack of quantitative information on metabolic changes resulting from the difference in egg size or hen age *per se*. Also, it is unclear as to the mechanisms that dictate the patterns and extents of utilization of substrates by the developing embryo. We speculated that AMPK plays a key role in coordinating nutrient use in developing embryos.

In the past fifteen years, a new field of metabolomics has come to the forefront of metabolic exploration. The beauty of metabolomics lies in the fact that, unlike genomics or proteomics, it is a direct reflection of the phenotype or the physiological state of a biological system (e.g. whole animal, organ or cell). The technique can be used to capture a 'metabolic snapshot' of the active metabolic events. In recent years, animal scientists have started to employ this approach to determine the specific metabolites and metabolic pathways for suboptimal growth and development in piglets (Lin et al., 2012; Getty et al., 2013).

Prior to this research project, our laboratory developed an *in ovo* stable isotope tracer (e.g. [U-^{13}C] glucose, [U-^{13}C] glycerol) injection approach to investigate changes in the flux of substrates towards major metabolic pathways such as gluconeogenesis and the Krebs cycle in developing chicken embryos (Sunny and Bequette, 2010; 2011). This approach employs ^{13}C-mass isotopomer distribution analysis (MIDA) of metabolic intermediates and end products of pathways to calculate the fluxes and partitioning of substrates (e.g., glucose and glycerol) through central metabolic pathways. Thus, MIDA establishes the enzyme pathways involved in substrate use and the relative activity of enzymes and associated pathways. In the current research project, we employed both metabolic profiling and stable isotope tracer approaches to investigate the influence of egg size and hen age on metabolic development of the embryo, and to quantify the changes in metabolic pathways in response to varying nutrient compositions.

Experiment Objectives

1. Establish the patterns of nutrient utilization and metabolism in developing chicken embryos (e11 to posthatch day 1) hatched from small *vs* large eggs (*Study One*). We hypothesized that the different nutrient environments of small and large eggs would

necessitate an *in ovo* energy-sensing mechanism(s) to coordinate embryo growth, and that AMPK mediates these alterations. Further, this study aimed to quantify the available substrates (carbohydrates and fatty acids) in albumen and residual yolk from the two sizes of eggs (Chapter 3).

2. Determine the influence of egg size and breeder age on metabolic events during the late periods of development (e14 to posthatch day 1) employing metabolomics (*Study Two*). This study aimed to test the hypothesis that the activity of metabolic pathways involved in macronutrient metabolism differs during development of chicken embryos and in posthatch chicks due to the varying nutrient environments of eggs of different sizes and those from different ages of hens (Chapter 4).
3. Develop a constant infusion tracer ([U-^{13}C] glucose and [U-^{13}C] glycerol) approach to establish the rates of gluconeogenesis and substrate utilization in e14 and e19 embryos (*Study Three*). It was hypothesized that glucose and non-essential amino acid synthesis (NEAA) would increase from e14 to e19 in embryos due to the greater needs for glucose for muscle and liver glycogen accumulation and NEAA for net tissue protein gain. The study aimed to attain a high level of incorporation of ^{13}C into metabolites of intermediary metabolism in embryos by employing a constant tracer infusion protocol (Chapter 5).

CHAPTER 2: LITERATURE REVIEW

The Significance of Egg Hatchability to the Industry

In the US, per capita consumption of poultry meat (96 lb) is nearly equal to that of beef and pork combined (104 lb) in recent years (USDA, 2013) because of the public's perception of chicken and turkey meat as being low in fat, wholesome and nutritious. Poultry production will need to continue to rise to keep up with this increasing demand (USDA, 2007). In response to higher feed costs and to meet the large meat demand, the poultry industry will have to increase production efficiency by improving nutritional efficiency and reducing productive losses. Although growth rate and meat yield of commercial poultry have improved linearly over the last few decades (Havenstein et al., 2003a, b; Havenstein et al., 2007), embryonic death and ~80% hatchability continue to represent the largest losses in potential productivity, costing the US broiler and turkey industries $500 M per annum (Schaal and Cherian, 2007). Another issue facing the poultry industry is that chicks hatched from small eggs experience poorer hatchability and suboptimal posthatch growth performance compared to those from typical and larger sized eggs (Peebles and Brake, 1987). It is estimated that reducing early chick mortality by 0.25% will save the broiler industry over $ 5M per annum (Peebles, 2007).

Currently in the poultry industry, meat birds reach market weight in ~6 weeks. Therefore, the period encompassing the 21-day incubation period plus 10 days post-hatch represents ~50% of the broiler's lifespan. Any factors that promote or delay growth and development during this neonatal period will have a marked effect on overall growth performance and health of chicks. Thus, this dissertation research will focus on the period between embryonic (e) day 11 and posthatch day 1 of broiler chick embryo development, a critical window during which the embryo undergoes rapid growth and development, as the chick

prepares for emergence and life outside the egg. This period is also important to chicken survival during the first 1-3 days posthatch when stored glycogen and residual yolk components aid in the transition to feed grains (Lilburn, 1998; Vieira and Moran, 1999).

From Egg to Chick

Once the ovum is fertilized in the infundibulum, germ development is initiated. Fertilized germinal disc development occurs during the first 24 h (42 °C) while egg formation is being completed. Germ development temporarily ceases when the egg is laid and the environment temperature drops below 27 °C (Romanoff, 1939). When incubation begins, germ development resumes. A visible vascular system aids the germ in the absorption of nutrients from the surrounding yolk (Litke and Low, 1975) and albumen (Deeming, 1989). Oxygen access is limited to simple diffusion at this point (Baumann and Meuer, 1992); therefore the energy supply is dependent on glycolysis of glucose to lactic acid until the chorioallantoic compartment is formed (Kucera et al., 1984, Moran, 2007).

Rapid vascular system development enables the exchange of O_2 and CO_2 with shell pores (Tullety and Board, 1976), and fatty acid β-oxidation becomes the primary energy source for embryo development. Around e 8, with chorioallantoic respiration established, the vascular system is fully developed to ensure O_2-CO_2 exchange (Levinsohn et al., 1984). The embryo is structurally completed by e14 (Moran, 2007), and oxygen consumption reaches a plateau (Christensen et al., 1996). A simplified display of embryo development is shown in **Figure2.1**. Embryo death occurring at this stage is mainly due to nutritional deficiency of the breeder (Moran, 2007).

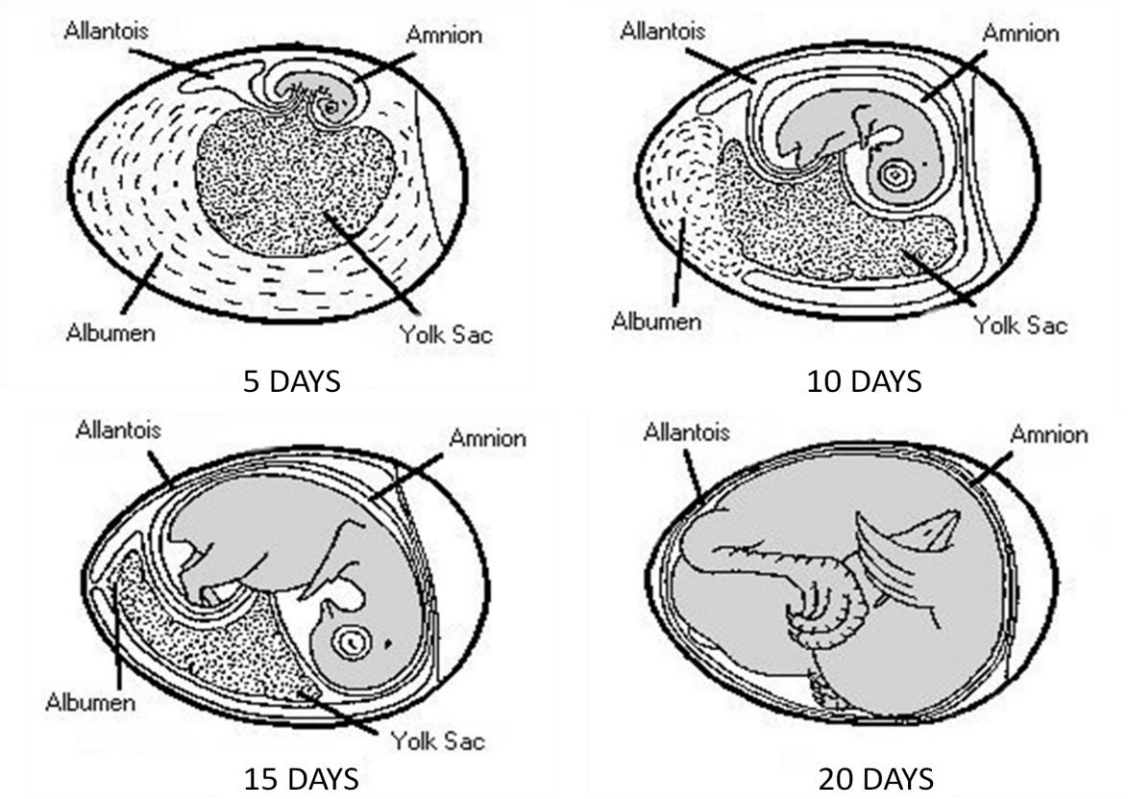

Figure 2.1 Chicken embryo development on e 5, e10, e15, e20, adapted from Romanoff (1939).

During the last week of embryo development, albumen enters the amniotic sac, and the amnion is orally consumed by the embryo. The albumen-amniotic mixture enters the yolk sac through the stalk to allow partial absorption of protein by enterocytes (Moran, 2007). Gluconeogenesis increases to ensure an adequate supply of glucose for glycogen accumulation in the liver and muscles.

Emergence is initiated when internal pipping occurs around e 20. Oxygen supply becomes limited, and energy support is mainly from glucose metabolism provided by the glycogen reserves. The metabolism of glucose to lactic acid reduces at this point once pulmonary respiration is initiated (Garcia et al., 1986; Hoiby et al., 1987). The remaining yolk sac is internalized and conserved for the transition during the first two days posthatch. Upon hatch, the liver and intestines continue to develop to prepare for the transition to feed consumption and digestion. During this latter period, dramatic changes in physiology and metabolism occur to ensure transition of the hatchling. Any interference during this transition period may significantly affect embryo survival, or result in suboptimal growth performance after hatch.

To summarize, embryo development can be divided into three phases. The first week of features the establishment of germ and chorioallantoic compartment formation. The second week is characterized by embryo completion and O_2-CO_2 exchange of chorioallantoic respiration. And, the last phase includes accumulation of glycogen in the liver and muscle tissues, beginning of pulmonary respiration, internalization of the remaining yolk sac, shell pipping and emergence. Major events during the entire incubation are displayed in **Figure 2.2**.

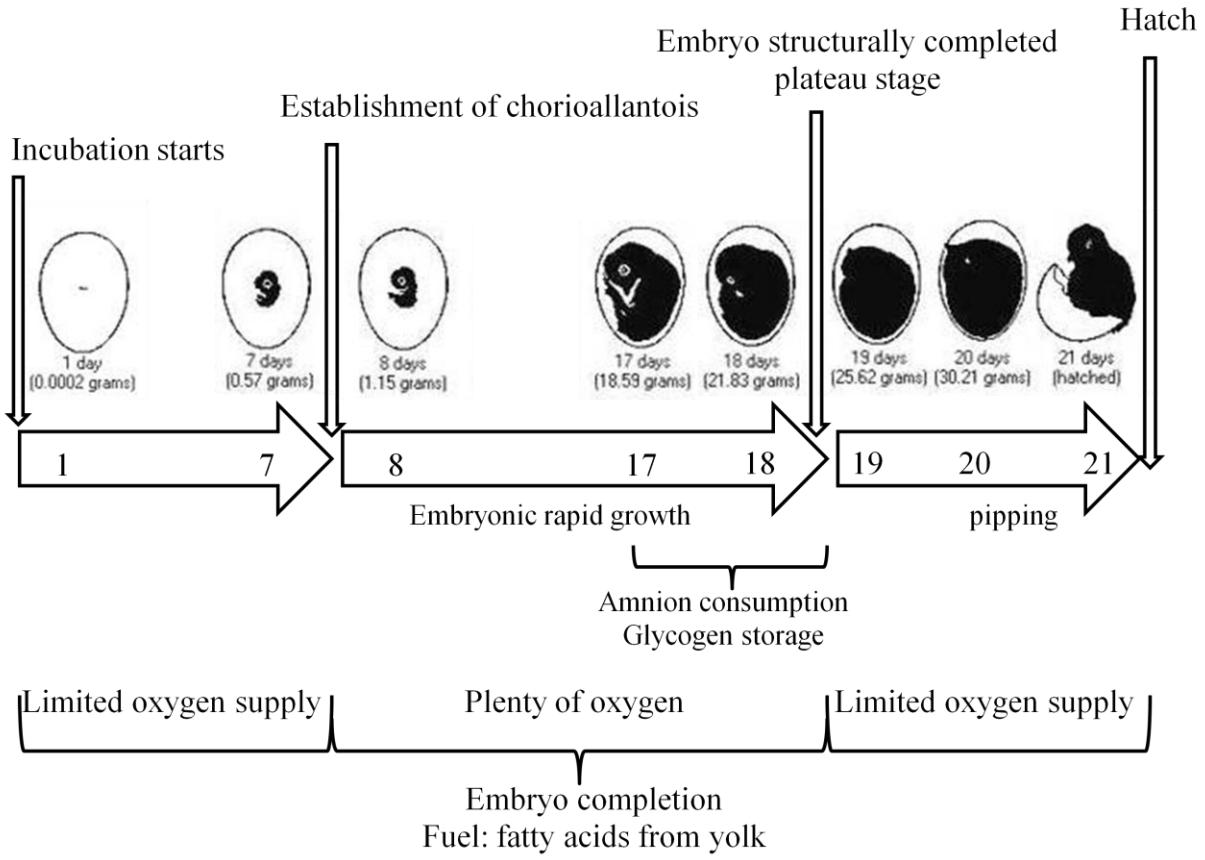

Figure 2.2 Chicken embryo development periods and major physiological and metabolic events, adapted from De Oliveira et al., (2008).

Factors Affecting Chicken Embryo Development

A variety of factors can affect chicken embryo development, such as the environment (temperature, humidity), seasonal variations, breeder genetics, nutritional status, and maternal age to name a few. These factors may directly contribute to hatchability and posthatch survival. Within a species, the breeder may lay eggs with enormous differences in size. The size difference can also occur within the same clutch (Surez et al., 1997; Mortola and Awam, 2010). If the embryonic growth trajectory is genetically conserved, then the weight difference of posthatch chicks and future growth performance of the hatchlings must be attributed to the egg nutrient supply.

Egg Size (weight)

It is well known that eggs of different sizes produce different size hatchlings (Mortola and Awam, 2010). Egg size differs due to several reasons, e.g. breeder age, nutritional status and laying time during a clutch. A strong positive correlation exists between egg weight at set and embryo weight on e 14, e 16, and e18 (Shanawany, 1984; Sunny and Bequette, 2010). Studies have shown that larger eggs have a greater surface area for O_2 diffusion. Because the availability of O_2 towards the end of embryo development is critical to energy metabolism, this may be more pronounced in the embryos of small eggs with smaller surface areas (Burton and Tullett, 1985; Tazawa et al., 1992). Hatchlings produced from large eggs also have a greater yolk residue (Williams, 1994; Lourens et al., 2006), which provides more nutrients for embryos during the transition period and results in heavier body weight at hatch (Mortola and Awam, 2010; Sunny and Bequette, 2010; Ulmer-Franco et al., 2010). Further, hatchling weight is positively correlated with blood glucose concentrations at hatch (Christensen et al., 2000). Lower blood glucose concentration is associated with lower hatchability in small eggs (Christensen et al., 2000). Not

surprisingly, hatchlings from small eggs also have relatively smaller breast muscle, liver and adipose tissue, which indicate less glycogen and fat storage for emergence.

Breeder Age

Breeder age is one of the most important factors that influence the yolk to albumen ratio in an egg (O'Sullivan et al., 1991). It is known that egg weight and the proportion of yolk both increase with increasing hen age (Suarez et al., 1997); however, egg shell thickness decreases with increasing hen age (Peebles et al., 2000). Shell thickness and pore number influence gas exchange and moisture loss during the incubation period (Wangensteen et al., 1970-1971; Reis et al., 1997; Peebles et al., 2001). While yolk provides more than 90% of the energy requirement of the developing embryo (Romanoff, 1960), a smaller proportion of yolk relative to albumen is disadvantageous to embryos from small eggs (Ulmer-Franco et al., 2010). The posthatch body weight differences and higher mortality rate were linked to small eggs derived from young hens may also lead to less development of physiological systems (McNaughton et al., 1978). Eggs from older hens hatch earlier than those from younger hens (Lowe and Garwood, 1977), probably because of efficient nutrient deposition into the eggs leading to optimal use during embryonic growth (Shanawany, 1984).

Relationship between Breeder Age and Egg size

In general, egg size increases with hen age; however, during a given laying cycle (clutch), breeders produce eggs of variable sizes. Therefore, egg size differences can be attributed to hen age or laying time during the clutch. Small eggs from young hens (32 wk) have a lower yolk to albumen ratio as compared to large eggs from older hens (41 wk) (Joseph and Moran, 2005). Surprisingly, small eggs laid at beginning and end of the clutch have a greater

proportion of yolk than large eggs from the same clutch (Vieira and Moran, 1998). Shanawany (1984) showed that e18 embryo weight increased with increasing breeder age, regardless of the initial egg weight.

Important Metabolic Pathways during Development

Metabolic pathways of greatest importance to the embryo are related to energy metabolism, and are dependent on the availability of O_2. Current information on regulation of metabolic pathways to support embryonic development is limited. The following sections elucidate the importance of various metabolic pathways during different stages of embryo development. **Figure 2.3** summarizes the central metabolic network.

Glycolysis and Krebs cycle

Glycolysis plays a particularly important role during early embryonic development when the chorioallantoic compartment is not completely formed. Through glycolysis, 1 mole of accessible glucose produces 2 mol of ATP and 2 units of pyruvate. When O_2 supply is limited, pyruvate is converted to lactate in order to maintain glycolysis self-functioning. Although carbohydrates are only 3% (DM basis) of egg content at set (Romanoff and Romanoff, 1967), this limited supply ensures the successful transition from anaerobic to aerobic metabolism. As the vascular system develops, pyruvate from glycolysis enters the Krebs cycle for further and complete oxidation rather than formation of lactate.

The Krebs cycle receives inputs into the acetyl-CoA pool from fatty acid β-oxidation to generate most of the energy required for embryo development. The Krebs cycle also provides intermediates for gluconeogenesis and non-essential amino acid (NEAA) synthesis, and reducing equivalents (including NADH and $FADH_2$) are formed to generate ATP via the electron

transport chain (Moran, 2007). Because the initial egg supply of glucose is finite, the glycolytic pathway is truncated at pyruvate at the beginning and end of embryo development when O_2 availability is marginal (Freeman, 1969; Tazawa et al., 1983).

Lipid Metabolism

The egg contains ~31% yolk (DM basis), which is comprised primarily of lipids (33%) (Burley and Vadehra, 1989; Deeming and Ferguson, 1991). Yolk lipids are the major source of energy and are important building blocks for tissue and brain development (Speake et al., 1998; Sato et al., 2006). Triglycerides and phosphoglycerides are the main forms in yolk lipids (92%) and are preferentially utilized to generate energy (Burley and Vadehra, 1989; Deeming and Ferguson, 1991). Triglyceride hydrolysis yields free fatty acids and glycerol. After the formation of the chorioallantoic compartment, acetyl-CoA generated from fatty acids β-oxidation enters the Krebs cycle to yield ATP (Krebs, 1972). Previous work in our laboratory demonstrated that glycerol is a significant substrate for gluconeogenesis in the developing chicken embryo (Sunny and Bequette, 2011).

Rapid cell proliferation in developing chicken embryos requires the formation of membrane phospholipid from yolk stores (Speake et al., 1998). Some n-3 and n-6 long chain polyunsaturated fatty acids are believed to be essential in the functional differentiation of certain organs and tissues. For example, docosahexaenoic acid (C22:6 n-3) is of importance in brain and retina development (Anderson et al., 1990; Cherian and Sim, 1992). The final week of embryogenesis features rapid transfer of lipid components in the form of lipoprotein particles from yolk to the embryonic circulation (Noble and Cocchi, 1990; Shand et al., 1993).

High levels of lipoprotein lipase activity were observed in adipose tissues of embryos (Speake et al., 1992) whereas lipogenesis from carbohydrate precursors was not active

(Goodridge, 1974). However, subcutaneous fat was detected in embryos as early as e12, which suggests that the growth of adipose tissue is dependent on uptake of yolk lipids (Langlow and Lewis, 1972; Ferkas et al., 1996).

Amino Acid Metabolism

Both yolk and albumen contain significant, but a fixed, amount of protein (amino acids) for tissue growth and development. Free albumen enters via the amniotic sac, and thus albumen-amniotic mixture is orally consumed by the embryo. The macronutrients in this mixture are absorbed by enterocytes in the duodenum and jejunum (Moran, 2007). Albumen can also enter the yolk sac through the stalk with the aid from antiperistaltic activity of the colon (Sugimoto et al., 1989; Bryk and Gheri, 1990). The amino acid profile of egg proteins remains the same throughout development, and utilization of amino acids from the yolk and albumen occurs at a constant rate (Ohta et al., 1999). Except for glycine and proline, which are required in higher proportions for collagen synthesis, the rate of use of most amino acids occurs at a similar rate (Ohta et al., 1999).

In addition to their essential role in tissue protein synthesis, amino acids also serve as important substrates for gluconeogenesis. Glutamine, glutamate, alanine, aspartate, serine and threonine are the major gluconeogenic amino acids, not only in avian species, but also in mammals (Heitmann et al., 1973; Lobley, 1992; Sunny and Bequette, 2010). Apart from tissue protein synthesis and gluconeogenesis, some amino acids, such as glycine and aspartate, are indispensible components of nucleotide bases. Glycine and glutamine also serve as important substrates for uric acid synthesis, the primary end product of amino acid catabolism in the embryo that is excreted into the allantois (Levenberg et al., 1956; Sonne et al., 1956).

Gluconeogenesis and Glycogenesis

Although glucose is initially catabolized to support early embryo development, glucose concentration increases in the plasma from < 100 mg/dl in early developmental stage to levels reaching 150-160 mg/dl at the time of hatch (Hazelwood, 1986). This phenomenon suggests that gluconeogenesis from non-glucose substrates must increase in activity as the embryo develops. A study of isolated chicken liver cells showed that lactate, pyruvate, and dihydroxyacetone were the top three substrates that contribute to glucose synthesis (Brady et al., 1979). In contrast to mammals, gluconeogenesis from lactate appears to be greater than from pyruvate in avian species. A possible explanation for this species difference relates to the increased gene expression of the liver mitochondrial (m) isoform of phosphoenolpyruvate carboxykinase (PEPCK) that predominants from e 13 to adulthood, whereas gene expression of the liver PEPCK cytosolic (c) isoform decreases from e13 to negligible levels by e20 (Savon et al., 1993). Gluconeogenesis requires the transfer of carbon substrates (pyruvate, amino acids and Krebs cycle intermediates) from the mitochondria to cytosol and the generation of cytosolic NADH from the conversion of malate to oxaloacetate. When the PEPCK (m) isoform predominates during later embryonic development, pyruvate exits the mitochondria as phophoenolpyruvate, without transfer of NADH. The oxidation of lactate to pyruvate generates one NADH in the cytosol. Only one NADH is consumed per each triosephosphate dehydrogenase reaction in gluconeogenesis. It is important to balance the cytosolic redox state by synthesizing phophoenolpyruvate in the mitochondria, as this obviates production of another NADH from the malate to oxaloacetate conversion in the cytosol (Yang et al., 2009). In addition to the three substrates mentioned above, glycerol has also been shown to be a significant substrate for gluconeogenesis, especially in embryos from small eggs (Sunny and Bequette, 2011).

Glucose arising from gluconeogenesis is predominantly stored in the liver and muscle as glycogen (Matthews and Holde, 1990; Christensen et al., 2001). Synthesis of glycogen is extremely critical for embryo survival, particularly during the last few days of development. Nevertheless, glycogenolysis is as important as glycogenesis, since glycogenolysis provides free glucose for energy. When the embryo approaches the plateau stage of O_2 consumption during later development, the energy supply switches from fatty acid β-oxidation to glycolysis utilizing glucose mobilized from glycogen storages (Donaldson and Christensen, 1991). Both glycogenesis and glycogenolysis are tightly regulated by hormones to maintain homeostasis.

Pentose Phosphate Pathway

The pentose phosphate pathway is important for cell proliferation and tissue growth, as it provides ribose, a necessary component for synthesis of nucleotides. It is known that the initial supply of preformed nucleic acids in freshly laid eggs is limited (Reddy et al., 1952), thus the ability to *de novo* synthesize nucleic acids becomes vital during embryo development. However, purines, but not pyrimidines, are mostly synthesized (> 95%) *de novo* by hens (Berthold et al., 1995), which suggests that the initial deposition of pyrimidines into the egg by the hen and the availability of precursors for purine biosynthesis by the embryo will greatly influence development. Furthermore, the pentose phosphate pathway generates reducing equivalents, NADPH and NADH, which enter the respiration chain to produce ATP and which are essential for reactions involving fatty acid and nucleic acid synthesis.

Hormonal Control of Metabolic Pathways

The endocrine system, including the pituitary, hypothalamus and pancreas, develops in chicken embryo during the first week of incubation. The hormones produced from these organs

determine metabolic patterns throughout development and influence the partition of nutrients and substrates during embryonic growth.

Plasma glucose can be detected in the chicken embryo as early as e4, and is found to increase gradually during the entirety of development. On e4, glucagon secreted from pancreatic A cells begins to circulate freely or loosely bound to plasma albumin (Hazelwood, 1986). It has been reported that glucagon levels are two to five times higher in avian plasma compared to that in mammals (Weir et al., 1976). Glucagon regulates carbohydrate, lipid and amino acid metabolism by counteracting the effects of insulin (Jiang and Zhang, 2003). The major physiological effect of glucagon is to increase plasma glucose by enhancing hepatic gluconeogenesis and glycogenolysis. Glucagon is also the primary hormone in avian species that stimulates lipid mobilization from adipose tissue, resulting in elevated plasma free fatty acid levels (Leclercq, 1984). Therefore, plasma glucose may be spared when fatty acids are utilized, which is largely under control of glucagon or the glucagon/insulin ratio. Glucagon plays an important role not only during embryogenesis, but also in the transition of the embryo from a high-fat, low-carbohydrate supply *in ovo* to a high-carbohydrate, low-fat diet after hatch (Langslow et al., 1979).

Insulin has been shown to accelerate chick embryonic growth and morphological development (De Pablo et al., 1990). The reversed effects of insulin, compared to glucagon, are to reduce glycogenolysis and simultaneously promote glycogenesis. The main target tissues, which are essentially the same as those in response to glucagon, include liver, muscle and adipose tissue (Dickson and Langslow, 1978; Hazelwood, 1986). *In vitro* and *in vivo* studies have shown that insulin appears to be more active in the liver of chickens than that in mammals. Possible explanations are greater affinity of chicken insulin for liver binding sites and a slower

dissociation rate of the insulin-receptor complex that further potentiates the role of insulin in metabolic regulation (Simon et al., 1974). The molar ratio of insulin to glucagon increases between embryonic e 12 to e15 and decreases during pipping and hatch, thus supporting the high energy demands of hatching (Lu et al., 2007).

Corticosterone is the primary glucocorticoid secreted by the avian adrenal cortex. In the chicken embryo, plasma glucocorticoid concentration reaches a peak around e 14-e16 (Wise and Frye, 1973) and immediately before hatch (Marie, 1981; Tanabe et al., 1986). Effective glucocorticoids stimulate gluconeogenesis, thus resulting in greater hepatic glycogen deposition. Extrahepatic amino acids are mobilized for gluconeogenesis by the action of glucocorticoids (McKay and Cidlowski, 2003; Hall, 2010). Hayward and Wingfield (2004) reported that corticosterone implanted into the hen was transferred to the quail egg yolk and resulted in slower growth of the hatchlings.

The catecholamines dopamine, norephinephrine and epinephrine are synthesized from tyrosine (Kubrusly et al., 2007), and at e9, catecholamines have been detected in embryo plasma, with levels increasing up until time of hatch (Hazelwood, 1986). Catecholamines enhance glycogenolysis and lipolysis which result in the elevation of blood glucose and free fatty acids (Connolly et al., 1991; Stevenson et al., 1991).

Growth hormone is abundant in neural tissues of the chicken embryo during the first week of incubation and localized to specific tissues and cells during later development (Harvey et al, 2001). The population of growth hormone secreting cells is increased by corticosterone between e11 and e13. The main functions of growth hormone include promotion of lipolysis and glycerol release and increase of gluconeogenesis and protein synthesis.

The thyroid hormones, triiodothyronine (T3) and thyroxine (T4), participate in numerous physiological processes in both mammals and avians, especially regulating heat production during chicken embryo development (Cogburn et al., 1989; McNabb, 2000). Plasma T3 was detected on e9.5 and remained unchanged until pulmonary respiration starts (McNabb, 2000; Reyns et al., 2003; Lu et al., 2007). The elevated plasma T4 level occurs during the middle period of development, which is because of increased thyroid hormone receptors in the liver and brain (Bellabarba et al., 1988). Both T3 and T4 are positively correlated with chicken embryo body weight, suggesting that these hormones are critical in maintaining normal embryo growth and development (Lu et al., 2007).

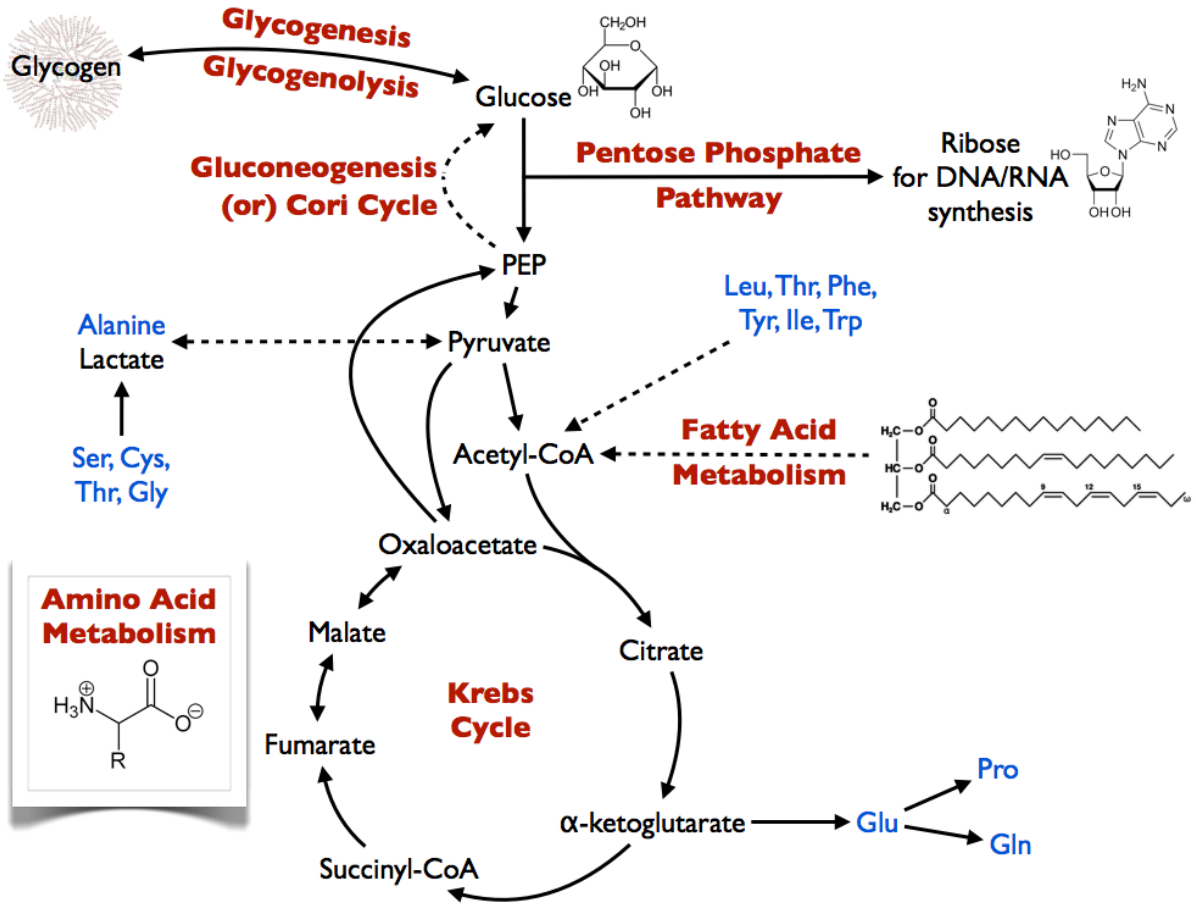

Figure 2.3 Central metabolic pathway networks in developing chicken embryos.

Energy Regulation during Embryo Development

Embryonic metabolism undergoes dramatic changes, especially during emergence. Sensing and regulating energy status is of particular importance in embryonic development, given the fixed supply of energy substrates available to the embryo throughout development. Reports over last 15 years clearly demonstrate that AMPK is a key sensor and regulator of cellular and whole body energy homeostasis in nearly all cell types and in many species. To date, clear demonstration of the role of AMPK in chicken embryo metabolism remains limited.

AMPK and Its Activation

AMP-activated protein kinase is a sensor and regulator of energy balance at both single-cell and whole-body levels (Kahn, 2005). The native form of AMPK is a hetero-trimer comprised of catalytic α subunits and regulatory β and γ subunits (Xiao et al., 2007, McBride et al., 2009). The α subunit includes two isoforms, α-1 and α-2, encoded by distinct genes in mammals. These subunits have conventional Ser/Thr kinase domains, with the conserved threonine residue which becomes phosphorylated in the activation loop once it is activated (Hawley, et al., 1996). The β subunit is regarded as a protein scaffold with glycogen-binding domains. The γ subunit contains four repeats of a structural motif which is referred to as cystathionine β-synthase. These motifs act in pairs to form two domains and are termed Bateman domains. Each Bateman domain preferentially binds to one molecule of AMP at five- fold higher affinity comparing to the binding of ATP molecules (Hardie, 2007a).

Similar to mammals, chicken AMPK is also composed of one catalytic and two regulatory subunits. Proszkowiec-Weglarz et al. (2006 a, b) identified two alpha, two beta and three gamma subunit isoforms in broiler chickens. However, studies have also shown that

expression of the α -1subunit is highest in the liver whereas the α-2 subunit is preferentially expressed in breast muscle (Proszkowiec-Weglarz and Richards, 2009).

AMPK is well known as a sensor of energy status in mammals as well as in broiler chickens (Hardie, 2007a; Proszkowiec-Weglarz et al., 2009). Activation of AMPK is brought about by metabolic stress signals, leading to production of ATP (Kahn et al., 2005). Once activated, a cascade of reactions turns on catabolic pathways to generate ATP, while the ATP-consuming processes are turned off (Hardie, 2007b). AMPK is activated through the binding of AMP by three different mechanisms: 1) AMP allosterically activates the AMPK complex, 2) AMP promotes activation of the AMPK complex by stimulating phosphorylation of Thr-172 residue in the activation loop by an upstream kinase, and 3) AMP inhibits dephosphorylation of Thr-172 by protein phosphatases. All three mechanisms ensure that the AMPK system is sensitive to small changes in the cellular AMP/ATP ratio (Kahn et al., 2005). AMPK monitors the cellular energy status not only through the AMP/ATP ratio, but also by glycogen (McBride et al., 2009). Activated AMPK inhibits the anabolic pathways which require ATP, e.g. liver gluconeogenesis is reduced by decreasing gene expression of PEPCK (c) and glucose-6-phosphatase (Lochhead et al., 2000).

Metabolic Investigation Approaches

The central pathways involving carbohydrates, lipids, and amino acids are largely interlinked. Carbon skeletons of substrates and intermediates are highly exchanged among several pathways. Intermediary fluxes through the entire metabolic network determine the partition and utilization of substrates. It may be misleading if we consider one pathway separately from others, because changes in one reaction can readily alter the subsequent

pathways which seem to be remotely connected (Reeds et al., 1997). Although various metabolic pathways intersect freely at the whole body level, specific pathways may be compartmentalized between tissues and within cells. Thus, metabolic pathway investigation must be performed at the whole tissue or animal level. However, most of the current understanding of nutrient metabolism has been derived from *in vitro* studies (Bequette et al., 2006). As a result, there is a need to focus on *in vivo* models to better understand the underlying mechanisms of metabolic regulation.

The technological advances in mass spectrometry (MS) have been increasingly applied to study dynamic metabolic processes and their integration at the whole body level (Owen et al., 2000). The review below includes two popular approaches currently being employed in the studies of metabolic pathways.

Metabolomics

Metabolomics refers to the study of the entire set of small molecules (< 1500 Da) in a biological sample (Wishart, 2007). As such, the metabolome is defined as a collection of small molecules produced by cells. It allows for investigating the relationship between mechanistic biochemistry and particular phenotypes (Patti et al., 2012). Metabolites are different from genes and proteins, the functions of which are influenced by epigenetic regulation and post-translational modifications. They provide the instantaneous information about the biochemical reactions ongoing in the organism and therefore are unequivocally correlated with the particular genotype. Metabolomics approaches allow for the analysis of hundreds of metabolites in a given biological sample to provide a snapshot of multiple metabolic pathways simultaneously (Scalbert et al., 2009). System-wide changes of metabolic pathways in response to specific phenotypic perturbations have been identified when applying metabolomics profiling approaches and

bioinformatic tools (Patti et al., 2012). Currently, nuclear magnetic resonance (NMR) spectroscopy and other diverse chromatographic platforms, such as gas chromatography (GC), liquid chromatography (LC) and capillary electrophoresis (CE) coupled to MS are the major instruments for metabolomics studies. MS techniques are particularly advantageous because of their sensitivity, selectivity and ease of use, and have been used extensively in the metabolomics studies. There are two separate approaches to metabolomics that are described in detail below.

Targeted Metabolomics

Targeted metabolomics focuses on absolute quantification of selected metabolites, which may relate to one or more pathways of interest. It is usually used to interrogate a particular biochemical question or to test hypotheses that are typically related to certain pathways (Koal and Deigner, 2010; Patti et al., 2012), e.g. the targeted approach is effective when measuring the influence of a gene modification(s) on a specific enzyme(s). Researchers monitor changes in metabolic activity which could be attributed to differential production of a particular metabolite involved in the pathway. The workflow of targeted metabolomics includes metabolite extraction, selected reaction monitoring, instrument setting optimization and standard curve construct, and data analysis (Patti et al., 2012; Roberts et al., 2012) (**Figure 2.4**).

Research on measuring targeted metabolites has long been in practice, dating back to 1974 (Davison et al., 1974). The targeted approach undoubtedly played an important role in the development of the metabolomics field. Advanced instrumentation, such as NMR and MS, provides a highly sensitive and reliable method to measure a large number of metabolites with high throughput. In a human patient study of diabetes, a target metabolomics approach was used to measure the patient response to glucose challenge (Shaham et al., 2008). Using the LC-MS/MS platform, the levels of three bile acids, i.e. glycocholic acid, glycochenodeoxycholic

acid and taurochenodeoxycholic acid, were found to be more than double within the first 30 min after glucose intake. The results were unexpected as those bile acids had never been correlated with glucose homeostasis.

However, since this approach only measures specific metabolites of interest to the researcher, the metabolites which are not well documented or identified are overlooked. This shortcoming will result in incomplete characterization of metabolic networks and pathways, and likely lead to misinterpretation of metabolic events. To overcome some of these shortcomings, an untargeted metabolomics approach can be applied.

Untargeted Metabolomics

Untargeted metabolomics approaches aim to identify or profile as many metabolites as possible in a given biological sample without bias (Vinayavekhin and Saghatelian, 2010; Patti et al., 2012). It is more global in assessment, and the datasets generated from high resolution instruments can be very complicated. Currently, metabolomic profiling can be performed using NMR and MS technologies. However, NMR is less sensitive than MS, and requires micromole amounts of metabolites. Thus, MS techniques are generally preferred to identify and quantify metabolites in samples. Although the detection limits of these instruments can be as low as picomoles, none of the individual methods can cover the complete metabolome. Therefore, a combination of all the instruments would be ideal to ultimately measure the metabolome of a biological sample. A typical untargeted metabolomics workflow by GC-MS features metabolite extraction, metabolite derivatization, ion chromatogram overlays, data alignment, database identification, and validation with standards (Scalbert et al., 2009; Patti et al., 2012) (**Figure 2.4**).

In contrast to the targeted metabolomics approach, untargeted metabolomics is often "hypothesis generating" rather than "hypothesis driven". Hence, it is important to design the

experiment to ensure maximum metabolite detection and quantitative reproducibility. This emphasizes the importance of sample collection and preparation, chromatographic separation and data acquisition (Patti et al., 2012). As a global profiling approach, untargeted metabolomics has aided in understanding of the comprehensive relationship between cellular/whole body level metabolism and specific phenotypes (Fiehn and Spanger, 2002; t'Kindt et al., 2010; Patti et al., 2012). It has also been useful in identifying key metabolites which can be targeted for therapeutic benefit. An example of the application of this approach is the discovery of rapid consumption of glycine in rapid cancer cell proliferation using LC-MS/MS (Jain et al., 2012). By measuring the consumption and release profiles of 219 metabolites from media across the cancer cell lines, glycine and related metabolites (i.e. sarcosine, serine, and threonine) were determined to represent a metabolic vulnerability in rapidly proliferating cancer cells.

The challenges of untargeted metabolomics include instrument detection limits, and metabolite identification and quantification (Dunn et al., 2013). GC-MS is a powerful and widely used tool which offers high separation efficiency and reproducibility. However, it requires derivitization of metabolites to make them volatile for GC separation, which can be a limitation for large molecules. Moreover, derivatives can be easily degraded. On the other hand, LC-MS does not require the samples to be derivatized for analysis of polar or high molecular weight metabolites, but the disadvantages are the retention time instability and ion suppression (Scalbert et al., 2009). Unknown metabolites may be difficult to identify, thus metabolite databases and identification software need further improvement.

Application of Metabolomics in Animal Sciences

The application of metabolomics in research has increased rapidly during the past decade. It is expanding to catch up with other analytical techniques such as genomics and proteomics but

still remains far less developed and less accessible to many researchers and labs (**Figure 2.5**).Although most often applied in plant science and human disease and nutrition research, the use of metabolomics in the animal sciences field has been increasing in recent years. It has been used to address questions such as the study of umbilical vein plasma metabolite differences between normal and growth restricted fetal pigs (Lin et al., 2011), milk metabolomics (Sundekilde et al., 2013) and arginine supplementation to the metabolic profile of the small for gestational age piglet (Getty et al., 2013).

Mass Isotopomer Distribution Analysis

Changes in one pathway may affect other pathways which seem remote from the initial metabolic change. Thus, it requires researchers to investigate the metabolic pathways and nutrient fluxes at the whole tissue or the whole animal level. The application of stable isotope tracer approaches in whole animals and cell cultures allows us to determine the dynamic processes underlying nutrient metabolism and intermediary metabolism. With the advancement of technologies in MS, coupled with mass isotopomer distribution analysis (MIDA), stable isotope tracers have been employed in a range of nutrient metabolism investigations in a variety of species (Brunengraber et al., 1997; Bequette et al., 2006).

MIDA, first developed in 1991 (Katz and Lee, 1991), is a technique for measuring the synthesis of biological polymers (e.g. lipids, carbohydrates and proteins) (Hellerstein and Neese, 1999). After introducing a stable isotope labeled precursor into a biological system (e.g. cell cultures, tissue cultures, whole animals), MIDA quantifies the relative abundance of molecular species of a compound differing only in mass (mass isotopomers). The mass isotopomer pattern, or distribution, is analyzed using a combinatorial probability model by comparing measured abundances to theoretical distributions. MIDA calculates the dilution in the precursor and

product pools, the precursor pool turnover rate, and fractional contribution from endogenous biosynthesis. Generally, MIDA provides a fundamental "equation for biosynthesis" (Hellerstein and Neese, 1999).

The stable isotopes (e.g. ^{13}C, ^{2}H, ^{15}N, ^{18}O, and ^{34}S) are particularly useful in biological studies. It is noteworthy that stable isotope enriched compounds are only available when the atom in the compound occurs naturally, 1 or 2 atomic mass units heavier. This way, derivatized stable isotope enriched molecules will fragment predictably to yield an identical ion spectrum signature as the unlabeled (naturally abundant) compound when using GC-MS. The largest molecular weight fragment ion and its associated heavier isotopomers are selectively monitored (Bequette et al., 2006). The stable isotope labeling pattern of the targeted compound provides important metabolic information that extrapolates to the metabolism in the cell, tissue or whole organism.

To better illustrate the above concepts, I will describe the predicted biochemical transformation of a [U-^{13}C] labeled compound (e.g. glucose, amino acids) administration *in ovo* to developing chicken embryos as an example (Sunny and Bequette, 2010). [U-^{13}C] Glucose is six mass units heavier, but it is metabolically indistinguishable from unlabeled glucose [M] when metabolized through the same pathways. During the course of metabolism of the labeled and unlabelled glucose through glycolysis and the Krebs cycle, isotopomer patterns (e.g. [M+1], [M+2], and [M+3]) are generated in intermediates in these pathways. The relative labeling pattern of two intermediates can be used to derive relative contributions of metabolites towards different metabolic pathways.

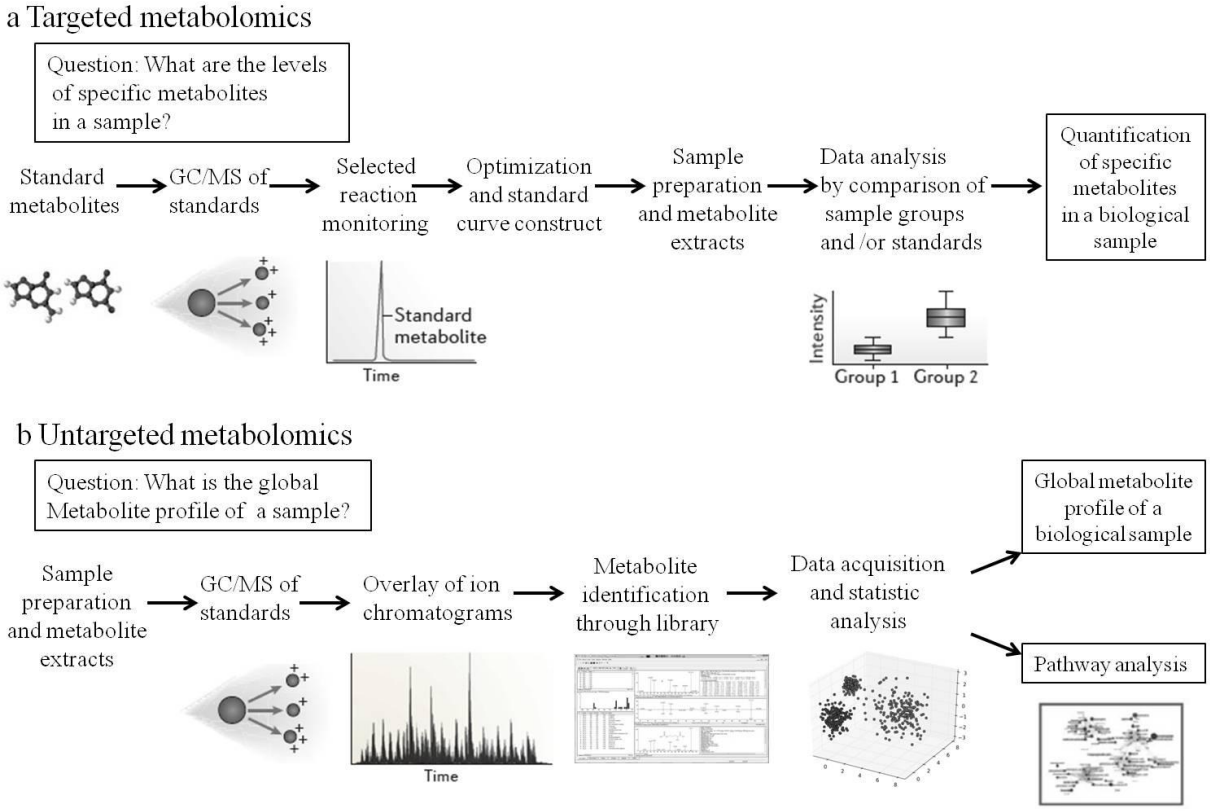

Figure 2.4 Targeted and untargeted metabolomics workflow, adapted from Patti et al., 2012.

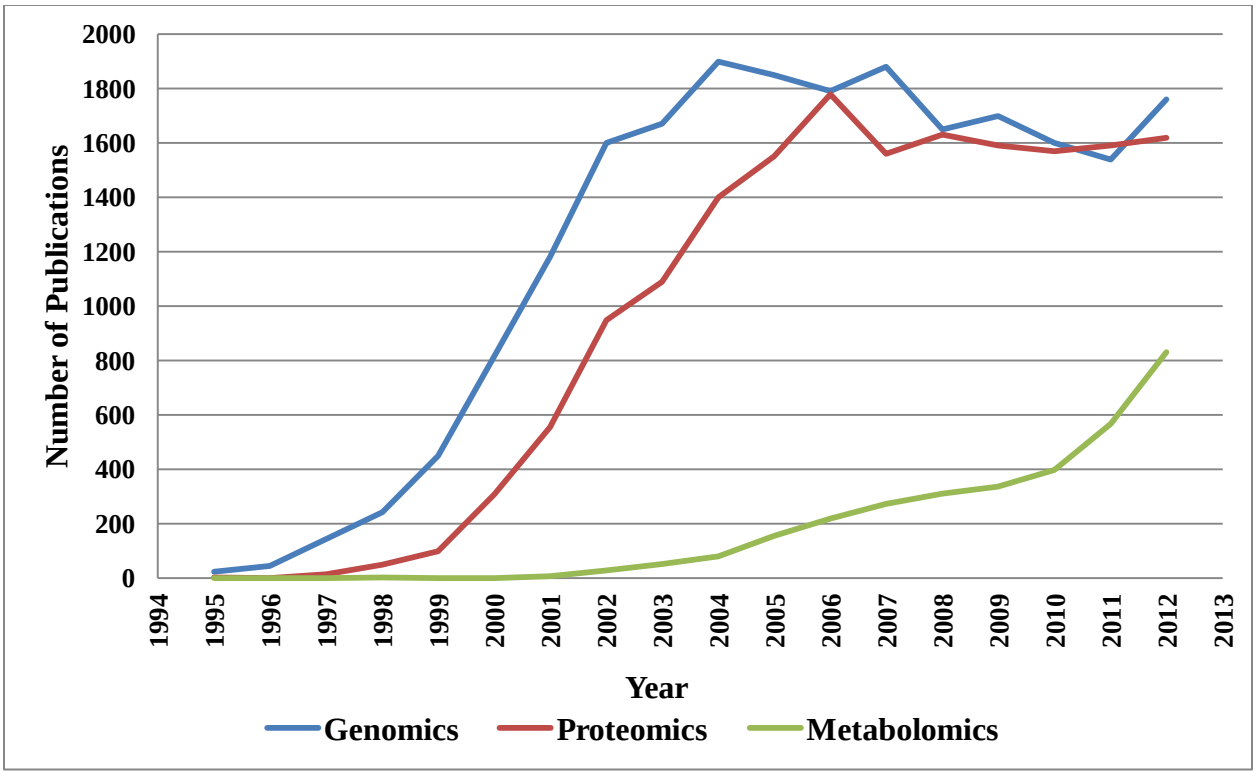

Figure 2.5 Publications of genomics, proteomics and metabolomics research from Year 1995-2012, data source: google scholar.

[U-^{13}C] Glucose was introduced *in ovo* in developing chicken embryos for three consecutive days to reach stable isotope steady state (Sunny and Bequette, 2010). Metabolism of [U-^{13}C] glucose involves several initial fates: 1) incorporated into glycogen, 2) metabolized via glycolysis to yield [M+3] pyruvate and/or 3) entry into the pentose phosphate pathway. Further metabolism of [M+3] pyruvate in the Krebs cycle can lead to synthesis of [M+2] acetyl-CoA and/or [M+3] oxaloacetate after carboxylation. [M+3] Oxaloacetate can either continue on through the Krebs cycle or be converted to [M+3] phosphoenolpyruvate which can be used to resynthesize glucose, thus leading to synthesis of the [M+3] glucose isotopomer. Thus, the ratio of [M+3] to [M+6] glucose isotopomers gives a minimal estimate of glucose carbon recycling and gluconeogenesis from pyruvate. However, this [M+3] glucose underestimates fractional gluconeogenesis due to the dilution of unlabelled carbon sources arising from: 1) entry into the pyruvate pool from metabolism of alanine, 2) entry of carbon sources from fatty acid β-oxidation and amino acid catabolism, and 3) the exchange and rearrangement of carbons due to oxaloacetate-fumarate cycling in the Krebs cycle, generating a mixture of ^{13}C-labeled oxaloacetate units where carbons 1-3 and carbons 2-4 of oxaloacetate are ^{13}C-labeled. Only oxaloacetate labeled in carbons 1-3 produces [M+3] glucose (Reeds et al., 1997).

The ^{13}C-labelling patterns of metabolites through metabolism of [U-^{13}C] glucose via the glycolytic pathway also provide information on enzyme pathway activity (Bequette et al., 2006). For example, to measure pyruvate dehydrogenase (PDH) activity, the unique labeling patterns of intermediates from metabolism of [M+3] pyruvate in the Krebs cycle are monitored. The [M+3] pyruvate isotopomer generates the [M+3] oxaloacetate isotopomer via activity of pyruvate carboxylase (PC). Eventually, further metabolism of the [M+3] oxaloacetate in the Krebs cycle leads to the synthesis of [M+3] α-ketoglutarate. Moreover, the [M+3] pyruvate can also be

metabolized via PDH to produce [M+2] acetyl-CoA which results in the formation of [M+2] α-ketoglutarate. However, the [M+2] α-ketoglutarate isotopomer can also result from oxaloacetate-fumarate cycling. Here, the decarboxylation step between citrate and α-ketoglutarate leads to the loss of carbon 1 of oxaloacetate which contributes to the [M+2] α-ketoglutarate isotopomer, thus necessitating a correction to the [M+2] α-ketoglutarate enrichment (Berthold et al., 1994). In the study of *in ovo* administration of [U-^{13}C] glucose described above (Sunny and Bequette, 2010), [M+2], [M+3] aspartate and [M+2], [M+3] glutamate enrichments were measured due to the technical challenges of direct measurement of tissue oxaloacetate and α-ketoglutarate enrichments. However, several studies have demonstrated that the isotopomer labeling patterns and enrichments of oxaloacetate and aspartate, and α-ketoglutarate and glutamate are nearly identical since these paired intermediates are in metabolic equilibrium (Katz et al., 1989; Wykes et al., 1998). Hence, PDH activity can be estimated by the ratio of [M+2] acetyl-CoA to [M+3] pyruvate (Berthold et al., 1994).

Summary

To date, several studies have evaluated the effect of egg size and breeder age on embryo growth and hatchability as well as other physiological parameters. However, most of these studies utilized different sizes of eggs from different age of hens, thus the effect of egg size on embryo development is often confounded with hen age. The answers to the following questions are not clear: 1) What is the influence of egg size or breeder age *per se* on embryo development? 2) What metabolic pathway changes does the embryo undergo to satisfy the metabolic and growth needs of cells, tissues and organs when there is a limited supply of nutrients throughout development? 3) Via what mechanisms are substrate utilization adapted and coordinated when the embryo is faced with a limited nutrient environment (e.g. small versus large eggs)?

Based on the available literature and results from previous experiments in our lab, we hypothesized that part of the adaptation and coordination of embryo energy metabolism is regulated by sensing through AMPK. Eggs of different sizes and laid by hens of different ages affects egg nutrient composition, thus requiring metabolic adaptations to accommodate the fixed nutrient supply to ensure appropriate utilization of nutrients during embryo development. These hypotheses will be tested in this dissertation with three experiments applying metabolomics profiling and stable isotope MIDA approaches.

The information generated from this project will provide information about the metabolic pathways that are important for embryo development. Proper pathways or metabolites may be determined accordingly to be biomarkers for optimal growth. Furthermore, knowledge about metabolic pathway changes and substrate utilization will improve our understanding of the nutrient needs of hatchlings. In this regard, appropriate diets could be formulated for breeders and hatchlings, respectively, to optimize egg content and composition to improve embryo survival and hatchling growth performance.

CHAPTER 3: EXPERIMENT 1

ENERGY-SENSING IN DEVELOPING CHICKEN EMBRYOS AND POST-HATCH CHICKS FROM DIFFERENT SIZE EGGS[1,2]

[1] Presented in part at the annual meetings of the Federation of American Societies for Experimental Biology: Hu, Q., U. Agarwal, K. R. Somers, K. M. Bailey, A. C. Brown, and B. J. Bequette, 2011. Energy balance regulation and carbohydrate utilization in developing chicken embryos. FASEB J. 25: 774.11

[2] Published in part in Poultry Science [Hu, Q., U. Agarwal, and B. J. Bequette, 2013. Energy-sensing in developing chicken embryos and post-hatch chicks from different size eggs. Poult. Sci. 92:1650-1654.]

ABSTRACT

The objective of this study was to quantify developmental changes in macronutrients in eggs of different sizes, and to explore an energy-sensing mechanism that may mediate nutrient metabolism. We hypothesized that 5'-AMP-activated protein kinase (AMPK), a ubiquitous energy-sensor, plays a key role in coordinating nutrient use in developing broiler breeder embryos. To test this hypothesis, we measured AMPK activity in the liver of embryos, and carbohydrates and fatty acids in the yolk and albumen of small *vs* large eggs. Small (53.2 ± 1.04 g) eggs from 26 wk-old and large (69.0 ± 1.86 g) eggs from 42 wk-old broiler breeder hens were acquired and measurements were made on embryonic day (e) 11, 14, 17, and 20 and on posthatch d1. The initial weight of dry yolk to albumen was higher (2.3 *vs* 1.7) in large *vs* small eggs, and embryo weight differed from e17 onwards. At set, glucose and mannose contents in albumen were 500-fold higher than fucose, but by e11 glucose content decreased to negligible levels whereas mannose and fucose contents remained constant. The proportion of palmitic and stearic acid in the yolk remained relatively constant during development for both egg sizes. However, palmitic acid accounted for a higher proportion ($P < 0.0001$) of yolk lipids in the small *vs* large eggs throughout development whereas linoleic and linolenic acid were 9% ($P = 0.0002$) and 22% ($P < 0.0001$) higher in yolk lipids from large eggs. AMPK activity was higher ($P < 0.05$) in livers of embryos from large *vs* small eggs on each sampling day, and activity peaked between e12 and e20 for both size eggs. We speculate that higher AMPK activity in livers of embryos from large eggs may reflect increased metabolism of nutrients to support their faster growth rate *in ovo*. Taken together, our results are the first to investigate the relationship between liver AMPK activity and egg size and egg nutrient composition in developing chicken embryos.

Key words: chicken embryo, post-hatch chicks, egg size, 5'-AMP-activated protein kinase, energy regulation, egg nutrient

Introduction

Broiler chicks hatched from small (< 55 g) compared to large size (65-70 g) eggs have greater embryonic and post-hatch mortality, and this has been linked to a lower glucose status and a lower ratio of yolk to albumen of smaller eggs. Chicks hatched from large eggs are heavier at hatch and have a larger residual yolk sac (Wilson, 1991; Lourens, et al., 2006). Lourens et al., (2006) reported that chicken body weight differences at hatch from small *vs* large eggs is due to the extra nutrient supply in large eggs. Given the positive correlation between egg weight and final hatchling weight, the economic importance of egg size is obvious (Wilson, 1991). To date, the mechanisms coordinating nutrient utilization in developing chicken embryos, in particular when egg size and nutrient composition varies, has received little attention.

Recently, AMPK has been found to regulate energy metabolism in response to nutrient and hormonal signals at the cellular and whole body levels (Towler and Hardie, 2007; Lage et al., 2008). AMPK, a heterotrimeric enzyme complex, is composed of a catalytic (α) and two regulatory (β and γ) subunits (Mitchelhill et al., 1994; Stapleton et al., 1996). Activation of AMPK by phosphorylation of threonine 172 on α subunit enhances activity of energy-generating pathways such as glycolysis, fatty acid oxidation, whereas activity of energy-consuming pathways, for example, gluconeogenesis, fatty acid synthesis and cholesterol synthesis, is reduced (Kahn et al., 2005). In broilers, the expression and activity of AMPK in various tissues, including the liver, has been characterized for developing embryos as well as for post-hatch chicks (Proszkowiec-Weglarz et al., 2006; 2009). AMPK was reported to repress gene

expression of PEPCK, a key enzyme in gluconeogenesis (Inoue and Yamauchi, 2006). Furthermore, activation of AMPK was found to down-regulate energy-consuming anabolic enzymes at the transcriptional level (Berasi et al., 2006). In a study of the effect of fasting and refeeding on liver AMPK mRNA, protein and activity levels in broiler chickens, Proszkowiec-Weglarz et al., (2009) found that phosphorylated AMPK level increased after a 48 h fast.

More than 90% of the energy requirement of chicken embryo development was supplied by the yolk fatty acid oxidation (Romanoff, 1960). Embryo and liver dry matter percentages were shown to be associated with various fatty acids in the yolk lipid (Peebles et al., 1999). Carbohydrate metabolism predominates during the first week of development (Moran, 2007). In chicken embryos, we speculate that the differences in nutrient supply and composition of large *vs* small eggs will be reflected in coordinated changes in AMPK activity in the liver as embryos develop. It is unknown whether carbohydrate and fatty acid composition differ in the small *vs* large eggs and whether these nutrients are selectively used during the embryo development. Therefore, the objectives of this study were to measure the nutrient content (carbohydrates and fatty acids) in egg yolk and albumen throughout development and to investigate the effect of nutrient composition and content on liver AMPK activity in chicken embryos during the later development.

Materials and Methods

Egg Incubation and Sample Collection

Fertile broiler breeder eggs of small (n = 60, 53.2 ± 1.04 g) and large (n = 60, 69.0 ± 1.86 g) sizes from 26 and 42 wk-old hens, respectively, were acquired from Perdue Farms, Inc (Herlock, MD). Ten eggs from each group were randomly selected for measurements of initial egg composition. The remaining eggs were incubated under standard conditions of 65% relative

humidity and 37.5°C. On embryonic (e) day 9, eggs were candled and undeveloped eggs removed. On e11, e14, e17, e20 and post-hatch day 1, a hole was made into the large end (air cell) of the egg with scissors, the crown removed, and the air-cell membrane removed to expose the embryo. The embryo and connecting compartments were transferred to a petri-dish on ice. The weights of the embryo, and residual yolk and albumen were recorded, and the whole liver immediately wrapped in aluminum foil before plunging into liquid nitrogen. Livers were stored at -80°C. Yolk and albumen were stored at -20°C for further analysis. The experimental protocol was approved by the Institutional Animal Care and Use Committee at the University of Maryland.

Fatty Acid Composition Analysis

For determination of individual fatty acid concentrations, frozen yolk was lyophilized to dryness (FreeZone Bulk Tray Dryer, Labconco, Kansas, MO) and pulverized in a liquid nitrogen freezer-mill (6850 SPEX CertiPrep Freezer/Mill, Wolf, Pocklington, York). To a known weight of dry yolk (50 mg) was added a known amount of a mixture of [U-^{13}C] fatty acids (^{13}C labeled algal fatty acids, Cambridge Isotope Laboratories, Inc., Andover, MA). Fatty acid methyl esters (FAME) were prepared using the method described by Christie (1982) and Kadegowda et al. (2008), with modified procedures for tissue samples. Briefly, 0.5 mL of 0.5 *N* NaOH/methanol was added to each sample and incubated in a 50°C water bath for 30 min. FAME were formed by adding 6.5 mL of 1.2 *N* H_2SO_4 in methanol and incubated in the dark at room temperature for 20 h. After extraction with hexane, FAME was analyzed on a gas chromatography-mass spectrometer (GC-MS, HP 6890 coupled with an HP 5973 Mass Selective Detector, Agilent) equipped with a 60 m × 0.25 mm × 0.25 µm capillary column (DB-23, Agilent Technologies, Palo Alto, CA). The inlet temperature was maintained at 250°C. The GC oven temperature

program was: 130°C for 1 min, increase 6.5°C per min to 170°C, increase 2.75°C per min to 215°C, 12 min at 215°C, increase 40°C per min to 230°C and 3 min at 230°C. The MS was operated in electron ionization mode and ions corresponding to the unlabelled fatty acid (M) and the labeled fatty acid (M+n, where n is the number of carbons in the fatty acid) were monitored and recorded. Fatty acid concentrations were calculated by isotope dilution.

Carbohydrate Composition Analysis

An initial analysis of the dry yolk and albumen indicated that the predominant carbohydrates were glucose, mannos and fucose (data not shown). A known weight of a mixture of [U-^{13}C] carbohydrates ([$^{13}C_6$] D-(+)-glucose, [1-^{13}C] D-(+)-mannose and [1-^{13}C] D-(+)-fucose, Cambridge Isotope Laboratories, Inc., Andover, MA) was added to a known weight of sample (albumen or yolk, 75 mg) and thoroughly mixed. Samples were incubated in 10% trifluoroacetic acid in distilled H_2O (v/v) at 105°C for 4 h. To saturate the solution, NaCl (1 g) was added to each sample and the samples placed on a vortex shaker for 15 min. Cold acetone (1 mL) was added and the samples vortex mixed for 15 min followed by centrifugation at 4,000 rpm for 10 min at room temperature. The top acetone layer was carefully removed and blown down to dryness under a stream of N_2 (2 psi) at 50°C. Carbohydrates were converted to their di-O-isopropylidene mono-acetone derivative by adding 100 µL of ethyl acetate:acetic anhydride (v/v, 1:1) and incubating at 60°C for 30 min. Derivatized carbohydrates were separated on a fused silica capillary column (HP-5; 30 m × 0.25 mm × 1 µm Hewlett-Packard, Palo Alto, CA) prior to MS under electron ionization conditions. Ions (mass-to-charge) monitored were 287 (unlabelled) and 293 (internal standard) for glucose, 287 and 288 for mannose, and 229 and 230 for fucose. Carbohydrate concentrations were determined by isotope dilution.

Tissue Protein Extraction

Frozen livers were homogenized in ice-cold lysis buffer containing 20mM Tris-HCl (pH 7.5), 150 mM NaCl, 1mM ethylene glycol tetraacetic acid, 1% Triton X-100, 1 mM EDTA, 1 mM phenylmethylsulfonyl fluoride, and 1× protease and phosphatase inhibitor cocktail (Pierce, Rockford, IL). The homogenate was centrifuged at 14,000 × *g* for 10 min at 4°C. The supernatant was allocated into tubes and stored frozen (-80 °C). Protein concentration of liver extracts was measured by Bradford Assay (Bio-Rad Laboratories, Hercules, CA).

AMPK Activity

Enzyme-linked Immunosorbent Assay (ELISA)

For determination of phosphorylated AMPK α level (AMPK activity), 30 µg of total protein was used and analyzed (AMPK α [pT 172] immunoassay kit, Invitrogen Corp., Camarillo, CA) according to the manufacture's protocol. Absorbance was recorded at 450 nm using a microplate reader (ThermoElectron, San Jose, CA). Final AMPK activity was calculated using standards supplied with the kit.

Western Blot Analysis

Tissue lysates (50 µg) were diluted in Laemmli sample buffer prior to SDS-polyacrylamide gel electrophoresis (SDS-PAGE). SDS-PAGE was performed using precast Bis-Tris 10% gradient polyacrylamide gels under reducing conditions (Bio-Rad Laboratories, Hercules, CA). Separated proteins were transferred to polyvinylidene fluoride membranes (Immobilon-P, Millipore Corp., Billerica, MA) using a semi-dry electro-blotting system (Bio-Rad Laboratories, Hercules, CA) for 1.5 h at 80 V at 4°C. Membranes were incubated in blocking buffer with 5% skim milk for 2 h and immunoblotted with phosphorylated AMPK α (Thr172) antibody (Cell Signaling Technology, Inc. Beverly, MA), AMPK α-1 antibody

(Millipore Corp., Billerica, MA), and α-tubulin antibody (Santa Cruz Biotechnology, Inc., Santa Cruz, CA) at 1:1000 dilution in 5% bovine serum albumin. Membranes were washed three times for 10 min with TBS (0.025M Tris-HCl [pH 7.6], 0.137 M NaCl) plus 1% milk and 0.1% Tween-20 (TBST). Membranes were then incubated with donkey anti-rabbit horseradish peroxidase conjugated secondary antibody (Amersham Biosciences, Piscataway, NY) diluted in TBST (1:10000) at room temperature for 1 h, and then washed for 15 min in TBST and three times for 5min in TBS. Signals were detected with ECL plus Western blotting detection reagent (Amersham Biosciences, Piscataway, NY), developed and scanned using Gel documentation system (Bio-Rad Laboratories, Hercules, CA). AMPK α-1 and α-tubulin signal detection was performed after stripping the membrane with stripping buffer (100 mM 2-Mercaptoethanol, 2% SDS, 62.5 mM Tris-HCl pH 6.7). Densitometry was used to quantify band intensities for phosphorylated AMPK α, AMPK α-1 and α-tubulin. Data are expressed as the ratio of phosphorylated AMPK α to AMPK α-1 intensity.

Statistical Analysis

All data were verified to meet assumptions of normality and homogeneity of variance. Results were analyzed by 2-way ANOVA using PROC MIXED procedure of SAS 9.2 (SAS Institute Inc., Cary, NC). The fixed factors were egg size and developmental age. The statistical model used was $Y_{ijk} = \mu + S_i + T_j + (ST)_{ij} + \varepsilon_{ijk}$, where Y_{ijk} is kth observation from the ith size at the jth developmental age, μ is the grand mean, S_i is the effect of ith size, T_j is the effect of jth developmental age, $(ST)_{ij}$ is the interaction between size and developmental age, and ε_{ijk} is the error term. Where the interaction was not significant, the main effect of the individual factor was compared. Means were compared by Tukey-Kramer multiple comparison test, and a probability of $P < 0.05$ was considered statistically significant.

RESULTS

Embryo Growth

Prior to set, absolute weights of yolk and albumen (dry matter basis) in large eggs were heavier ($P < 0.01$) than those in small eggs (**Table 3.1**). And, the dry yolk to albumen ratio was greater in large compared to small eggs ($P < 0.0001$). Fresh embryo weight was greater ($P < 0.05$) for large eggs from e17 onwards (**Figure 3.1**). Thus, chicks from large eggs were 29.9% heavier ($P < 0.01$) compared to chicks from small eggs on posthatch d1.

Albumen and Yolk Carbohydrates

In albumen, glucose and mannose contents prior to set were similar (25 mg/g dry weight) and ~500-fold higher compared to fucose (**Figure 3.2 a, b, c**). The glucose content of albumen, but not mannose and fucose, decreased dramatically by e11 (~1 mg/g). Yolk glucose concentration did not change in large eggs from e11 to posthatch compared to the initial value (at set). However, surprisingly, glucose concentration increased from e17 to posthatch day 1 in yolk of small eggs, and these levels were greater than in large eggs at e17, e20 and posthatch d1 ($P < 0.05$). Yolk mannose content did not differ between small and large eggs during most time points measured except on e20. Moreover, yolk mannose content did not change much overall during later development.

Table 3.1: Initial weights of egg components[1]

Egg size	Fresh egg wt (g)[2]	Dry egg content/fresh egg (%)	Dry yolk wt (g)	Dry albumen wt (g)	Dry yolk/albumen
Large	69.0 ± 1.86**	22.7 ± 1.39*	10.8 ± 0.84**	4.7 ± 0.39**	2.3 ± 0.32**
Small	53.2 ± 1.04	21.6 ± 0.44	7.1 ± 0.35	4.3 ± 0.24	1.7 ± 0.13

[1]Values are expressed as means ± SD.
[2] *$P < 0.05$, ** $P < 0.01$

Yolk Fatty Acid Composition

The proportions of palmitic and stearic acids of all fatty acids in yolk remained relatively constant during development for both egg sizes (**Table 3.2**). However, palmitic and palmitoleic acids accounted for a higher ($P < 0.0001$) proportion of yolk fatty acids in small compared large eggs throughout development whereas the proportions of linoleic and linolenic acids were 9% ($P = 0.0002$) and 22% ($P < 0.0001$) higher in yolk from large eggs. Lastly, arachidonic acid represented a greater ($P < 0.05$) proportion of total fatty acids in large eggs during later development compared to that in small eggs.

Liver AMPK Activity and Phosphorylation State

For both sizes of eggs, AMPK activity (phospho-AMPK α by ELISA) was highest ($P < 0.0001$) in liver of e14 embryos (**Figure 3.3**). There was a main effect due to egg size for liver AMPK activity ($P < 0.05$). AMPK α phosphorylation state (Western blot analysis) tended (P = 0.12) to differ across stages of development but did not differ between egg sizes (**Figure 3.4**, **3.5**).

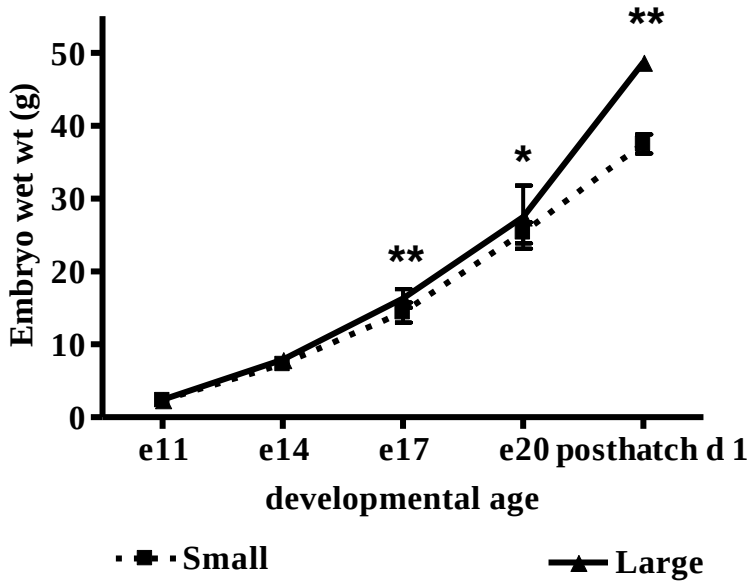

Figure 3.1: Fresh embryo weights of small (53.2 ± 1.04 g) and large (69.0 ± 1.86 g) eggs on e11, e14, e17, e 20 and post hatch day 1. Values on the figure were presented as mean ± SD, n = 4-10, *$P < 0.05$, ** $P < 0.01$.

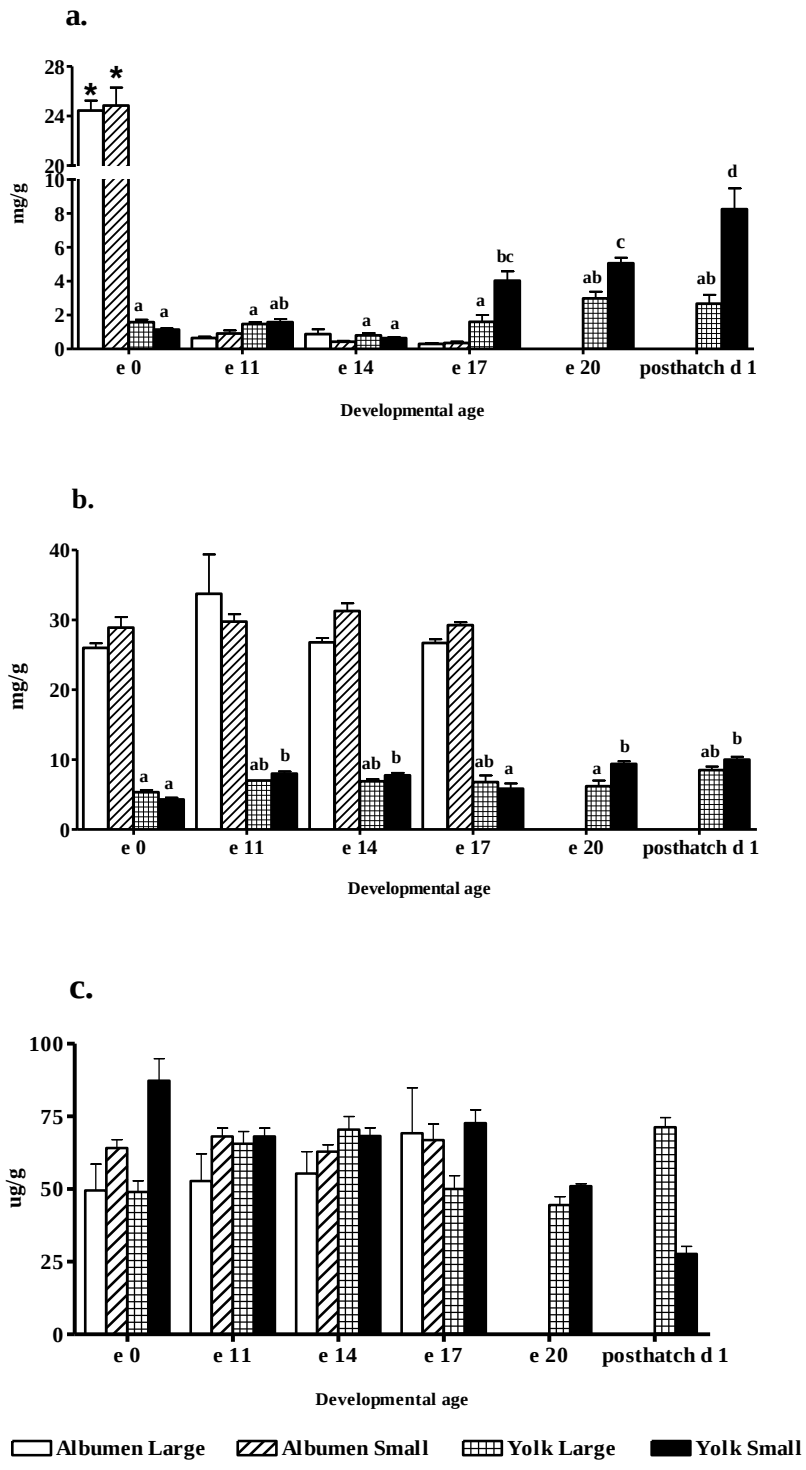

Figure 3.2: Initial and developmental changes in glucose (a), mannose (b) and fucose (c) content in dry yolk and albumen of small (53.2 ± 1.04 g) and large (69.0 ± 1.86 g) eggs. Each bar represents the average of ten eggs and values are expressed as the mean ± SEM. Bars bearing different letters differ ($P < 0.05$).

DISCUSSION

In the current study, the initial weights of yolk and albumen as well as the ratio of yolk to albumen were greater in large compared to small eggs. Thus, embryos in large eggs had access to a greater and more energy-dense substrate supply for development and growth. As would be expected, embryos from large eggs were heavier compared to those from small eggs from e17 onwards, which is consistent with our previous studies (Sunny and Bequette, 2010, 2011). Theoretically, embryos with the same genetic background, as in the current study, should have the same growth potential, irrespective of egg size. Thus, we hypothesized that the different nutrient environments of the two sizes of eggs would necessitate an *in ovo* energy-sensing mechanism(s) to coordinate embryo growth appropriately, and that AMPK serves this role in mediating changes in energy metabolism.

The initial carbohydrate amount in the albumen was about 240 mg at time of set. The content of mannose in albumen remained fairly constant, whereas glucose content dramatically decreased by e11 compared to the value at set. These observations suggest that the embryo selectively metabolizes glucose up until e11 while mannose metabolism predominates up until hatch. Furthermore, this higher dependence on glucose metabolism for energy expenditures early in development is consistent with previous observations of high rates of glycolysis during this period (Kucera et al., 1984). It is important to note that although mannose is influential for the glycosylation of certain proteins in mammals (Freeze et al., 2010), mannose can be converted to fructose-6-phosphate for metabolism in liver cells (Alton et al., 1997).We observed higher yolk glucose concentration at later development, which was consistent with another study (Yadgary et al., 2010). Surprisingly, yolk glucose concentration was observed to be higher in small eggs on e17, e20 and posthatch day 1, which suggests greater gluconeogenesis than that in large eggs.

Yadgary et al., (2010) showed that carbohydrate synthesis in the yolk sac, and the amount of carbohydrate reached the peak by e19. Increased yolk glucose content provides available energy for chicken embryo during hatching and pipping. Fucose is a common component of glycans and glycolipids in nearly all species. Through a nucletotide-activated form, GDP-fucose is essential in the construction of fucosylated oligosaccharides and can also be transformed from GDP-mannose (Becker and Lowe, 2003).The concentration of fucose in the yolk and albumen in our current study did not change during development. This phenomenon is not surprising because fucose-containing glycan has important roles in blood transfusion reactions and numerous ontogenic events (Becker and Lowe, 2003). The embryo must maintain a constant concentration of fucose for the high demand of embryogenesis during development.

The proportions of linoleic, linolenic, and arachidonic acid in total fatty acids were higher in the yolk of large egg at set, and thus development of the embryos in large eggs was aided by a greater supply of essential fatty acids (EFA). The greater absolute and relative availability of these three EFAs in the yolk of large eggs may allow for optimal embryonic growth and hatchability.

We observed higher liver AMPK activity from e11 to post-hatch day 1 in large egg embryos. The higher AMPK activity in liver of the large egg embryos may serve to enhance activity of pathways that generate energy to fuel their higher rate of growth during the later stages of development compared to the small egg embryos. This view is in agreement with our previous observations (Sunny and Bequette, 2010) where blood amino acid (glycine, glutamine, valine, leucine, isoleucine, threonine, arginine and tyrosine) concentrations were higher in large embryos on e16 and e18, suggesting a greater availability of amino acids for the higher rates of tissue protein synthesis needed to support this increased growth rate. Furthermore, by e20, the

large egg embryos had metabolized a larger (+6.2 % more) proportion of their original yolk weight as compared to small egg embryos. The higher yolk glucose content in the small eggs may indicate greater gluconeogenesis at the last several days of development. This again demonstrated higher AMPK activity in large egg embryos may suppress the energy-consuming pathways, which result in a lower glucose concentration in the yolk of large eggs.

Liver AMPK activity was at its highest on e14 in embryos from both size eggs. Similarly, AMPK activity was found to be highest in liver of chicken embryos on e16 (Proszkowiec-Weglarz and Richards, 2009). That study measured AMPK activity on e12, e16, e20 and post-hatch day 1, whereas in our study activity was measured on e11, 14, e17, e20 and post-hatch day 1, hence, giving a better resolution of AMPK activity during later development. Overall, the high liver AMPK activity from e12 to e20 reflects the period of embryo development when growth rate is highest and thus when energy demands are greatest (Sato et al., 2006; Moran, 2007).

AMPK activity as determined by Western blot analysis was expressed as the ratio of phospho-AMPK α to AMPK α-1 band intensity whereas the ELISA method measures phospho-AMPK α (Thr172) amount. Studies have shown that chicken liver preferentially expresses the AMPK α-1 subunit (Proszkowiec-Weglarz et al., 2006), unlike mammals which express both α-1 and α-2 subunits that contribute roughly equally to total AMPK activity in liver (Woods et al., 1996). Therefore, the AMPK α-1 antibody was preferred instead of AMPK α (α-1 and α-2) since the former is 94% homologous between mammals and chickens (Proszkowiec-Weglarz and Richards, 2009), and thus is the most suitable commercial product available. Western blot analysis of AMPK phosphorylation state followed a similar pattern (peaking between e12 and

e20) to that of the ELISA results; however, larger within group variation for the Western blot analysis precluded detection of statistical differences.

This study is the first to link embryonic liver AMPK activity with different nutrient compositions of broiler breeder eggs. Further studies are required to investigate whether specific substrates link AMPK activity and nutrient utilization *in ovo*, and the metabolic mechanisms that underlie coordination of egg nutrient use during embryo development.

Table 3.2: Fatty acid composition in the yolk at set (e0), and from e11 to posthatch day 1 of development[1]

Fatty acid	size	e 0	e 11	e 14	e 17	e 20	Post hatch day 1	SEM	*P* value	
									time effect[2]	size effect
Palmitic acid	small	23.0^{ab}	24.4^{ab}	23.4^{ab}	23.9^{ab}	26.3^{b}	24.6^{ab}	0.22	NS[3]	<0.0001
C16:0	large	21.8^{a}	22.6^{a}	21.4^{a}	22.9^{a}	21.5^{a}	21.6^{a}	0.35		
Palmitoleic acid	small	3.6^{ab}	3.7^{a}	3.3^{abc}	3.2^{abc}	3.2^{abc}	2.6^{abc}	0.09	0.0203	0.0005
C16:1 n-7	large	2.8^{abc}	3.1^{abc}	2.7^{abc}	3.0^{abc}	2.4^{bc}	2.3^{c}	0.13		
Stearic acid	small	6.5	6.5	6.3	6.3	6.4	6.0	0.10	NS	NS
C18:0	large	6.4	6.6	6.3	6.0	6.5	6.2	0.11		
Oleic acid	small	37.2^{a}	33.4^{ab}	37.0^{ab}	35.9^{ab}	29.6^{b}	39.1^{a}	0.42	0.0097	NS
C18:1 n-9	large	37.0^{ab}	33.2^{ab}	36.5^{ab}	36.3^{ab}	35.7^{ab}	36.3^{ab}	0.94		
Linoleic acid	small	16.2^{a}	19.0^{abc}	18.3^{ab}	19.2^{abc}	22.5^{c}	20.0^{abc}	0.30	<0.0001	0.0002
C18:2 n-6	large	19.0^{abc}	21.4^{bc}	20.9^{bc}	20.6^{bc}	21.4^{bc}	22.6^{c}	0.49		
Linolenic acid	small	0.39^{ab}	0.37^{ab}	0.39^{ab}	0.37^{ab}	0.39^{ab}	0.24^{b}	0.01	0.0186	<0.0001
C18:3 n-3	large	0.43^{a}	0.48^{a}	0.48^{a}	0.43^{a}	0.41^{a}	0.39^{ab}	0.01		
Arachidonic acid	small	12.4^{a}	12.7^{a}	11.4^{a}	11.2^{a}	11.5^{a}	7.5^{b}	0.23	<0.0001	0.0414
C20:4 n-6	large	12.7^{a}	12.6^{a}	11.7^{a}	10.8	12.0^{a}	10.6^{a}	0.36		

[1] Results are presented as percentages of all fatty acids measured.
[2] Time effect refers to day of incubation effect.
[3] NS = Not significantly different
Values within rows bearing different superscript letters differ ($P < 0.05$).

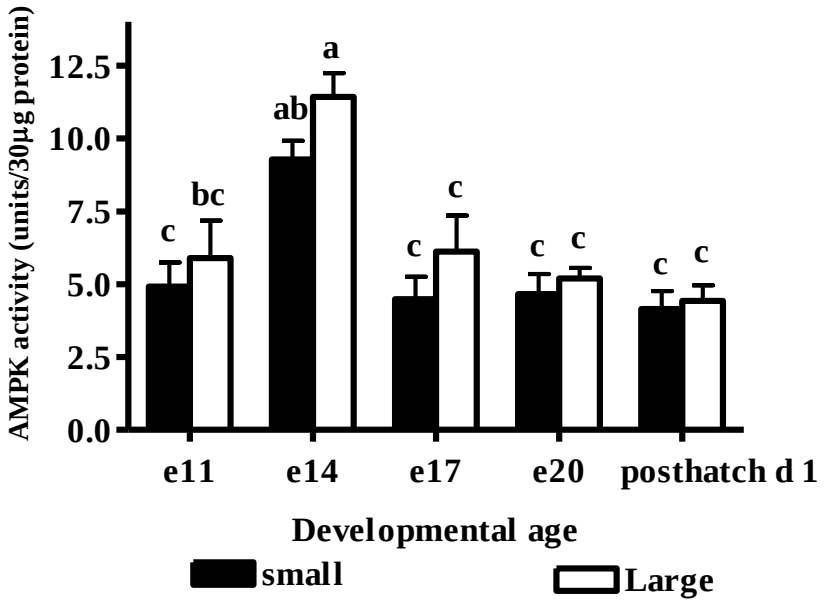

Figure 3.3: AMPK activity in liver of small and large egg embryos determined by ELSIA. Bar values (n = 4) are expressed as the mean ± SEM of phospho-AMPK α level. Bars bearing different letters differ ($P < 0.05$).

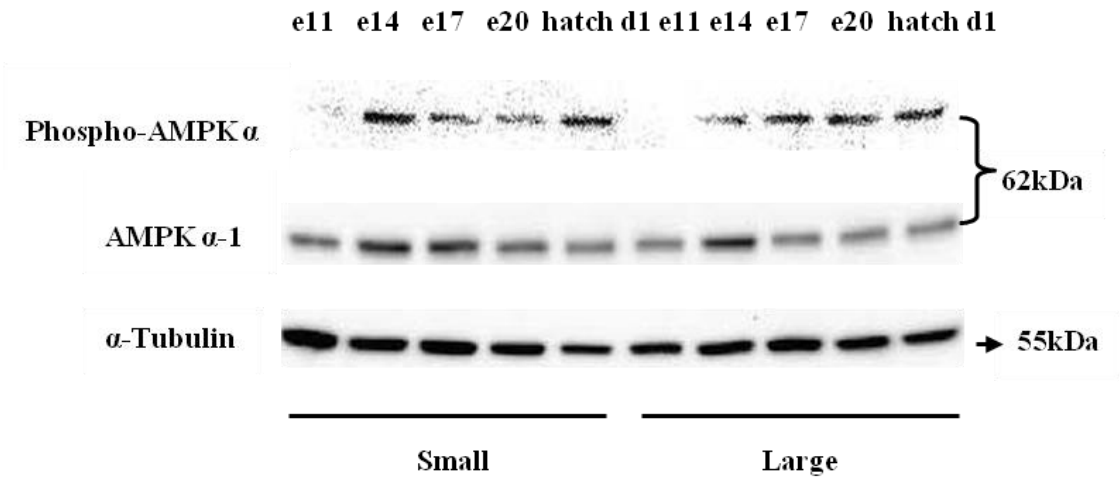

Figure 3.4: Representative Western blot of phospho-AMPK α, AMPK α-1, and α-tubulin in liver of small and large egg embryos.

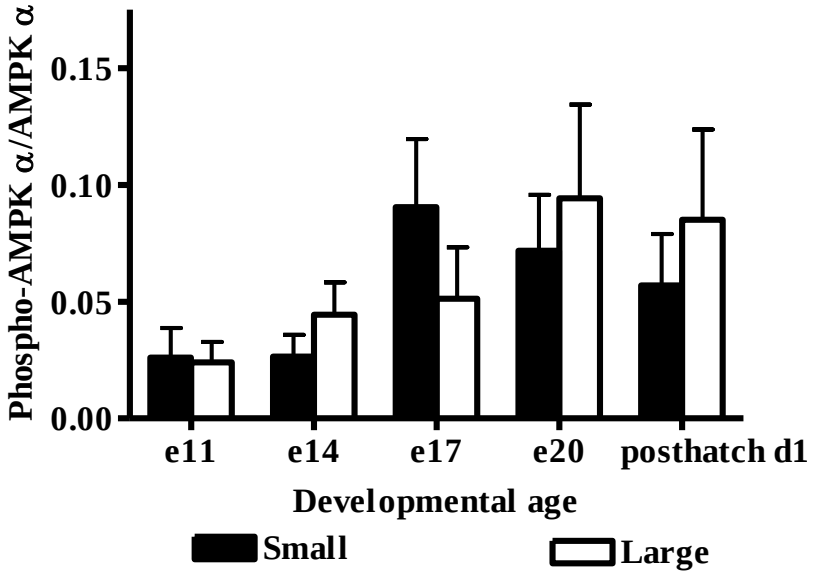

Figure 3.5: Quantitative results from Western blots. Bar values (n = 4) were expressed as the mean ± SEM of phospho-AMPK α intensity to AMPK α-1 intensity ratio.

CHAPTER 4: EXPERIMENT 2

METABOLOMIC PROFILING IN DEVELOPING CHICKEN EMBRYOS AND POSTHATCH CHICKS REVEALS METABOLIC DIFFERENCES[1,2,3]

[1] Q. Hu, U. Agarwal, and B. J. Bequette, 2013. Investigation of metabolic adaptation in developing chicken embryo and posthatch chicks by blood metabolomics. FASEB J. 27:1037.5

[2] Q. Hu, U. Agarwal, and B. J. Bequette. 2012. Metabolomic profiling of the liver in developing chicken embryos and posthatch chicks reveals unique metabolic differences. J Anim Sci., 2012. Vol. 90 (Suppl. 3):178

[3] Presented in part at the 8th Annual International Meeting of the Metabolomics Society, Washington D.C., 2012

Abstract

The aim of this study was to apply a metabolomic profiling approach to determine the influences of breeder age (32 wk *vs* 51 wk-old hens) and egg size (small *vs* large) and composition on developmental patterns of metabolism in embryos and posthatch chicks. Results showed that the proportions of palmitic and palmitoleic acids in the yolk of eggs from 32 wk-old hens were higher than those from 51 wk-old hens prior to set and throughout development in the residual yolk. Oleic and linolenic acids accounted for a higher proportion of yolk fatty acids in eggs from 51 wk-old hens at each developmental age that was evaluated. Gas chromatography-Mass spectrometry (GC-MS) was employed to evaluate the metabolome of the liver and blood of embryos on embryonic (e) days e14, e17 and e20 and on posthatch day 1. Principal component analysis (PCA) revealed that e14 and e20 liver metabolites, and e14 blood metabolites formed two separate clusters corresponding to 32 wk and 51 wk-old hens. However, clear separation of liver and blood metabolites was not observed in embryos from small *vs* large eggs at any developmental age. Pathway analysis on e14 and e20 liver metabolites in embryos from two ages of hens featured differences in branched-chain amino acid (BCAA), glycine, serine and threonine metabolisms ($P < 0.05$). Moreover, using PCA and hierarchical clustering analysis (HCA), it was observed that liver metabolites in embryos from either 32 wk or 51 wk-old hens formed four clusters in relation to the four developmental ages. The closer clusters corresponded to liver metabolites from e14, e17 and e20 embryos, whereas the posthatch day 1 liver metabolites clustered separately from the other clusters. The synthesis and degradation of ketone bodies, and glycerolipid and glutathione metabolism were the unique pathways that significantly differed during development in embryos from 51 wk-old hens. Overall, this study represents the first application of a metabolomic profiling approach to globally detail embryo metabolism and to

systematically evaluate the influences of hen age and egg size on embryo metabolism and growth during later development. The results from this study indicate a number of implications regarding the influences of maternal age and nutrient environment on overall development of the chicken embryo and posthatch chick.

Key words: hen age, egg size, GC-MS, metabolomic profiling, embryo metabolism

Introduction

Greater embryo and posthatch mortality are associated with broiler chicks from small (< 55 g) compared to large eggs (65-70 g). Studies have shown that broiler breeder age influences subsequent embryo development and hatchability (Shanawany, 1984; O'Sullivan et al., 1991; Latour et al., 1996, 1998; Ulmer-Franco et al., 2010). Yolk deposition in the egg (Peebles et al., 2000) and egg size (Suarez et al., 1997) increase with the age of hen. However, hen age is not the only factor that contributes to egg size differences. Other contributors include nutritional status (hen diet), breed and physiological status of the hen (Surez et al., 1997; Mortola and Awam, 2010). Egg size is positively correlated with subsequent poult weight in both broiler chickens and turkeys (Reinhart and Moran, 1979; Shanawany, 1987). The average chick weight at hatch is approximately 68% of the initial egg weight (Shanawany, 1987). The proportion of egg nutrient components, however, does not increase in proportion to egg weight. A study in turkeys found that by 24 wks of age, egg weight increased by about 11% compared to eggs laid at the onset of the lay period (Reidy et al., 1994), whereas the increases in yolk and albumen weight were 21% and 7% respectively. The yolk to albumen ratio was found to be higher in eggs from older hens compared to eggs from younger hens (Shanawany, 1984; Wilson, 1991; Applegate and Lilburn,

1996). Further, the smaller eggs laid in the clutch have a greater proportion of yolk than the larger eggs in the clutch from the same hens (Vieira and Moran, 1998).

Embryos from young breeders are associated with inefficient yolk lipid mobilization, transport and metabolism (Noble et al., 1986; Yafei and Noble, 1990). In addition, McNaughton et al., (1978) reported a higher mortality rate (2.4%) during 8 wks of growth in chicks from 29 wk vs 58 wk-old broiler breeders. This higher mortality rate occurred in the poults hatched from small eggs (47-54 g) by young hens (29 wk). This may reflect the less developed physiological systems of younger hens. In contrast, embryos from very old breeders have less hepatic and cardiac glycogen stores. Plasma glucose and thyroxine (T_4) concentrations are lower in embryos from old hens (Christensen et al., 1996). To date, there have been few studies that have investigated the independent influences of hen age and egg size (Shanawany, 1984; Applegate and Lilburn, 1996; Ulmer-Franco et al., 2010) on embryo metabolism, growth and physiology. Small eggs from young hens were used in most studies which might result in confounded effects of maternal age and egg size.

Metabolomics is an emerging field that uses diverse high-throughput analytical platforms, such as NMR, LC-MS/MS, GC-MS to provide an unbiased qualitative and quantitative assessment of the complete set of metabolites produced by an organism at a certain physiological state. Compared to other 'omics' approaches, metabolomics has numerous benefits. For instance, it reflects instantly the system perturbations in the metabolome that can be related to biochemical and phenotypic changes in the system (Dunn et al., 2011). Metabolomics has offered new perspectives in the animal science field, allowing scientists to investigate the metabolic pathway network changes in response to diet, physiological state, and disease to name a few. Thus far, the number of studies that have used metabolomic profiling approaches to

address questions of animal nutrition and production are still relatively few. With limited applications in pig and dairy cow studies, there is still no report about the utilization of metabolomic profiling in the chickens. Hence, in this study, we hypothesized that hen age and egg size would influence embryo metabolism, which may ultimately lead to differences in development and physiology of the embryo and posthatch chick.

Materials and Methods

Egg Incubation and Sample Collection

The experimental protocol (R-13-32) was approved by the Animal Care and Use Committee of the University of Marylan.

Fertile eggs from broiler breeders of different ages (Exp. 1: 32 wk, n = 60 *vs* 51 wk, n = 60, same egg weight, 63.2 ± 1.1 g,) and of two sizes laid by 45 wk old breeders (Exp. 2: 55.8 ± 1.2 g, n = 60 *vs* 67.7 ± 1.1 g, n = 60) were acquired from Perdue Farms, Inc (Salisbury, MD). Ten eggs from each group were randomly selected for measurements of initial egg composition. The remaining eggs were incubated under the standard condition of 65% relative humidity and 37.5°C. On embryonic (e) day 9, eggs were candled and undeveloped eggs removed. On e11, e14, e17, e20 and post-hatch day 1, a hole was made into the large end (air cell) of the egg with scissors, the crown removed, and whole egg contents were carefully transferred to a petri-dish on ice. The vitelline vessels (artery and vein) were exposed on the top and clearly visible. Embryos were bled by making a nick across the vitelline vessels and blood was drawn using a glass pasture pipette. Blood was transferred to a 600-µL blood collection tube with a solid lithium heparin ring (Multivette®, Sarstedt AG & Co., Nuembrecht, Germany). The weights of embryos, and residual yolk and albumen were recorded, and the whole liver immediately wrapped in

aluminum foil before plunging into liquid nitrogen. Livers and blood samples were then stored at -80°C. Yolk and albumen were stored at -20°C for later analysis.

Fatty Acid Composition Analysis

For determination of individual fatty acid concentrations, frozen yolk was lyophilized to dryness (FreeZone Bulk Tray Dryer, Labconco, Kansas city, MO) and later pulverized into a fine powder for analysis. To a known weight of dry yolk (50 mg), was added a known amount of a [U-^{13}C] fatty acid mixture (^{13}C labeled algal fatty acids, Cambridge Isotope Laboratories, Inc., Andover, MA). Fatty acid methyl esters (FAME) were prepared using the method described by Christie, (1982) and Kadegowda et al., (2008), with modified procedures for tissue samples. Briefly, 0.5 mL of 0.5 *N* NaOH/methanol was added to each sample and incubated in a 50°C water bath for 30 min. FAME were formed by adding 6.5 mL of 1.2 *N* H_2SO_4 in methanol and incubated in the dark at room temperature for 20 h. After extraction with hexane, FAME were analyzed on a gas chromatography-mass spectrometer (GC-MS, HP 6890 coupled with an HP 5973 Mass Selective Detector) equipped with a 60m × 0.25mm × 0.25µm capillary column (DB-23, Agilent Technologies, Palo Alto, CA). The inlet temperature was maintained at 250°C. The GC oven temperature was: 130°C for 1 min, increased at 6.5°C per min to 170°C, increase 2.75°C per min to 215°C and held for 12 min, increased at 40°C per min to 230°C and held for 3 min. Ions corresponding to the unlabelled fatty acid (M) and the labeled fatty acid (M+n, where n is the number of carbons in the fatty acid) were monitored and recorded. Fatty acid concentrations were calculated by isotope dilution using a standard curve.

Untargeted Metabolomic Profiling

Sample Preparation

Blood and liver samples were processed according to Want et al., (2006), Pasikanti et al., (2008) and Kouremenos et al., (2010) with modifications. Briefly, two liver samples were pooled (60 mg), and to the sample was added a known weight of L-norleucine (200 µL, 1.0 mg/mL, freshly prepared and stored at 4°C, Tokyo Chemical Industry Co., Ltd, Tokyo, Japan). Samples were extracted with 1 mL of ice-cold mixture of distilled H_2O:CH_3OH:$CHCl_3$ (2:5:2, v/v/v) in an ice-bath using a hand held homogenizer (VWR PowerMax AHS 200, VWR International, Radnor, PA). The homogenates were centrifuged at 15,000 × *g* for 15 min at 4 °C, and the supernatant reduced to dryness under N_2 gas at room temperature. To the dried extract, 80 µL of methoxylamine hydrochloride (15 mg/mL, 98% purity, Sigma-Aldrich Co. LLC., St. Louis, MO) in pyridine and 80 µL of *N*,*O*-bis-(trimethylsilyl)trifluoroacetamide (BSTFA) containing 1% trimethylchlorosilane (TMCS, Supelco, Sigma-Aldrich Co. LLC) were added, and the samples were vigorously vortexed. Derivatization of metabolites was carried out by microwaving for 90 sec at 200 watts prior to GC separation and MS analysis.

For blood samples, a known weight of internal standard (50 µL of L-norleucine, 0.33 mg/mL) was added to a known weight (50 mg) of blood. Blood metabolites were extracted with 1 mL ice-cold methanol. Samples were gassed with N_2 and vortexed vigorously for 15 min, followed by centrifugation at 13,400 × *g* for 10 min at room temperature. The supernatant was carefully transferred to a v-vial and reduced to dryness under N_2 gas at room temperature. Derivatization of metabolites was carried out by adding 40 µL of methoxylamine hydrochloride (30 mg/mL, Sigma-Aldrich Co. LLC.) in pyridine and 40 µL of BSTFA (1% TMCS) (Supelco, Sigma-Aldrich Co. LLC), then the samples were sealed and vortexed vigorously. To expedite

derivatization, samples were microwaved for 90 sec at 200 Watts prior to GC separation and MS analysis.

GC-MS Analysis

The trimethylsilyl derivatives were separated by GC with a a 30m × 0.25mm × 0.25µm capillary column (HP 50+, J&W Scientific, Agilent Technologies, Palo Alto, CA). The front inlet temperature was maintained at 250°C. The initial GC oven temperature was 70°C for 5 min, increased at 5°C per min to 310°C and held for 5 min, and 40°C per min to 70°C and held for 5 min. The MS was operated in electron impact mode and analyte ions were monitored in full mode. ChemStation Data Analysis software (Version Rev.D.01.02; Agilent Technologies) was used for manual review of chromatograms and ion spectra and quantification of ion intensity. Representative ion areas of each compound were corrected by using the internal standard ion 158.0.

Metabolite Identification

Classification and identification of metabolites were performed using the NIST mass spectral library with search program (2008) and Agilent Fiehn GC/MS metabolomics RTL library (2008). Metabolites were confirmed by both retention time and mass spectra in the library. Match probability over 60% was considered to be the corresponding compound. Missing values were assumed to result from areas falling below the instrument detection limits.

Statistical Analysis

Embryo body, egg content, and egg shell weights, and fatty acid composition are expressed as means ± SD or mean ± SEM and analyzed by 2-way ANOVA using PROC MIXED procedure of SAS 9.2 (SAS Institute Inc., Cary, NC). For eggs of different sizes, the fixed factors were egg size and developmental age. The statistical model used was

$$Y_{ijk} = \mu + S_i + T_j + (ST)_{ij} + \varepsilon_{ijk},$$

where Y_{ijk} is the kth observation from the ith size at the jth developmental age, μ is the grand mean, S_i is the effect of ith size, T_j is the effect of jth developmental age, $(ST)_{ij}$ is the interaction between size and developmental age, and ε_{ijk} is the error term. For eggs of the same weight, but from different ages of hen, the fixed factors were maternal age and developmental age. The statistic model used was

$$Y_{ijk} = \mu + A_i + T_j + (AT)_{ij} + \varepsilon_{ijk},$$

where Y_{ijk} is kth observation from the ith hen age at the jth developmental age, μ is the grand mean, A_i is the effect of ith age, T_j is the effect of jth developmental age, $(AT)_{ij}$ is the interaction between maternal age and developmental age, and ε_{ijk} is the error term. Where the interaction was not significant, the main effects of the individual factor were compared. Means were compared by Tukey-Kramer multiple comparison test, and a probability of $P < 0.05$ was considered statistically significant.

Data mining and multivariate statistic analysis of metabolomics profiling data were performed using MetaboAnalyst 2.0 (http://www.metaboanalyst.ca) (Xia et al., 2009, 2011, 2012) and XCMS online (https://xcmsonline.scripps.edu/). The data were semi-quantitative, and fold changes were compared between groups. Data was first normalized by log transformation and scaled by Pareto Scaling. Transformed data within different hen age at each embryonic developmental age or within two egg sizes at each developmental age were compared using a Student's t-test. Principal component analysis (PCA) was employed to identify the relationships between classes of transformed data. A loading plot was constructed to show the variables (metabolites) responsible for the variation within the dataset and correlations among the individual metabolites corresponding to the first two principal components (PC1 and PC2).

Hierarchical clustering analysis (HCA) with Euclidean distances measures and Ward's linkage were performed to explore the presence of clustering patterns among all the samples. Identified metabolites were applied to MetaboAnalyst 2.0 to perform pathway analysis using the Kyoto Encyclopedia of Gene and Genome (KEGG) pathway for *Gallus gallus*.

Results

Embryo Growth

Initial yolk weight (dry matter basis) was heavier ($P < 0.01$) in eggs from 51 wk *vs* 32 wk-old hens whereas the albumen weight was heavier ($P < 0.05$) in eggs from 32 wk *vs* 51 wk-old hens (Exp. 1) (**Table 4.1**). And, the yolk to albumen ratio was higher ($P < 0.01$) in eggs from 51 wk-old hens. However, both embryo and liver weights did not differ between different age breeders throughout later development (**Figure 4.1 a, c)**.

For eggs of different sizes, but from the same age (45 wk) of hens (Exp. 2), the weights of yolk and albumen prior to set were heavier ($P < 0.01$) in large compared to small eggs (**Table 4.1**). The yolk to albumen ratio tended ($P = 0.067$) to be lower in the large eggs, and their embryo weight was greater from e20 through posthatch day 1. Liver weight differences followed the same pattern as embryo weight (**Figure 4.1 b, d**). At hatch, chick weight was 26.6% greater for large compared to those from small eggs.

Yolk Fatty Acid Composition

The proportions of both palmitic and palmitoleic acids in egg yolks from 32 wk-old hens were higher ($P < 0.01$) than those from 51 wk-old hens at set (e0) and this pattern remained throughout development (**Table 4.2**). However, oleic and linolenic acids accounted for a higher proportion ($P < 0.01$) of yolk fatty acids for eggs from 51 wk-old hens at each developmental age

that was monitored. For both ages of breeders, the rate of yolk utilization oleic acid was less at e20 and posthatch day 1 compared to the earlier developmental ages. Relatively more yolk linoleic acid was mobilized for embryo use closer to hatch ($P < 0.01$).

The pattern of yolk fatty acids in small and large eggs from 45 wk-old hens did not differ throughout development (**Table 4.3**). The proportion of yolk palmitic acid was highest in both sizes of eggs on day 1 posthatch. In contrast, the proportions of myristic, myristoleic, oleic, stearic, and linolenic acids were highest on e20 and posthatch day 1 compared to e0 and earlier developmental ages (e11- e17).

Liver Metabolic Profiling

Hen age (32 wk vs 51 wk)

Based on PCA analysis, global liver metabolites clustered separately for embryos from 32 wk *vs* 51 wk-old hens on both e14 and e20 (**Figure 4.2a, Figure 4.3a**). Data were visualized by constructing PC scores, where each point on the plot represented a single sample (pooled by two original samples). Liver samples from e11 embryos were not included in this analysis due to insufficient replication. For e14 liver metabolites, PC1 and PC2 represented 45 and 21.1% of variation, respectively. The first two PC explained 68.5% of the total variance within the data for e20 embryos. However, we did not observe group separation for liver metabolites on e17 and posthatch day 1 (**Appendix a, b**).

Loading plots (**Figures 4.2 b and 4.3 b**) showed the individual liver metabolites responsible for the variation of the first two eigenvalues (PC1 and PC2). Metabolites with the similar distance from 0 and with the same direction are positively correlated, and those in the opposite direction are negatively correlated. For e14 liver samples, palmitic, stearic and linoleic acids, the BCAA, phenylalanine, glutamine, glycerol and lactate were positively correlated with

each other for PC1. However, these metabolites were negatively correlated with succinate, glycine, threonine and oleic acid. For PC2, a contrast appears to exist between succinate, threonine, aspartate and the BCAA as well as for β-hydroxybutyric acid. Oleic acid appears to be an important metabolite influencing the separation for both PC. For e20 liver metabolites, the first PC highlights the contrast between alanine, aspartate, uridine and several fatty acids. The second PC shows the contrast between glycine, threonine, succinate, malate, cholesterol and glycerol as well as pyrimidine.

A widely used pattern recognition method, partial least squares regression discriminant analysis (PLS-DA), was carried out to construct and validate the classification model. The results from PLS-DA on e14 and e20 liver metabolites showed clearly distinct groups in clustering between eggs derived from 32 wk and 51 wk-old hens (**Figure 4.4 a, b**).

Pathway analysis showed that 16 metabolic pathways in e14 embryo livers and nine pathways in e20 embryo livers were different for embryos from 32 wk *vs* 51 wk-old hens ($P < 0.05$) (**Tables 4.4** and **4.5**). Metabolic pathways that differed in e14 and e20 embryos mainly involve amino acid and glucose metabolism. Although some of the fatty acids, i.e., palmitic, oleic and linoleic acids, contribute to the differences in embryos from 32 wk *vs* 51 wk- old hens shown on the loading plots, they were not involved in the metabolic pathways that were significantly different between the two ages of breeders in the current study.

Egg size (small vs large)

PCA results did not show group separation in liver metabolites of embryos from small *vs* large eggs on e14, e17, e20 and posthatch day 1(Appendix **c, d, e, f**).

Table 4.1: Initial weights of eggs and components[1]

	Hen age (wk)	Fresh egg wt (g)[2]	Dry egg content/fresh egg (%)	Dry yolk wt (g)	Dry albumen wt (g)	Dry yolk/albumen	Dry egg shell/ fresh egg (%)
Exp. 1	32	62.9 ± 1.2	21.8 ± 0.5	8.8 ± 0.6**	4.9 ± 0.4*	1.8 ± 0.3**	8.8 ± 0.4
	51	62.8 ± 1.0	22.6 ± 1.0	9.6 ± 0.7	4.5 ± 0.3	2.1 ± 0.2	8.7 ± 0.6
Exp. 2	45	55.8 ± 1.2**	23.2 ± 1.0	9.1 ± 0.6**	3.9 ± 0.3**	2.4 ± 0.3	9.1 ± 0.4
	45	67.7 ± 1.1	22.7 ± 0.5	10.4 ± 0.6	5.0 ± 0.4	2.1 ± 0.3	9.0 ± 0.5

[1]Values are expressed as means ± SD, comparisons were made within Exp. 1, 32 wk (n = 60) *vs* 51 wk (n = 60); Exp. 2, small (n = 60) *vs* large (n = 60) eggs.
[2] $*P < 0.05$, $** P < 0.01$

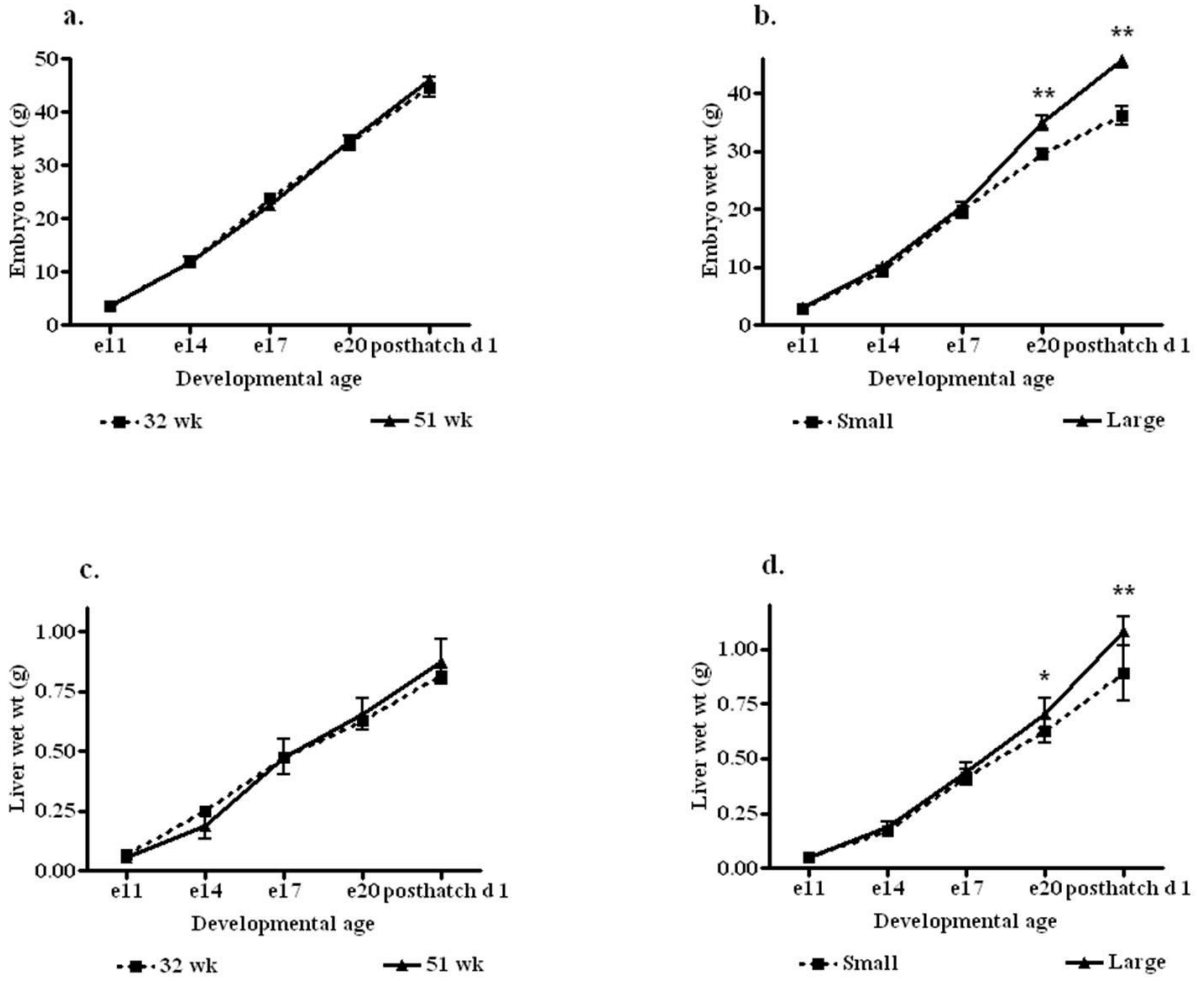

Figure 4.1: Embryo weights from e11 to posthatch day 1. **a**. Embryo weights in eggs of the same size but from different age hens (32 wk *vs* 51 wk); **b**. Embryo weights in large *vs* small eggs from 45 wk- old hens (Exp. 2); **c**. Liver weights of embryos from the same size eggs but different ages of hens (32 wk *vs* 51 wk; Exp. 1); **d**. Liver weights of embryos from small *vs* large eggs from 45 wk- old hens (Exp. 2). Values on the figures were presented as means ± SD, n = 8-10 at each developmental age, * $P < 0.05$, ** $P < 0.01$.

Table 4.2: Yolk fatty acid composition of eggs from 32 wk and 51 wk-old hens at set (e 0), and on e11 to posthatch day 1 of development (Exp. 1)[1]

Fatty acid	Hen age	e0	e11	e14	e17	e20	Post hatch day 1	SEM	*P* value[2]	
									Time effect[3]	Hen age effect
Myristic acid	32 wk	0.20^{a}	0.22^{ac}	0.20^{ad}	0.29^{bc}	0.27^{bc}	0.36^{bc}	0.01	<0.0001	NS
C14:0	51 wk	0.19^{a}	0.23^{ac}	0.20^{ad}	0.26^{bcd}	0.26^{bcd}	0.32^{bc}	0.009		
Myristoleic acid	32 wk	0.02^{a}	0.03^{ae}	0.02^{a}	0.06^{cde}	0.06^{cde}	0.09^{b}	0.004	<0.0001	NS
C14:1 n-9	51 wk	0.02^{a}	0.04^{ac}	0.02^{a}	0.06^{cde}	0.06^{cde}	0.08^{bd}	0.004		
Palmitic acid	32 wk	22.7^{a}	23.2^{a}	22.4^{a}	22.2^{a}	22.0^{ab}	21.4^{ab}	0.17	0.001	0.0005
C16:0	51 wk	21.4^{ab}	21.5^{ab}	22.6^{a}	21.6^{ab}	20.9^{ab}	20.1^{b}	0.23		
Palmitoleic acid	32 wk	2.6	2.8	2.4	2.3	2.6	2.5	0.07	NS	0.003
C16:1 n-7	51 wk	2.1	2.4	2.5	2.1	2.2	2	0.07		
Stearic acid	32 wk	7.0	6.8	6.8	7.1	6.7	7.2	0.08	NS	NS
C18:0	51 wk	6.9	6.8	6.9	7.2	6.9	6.9	0.1		
Oleic acid	32 wk	57.3^{a}	57.5^{ac}	58.3^{ab}	57.5^{ac}	59.4^{ab}	59.8^{ab}	0.28	0.0002	0.004
C18:1 n-9	51 wk	59.1^{ab}	59.3^{ab}	57.8^{ac}	58.7^{ab}	60.9^{bc}	61.1^{b}	0.33		
Linoleic acid	32 wk	10.0^{ab}	9.3^{ab}	9.6^{ab}	10.3^{a}	8.8^{ab}	8.4^{b}	0.18	0.003	NS
C18:2 n-6	51 wk	10.0^{ab}	9.3^{ab}	9.8^{ab}	9.8^{ab}	8.6^{ab}	9.2^{ab}	0.18		
Linolenic acid	32 wk	0.20^{a}	0.21^{ab}	0.20^{a}	0.26^{ab}	0.20^{a}	0.22^{a}	0.008	NS	<0.0001
C18:3 n-3	51 wk	0.29^{b}	0.31^{b}	0.30^{b}	0.30^{b}	0.25^{ab}	0.31^{b}	0.006		

[a,b,c,d] Values within a row bearing different superscript letters differ ($P < 0.05$), NS = Not significantly different.
[1] Results are presented as percentages of all fatty acids measured.
[2] No interaction exists between hen age effect and time effect.
[3] Time effect refers to day of incubation effect.

Table 4.3: Yolk fatty acid composition of small *vs* large eggs (45 wk) at set (e 0), and on e11 to posthatch day 1 (Exp. 2)[1]

Fatty acid	size	e0	e11	e14	e17	e20[2]	Post hatch day 1	SEM	*P* value[3]	
									Time effect[4]	Size effect
Myristic acid	small	0.20[a]	0.23[a]	0.21[a]	0.24[a]	-	0.34[b]	0.009	<0.0001	NS
C14:0	large	0.19[a]	0.24[a]	0.18[a]	0.22[a]	0.25	0.34[b]	0.009		
Myristoleic acid	small	0.02[a]	0.04[a]	0.02[a]	0.03[a]	-	0.08[b]	0.003	<0.0001	NS
C14:1 n-9	large	0.02[a]	0.04[a]	0.02[a]	0.02[a]	0.05	0.08[b]	0.004		
Palmitic acid	small	22.2[ab]	22.2[a]	23.1[b]	22.4[ab]	-	20.6[a]	0.199	0.0003	NS
C16:0	large	22.5[b]	21.9[a]	21.8[ab]	21.9[ab]	21.5	20.4[a]	0.207		
Palmitoleic acid	small	2.3	2.5	2.6	2.5	-	1.9	0.076	NS	NS
C16:1 n-7	large	2.3	2.2	2.2	2.2	2.3	2.1	0.061		
Stearic acid	small	6.8[ab]	6.9[ab]	6.4[a]	6.8[ab]	-	7.4[b]	0.082	<0.0001	NS
C18:0	large	6.5[a]	7.5[b]	6.5[a]	6.6[a]	6.7	7.6[b]	0.096		
Oleic acid	small	59.6[ab]	57.7[ab]	57.7[b]	58.4[ab]	-	60.9[a]	0.308	0.0062	NS
C18:1 n-9	large	58.6[ab]	58.6[ab]	60.4[ab]	59.5[ab]	60.1	60.9[a]	0.321		
Linoleic acid	small	8.8	10.2	9.8	9.4	-	8.4	0.23	NS	NS
C18:2 n-6	large	9.7	9.3	8.6	9.3	8.9	8.4	0.183		
Linolenic acid	small	0.19[a]	0.26[b]	0.19[ab]	0.22[ab]	-	0.24[ab]	0.008	0.0072	NS
C18:3 n-3	large	0.20[ab]	0.23[ab]	0.22[ab]	0.22[ab]	0.21	0.24[ab]	0.006		

[a,b] Values within a row bearing different superscript letters differ ($P < 0.05$), NS = Not significantly different.
[1] Results are presented as percentages of all fatty acids measured.
[2] e20 yolk fatty acids from small eggs were not quantified due to the limited amount of internal standards.
[3]No interaction existed between hen age and time effects.
[4]Time effect refers to day of incubation effect.

Liver metabolism during development (e14-posthatch day 1)

PCA and HCA were performed on liver metabolites in embryos from 32 wk and 51 wk-old hens (Exp. 1) and from two egg sizes (45 wk-old hens, Exp. 2) to investigate shifts in embryo liver metabolism. The PCA results on liver metabolites of embryos from 32 wk-old hens revealed the presence of four clusters corresponding to each developmental age, with metabolite clusters on e17 and e20 overlapping (**Figure 4.5a**). The first two PC represented 73.1% of the total variation. Likewise, PCA results of embryo liver metabolites from 51 wk-old hens showed clear separation amongst the four developmental ages (**Figure 4.5b**). On the PCA score plot, 83.8% of the total variation was explained by the first two PC.

For small and large eggs from 45 wk-old hens, results indicated that for embryos from the small eggs, there were two clusters corresponding to e14 and e17 liver samples. However, the separations of e20 and posthatch day 1 livers were not evident (**Figure 4.6a**). The distinct separation of liver metabolites from large eggs corresponded to the four developmental ages which is clearly shown on the PCA score plot (**Figure 4.6b**).The results of HCA are graphically presented in **Figures 4.7- 4.10**. The dendrograms show the presence of different sub-clusters of individual samples and of different metabolites with various degrees of similarity. The levels of different metabolites (variable) with respect to developmental age are indicated with the color intensity change on the heat map. The individual samples or different metabolites with higher similarity are positioned together with shorter branch heights. The HCA in the current study shows four clusters corresponding to the four developmental ages for embryos from both 32 wk and 51 wk-old hens. Similarly, four clusters were formed for e14, e17, e20 and posthatch day 1 liver metabolites in embryos from large eggs derived from 45 wk-old hens. Although there were four clusters presented on the dendrogram for embryos from small eggs (45 wk-old hens), one

e20 sample did not cluster with the other e20 liver metabolite samples, which might indicate the existence of an outlier. Interestingly, the HCA revealed the presence of three clusters of metabolites for embryos from both 32 wk and 51 wk-old hens. One cluster of metabolites consisting of arachidonic acid, alanine, proline, serine and glucose showed a clear increase with embryo development whereas another cluster consisting of palmitic and stearic acids, and leucine, glutamine and succinate reflected a decrease with advancing developmental age. However, the clustering of liver metabolites in embryos from small and large eggs derived from 45 wk-old hens was not as distinct. To elucidate the metabolic pathways that shift in activity and to investigate whether hen age and egg size affect developmental metabolism, pathway analysis was performed on liver samples on e14, e17, e20 and posthatch day 1 from 32 wk and 51 wk-old hens (Exp. 1), and on small and large eggs from 45 wk-old hens (Exp. 2), respectively. For embryos from 32 wk-old hens, the metabolic pathways that were significantly different with advancing developmental age included amino acid metabolism ($P < 0.05$), in particular glycine, serine and threonine metabolism, and fatty acid biosynthesis, energy-related metabolism and nucleotide metabolism (**Table 4.6**). While the metabolic pathways that differed in embryo livers from 51 wk-old hens included the same categories of metabolism as those from 32 wk-old hens (**Table 4.7**), differences in several pathways were unique to embryos from 51 wk-old hens ($P < 0.05$), most notably synthesis and degradation of ketone bodies, and glycerolipid and glutathione metabolism.

The pathways that contributed to the developmental changes in metabolism of embryos from small and large eggs (45 wk-old hens) featured amino acid, fatty acid and energy-related metabolism ($P < 0.05$) (**Tables 4.8** and **4.9**). However, developmental shifts in steroid

biosynthesis, and glycerolipid, cysteine and methionine metabolism were unique to embryos from large eggs.

Blood Metabolic Profiling

Hen age (32 wk vs 51 wk)

PCA analysis of blood metabolites revealed group separation on e14 (**Figure 4.11a**) but not on e17, e20 nor posthatch day 1 (**Appendices g, h, i**). The first two PC for e14 blood samples explained 65.2% of the total variation. Loading plot results revealed a contrast between β-aminoisobutyric acid, aspartate, methionine, linoleic acid and β-hydroxybutyric acid as well as glycine for PC1 (**Figure 4.11b**). PC2 featured the contrast between BCAA and glycerol.

We further performed pathway analysis to identify the pathways that contributed to the differences in e14 embryo metabolism in eggs from 32 wk *vs* 51 wk-old hens (**Table 4.10**). These results indicated differences in BCAA and glycerolipid metabolism, and fatty acid biosynthesis and metabolism.

Egg size (Small vs Large)

PCA was applied to investigate whether the metabolism of embryos differed due to egg size. Separation of blood metabolites on e14, e17, e20 and posthatch day 1 from small *vs* large eggs was not observed (**Appendices j, k, l, m**).

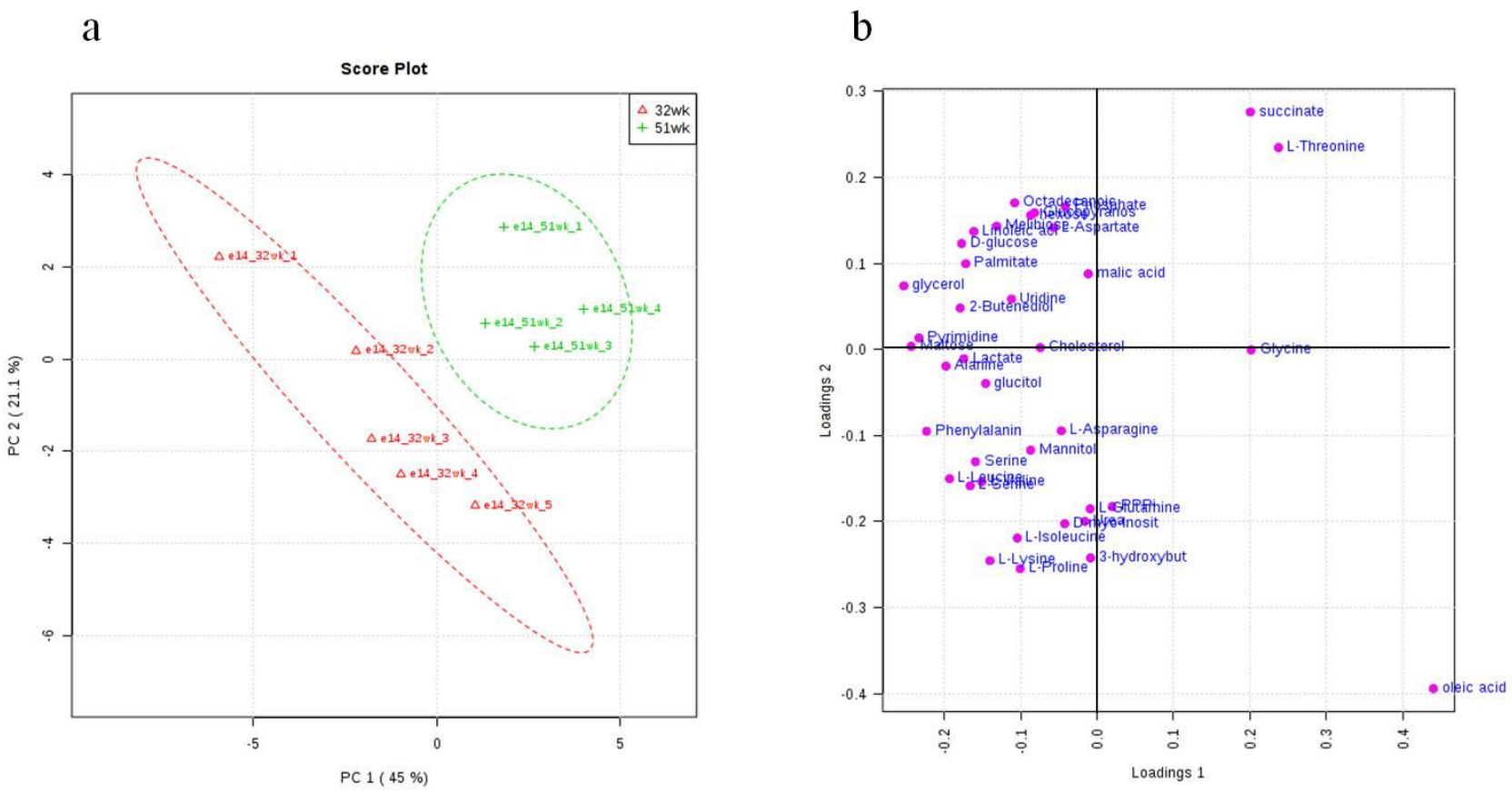

Figure 4.2 Principal component analysis (PCA) of e14 liver metabolomic profile (Exp. 1). **a.** The PCA score plot distinguishes the metabolic profiles of liver metabolites in eggs from 32 wk (Δ) *vs* 51 wk (+) old hens on e14. The first three characters represent the embryo developmental age (e14) followed by age (32 wk, 51 wk) and replicates (1-5 samples). **b.** Loading plot shows the correlations among individual liver metabolite of PC1 and PC2 (eigenvalues). Variables (metabolite) with the same distance from zero with similar positions are positively correlated. Those in the opposite direction are negatively correlated.

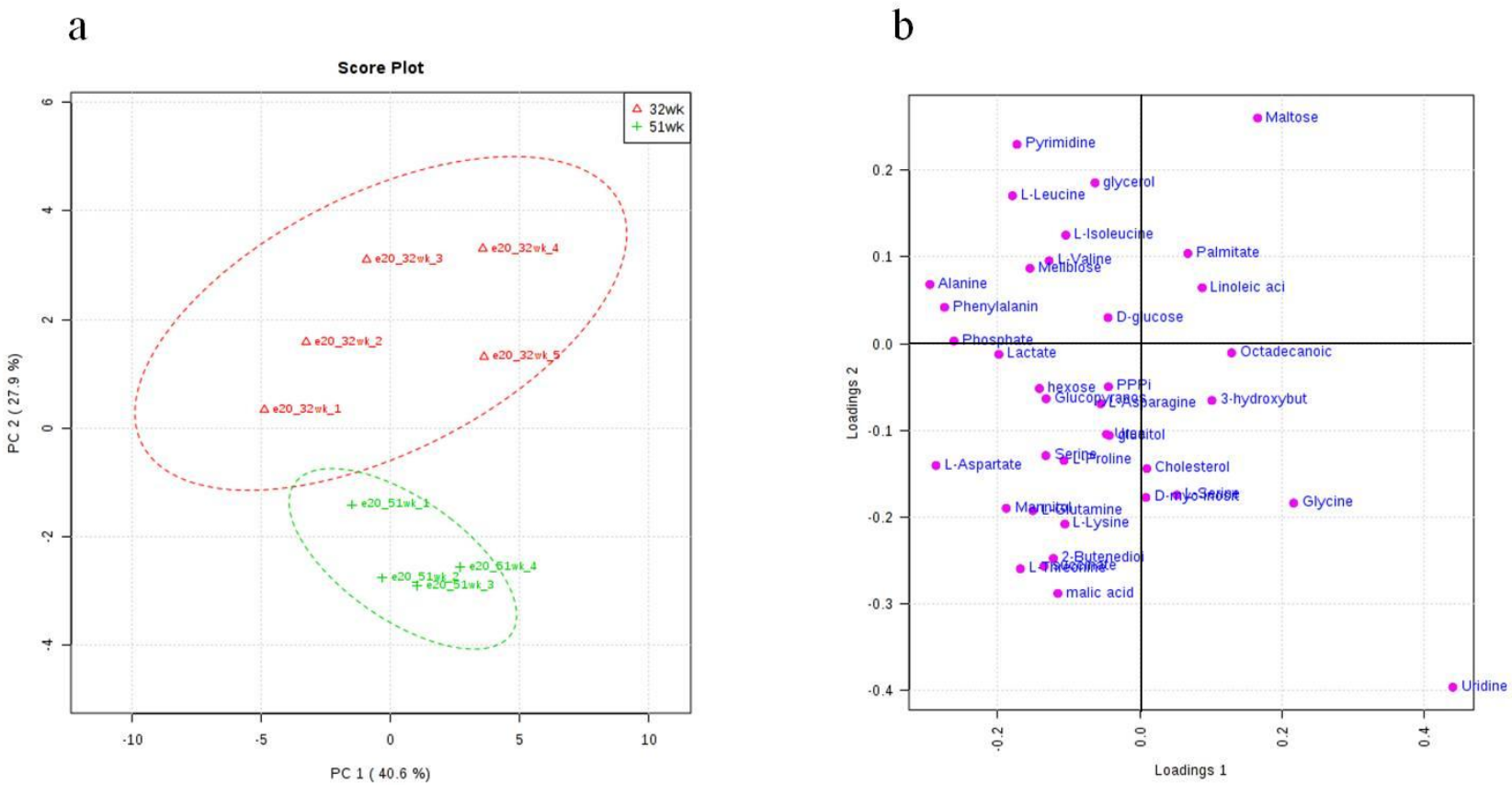

Figure 4.3 Principal component analysis (PCA) of e20 liver metabolomic profile (Exp. 1). **a.** The PCA score plot distinguishes the metabolic profiles of liver metabolites in eggs from 32 wk (Δ) *vs* 51 wk (+) old hens on e20. The first three characters represent the embryo developmental age (e14) followed by age (32 wk, 51 wk) and replicates (1-5 samples). **b.** Loading plot shows the correlations among individual liver metabolite of PC1 and PC2 (eigenvalues). Variables (metabolite) with the same distance from zero with similar positions are positively correlated. Those in the opposite direction are negatively correlated.

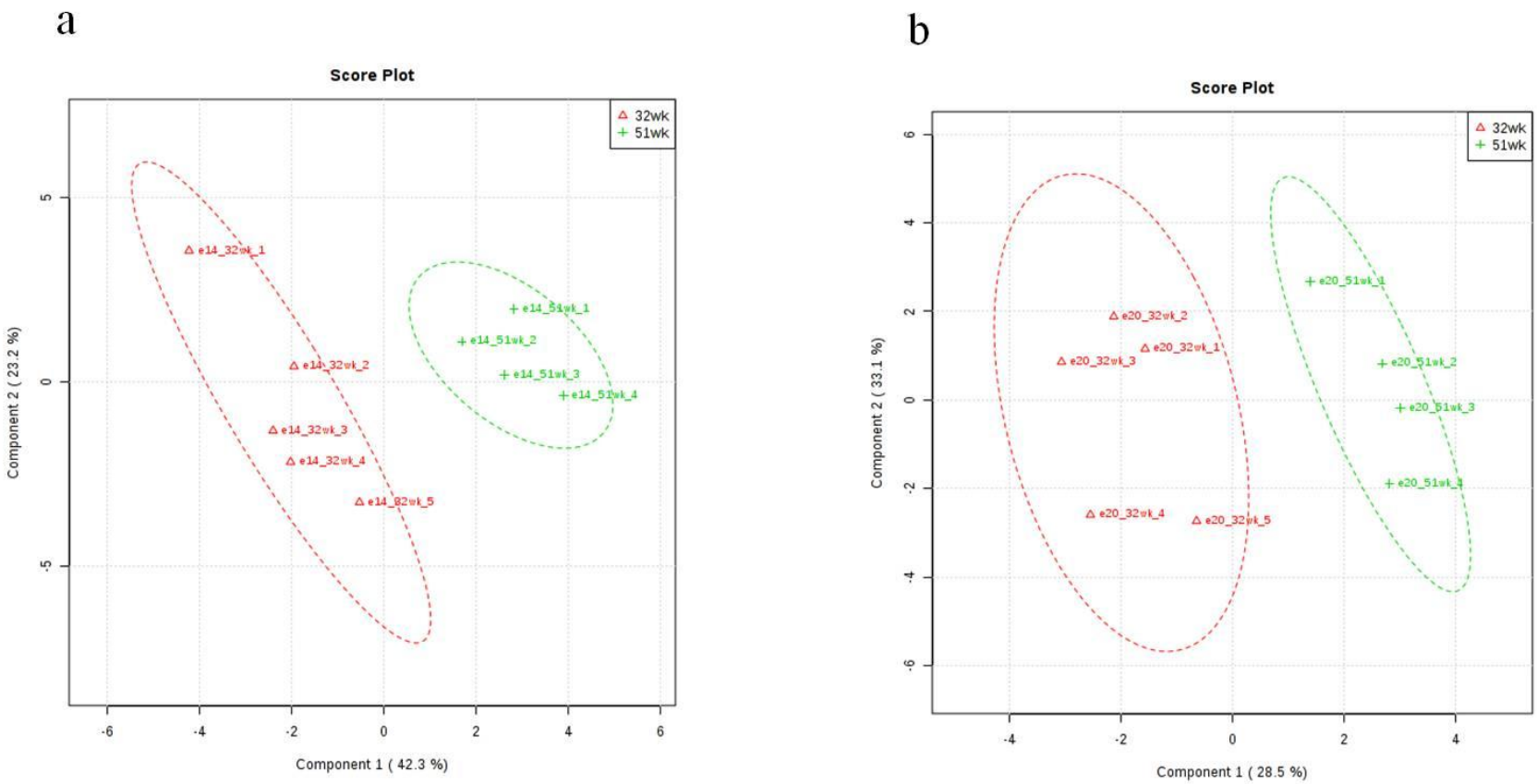

Figure 4.4 Partial least squares-discriminant analysis (PLS-DA) of e14 and e20 liver metabolites (Exp. 1). **a.** PLS-DA score plot shows clear group clustering in e14 liver metabolites from 32 wk *vs* 51 wk-old hens. **b**. PLS-DA score plot discriminates e20 liver metabolites from 32 wk *vs* 51 wk-old hens.

Table 4.4 Liver metabolic pathways that were significantly different in e14 embryos from 32 wk vs 51 wk-old hens (Exp. 1)[1]

Pathway Name	Metabolites[2]	*P* value	FDR[3]
Propanoic acid metabolism	Succinate	<0.0001	0.0021
Valine, leucine and isoleucine metabolism	Valine, Leucine, Isoleucine, Threonine	0.00012	0.0021
Butyric acid metabolism	Succinate, β-hydroxybutyric acid	0.00020	0.0021
Citrate cycle (TCA cycle)	Succinate, Malate	0.00021	0.0021
Aminoacyl-tRNA biosynthesis	Aspargine, Serine, Phenylalanine, Glutamine, Glycine, Aspartate, Lysine, Leucine, Isoleucine, Threonine, Proline	0.00045	0.0032
Pantothenate and CoA biosynthesis	Valine	0.00046	0.0032
Alanine, aspartate and glutamate metabolism	Succinate, Aspartate, Aspargine, Glutamine	0.00130	0.0075
Glycine, serine and threonine metabolism	Serine, Glycine, Threonine	0.00401	0.0183
Phenylalanine, tyrosine and tryptophan metabolism	Phenylalanine	0.00744	0.0278
Glutathione metabolism	Glycine	0.020	0.0592
Lysine degradation	Lysine	0.022	0.0592
Biotin metabolism	Lysine	0.022	0.0592
Pyruvate metabolism	Lactate, Malate	0.034	0.0874
Fructose and mannose metabolism	Glucitol	0.036	0.0874
Glycolysis or Gluconeogenesis	Glucose, Lactate	0.048	0.110

[1] Metabolic pathways that are different based on normalized e14 liver metabolite data in eggs from 32 wk *vs* 51 wk-old hens.
[2] Metabolites that were involved in the listed metabolic pathways are shown.
[3] False discovery rate (FDR) = the rate that significant features are truly null.

Table 4.5 Liver metabolic pathways that were significantly different in e20 embryos from 32 wk *vs* 51 wk-old hens (Exp. 1)[1]

Pathway Name	Metabolites[2]	*P* value	FDR[3]
Glycine, serine and threonine metabolism	Glycine, Serine, Threonine	0.00336	0.138
Valine, leucine and isoleucine metabolism	Valine, Leucine, Isoleucine, Threonine	0.0109	0.205
Methyl group metabolism	Glycine, Serine	0.0296	0.205
Glyoxylate and dicarboxylate metabolism	Malate	0.0340	0.205
Citrate cycle (TCA cycle)	Malate, Succinate	0.0345	0.205
Glutathione metabolism	Glycine	0.0388	0.205
Butyric acid metabolism	Succinate, β-hydroxybutyric acid	0.0401	0.205
Propanoic acid metabolism	Succinate	0.0472	0.215

[1] Metabolic pathways that are different based on normalized e20 liver metabolites data in eggs from 32 wk *vs* 51 wk-old hen.
[2] Metabolites that were involved in the listed metabolic pathways are shown.
[3] False discovery rate (FDR) = the rate that significant features are truly null.

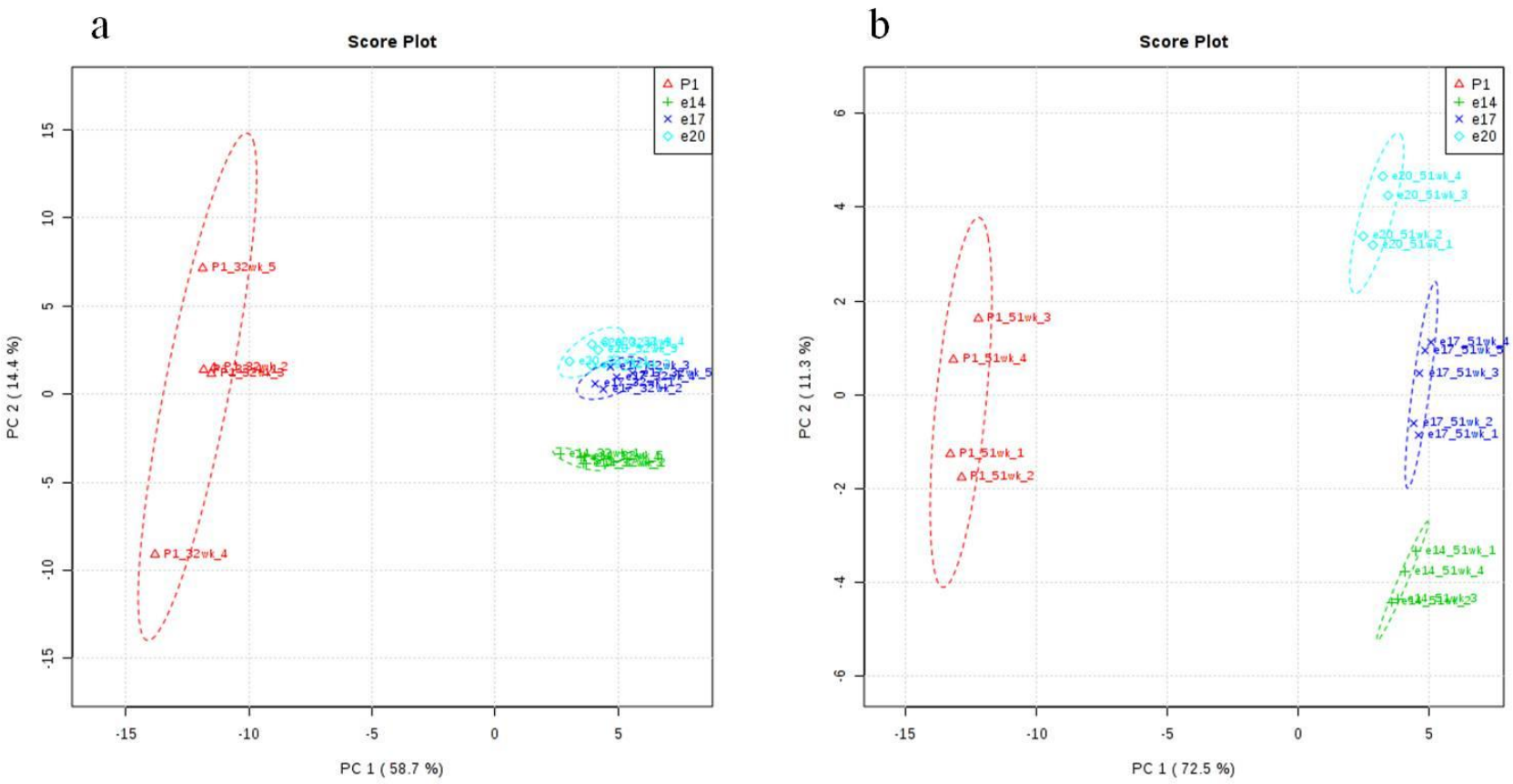

Figure 4.5 Principal component analysis (PCA) of liver metabolomic profile in eggs from 32 wk and 51 wk-old hens during development (Exp. 1). **a.** The PCA score plot showed a good separation in liver metabolites of embryos from 32 wk-old hens. **b** The PCA score plot revealed a distinct group separation in liver metabolites of embryos from 51 wk-old hens.

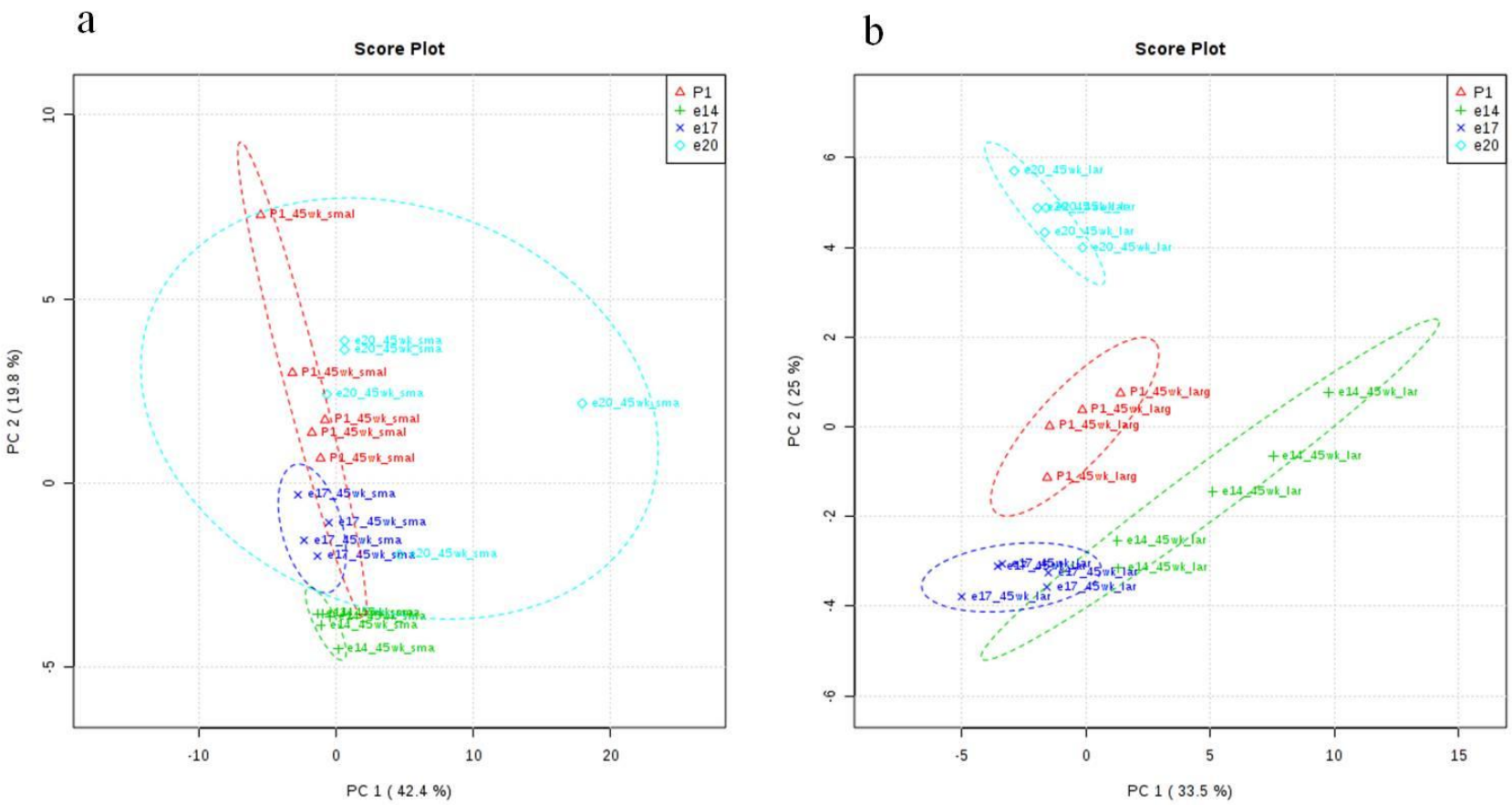

Figure 4.6 Principal component analysis (PCA) of liver metabolomic profile in small and large eggs (45 wk) during development (Exp. 2). **a.** The PCA score plot showed a separation of e14 and e17 liver metabolites of embryos from small eggs, but not a clear cluster for e20 and posthatch day 1 samples. **b** The PCA score plot showed four groups separation in liver metabolites of embryos from large eggs.

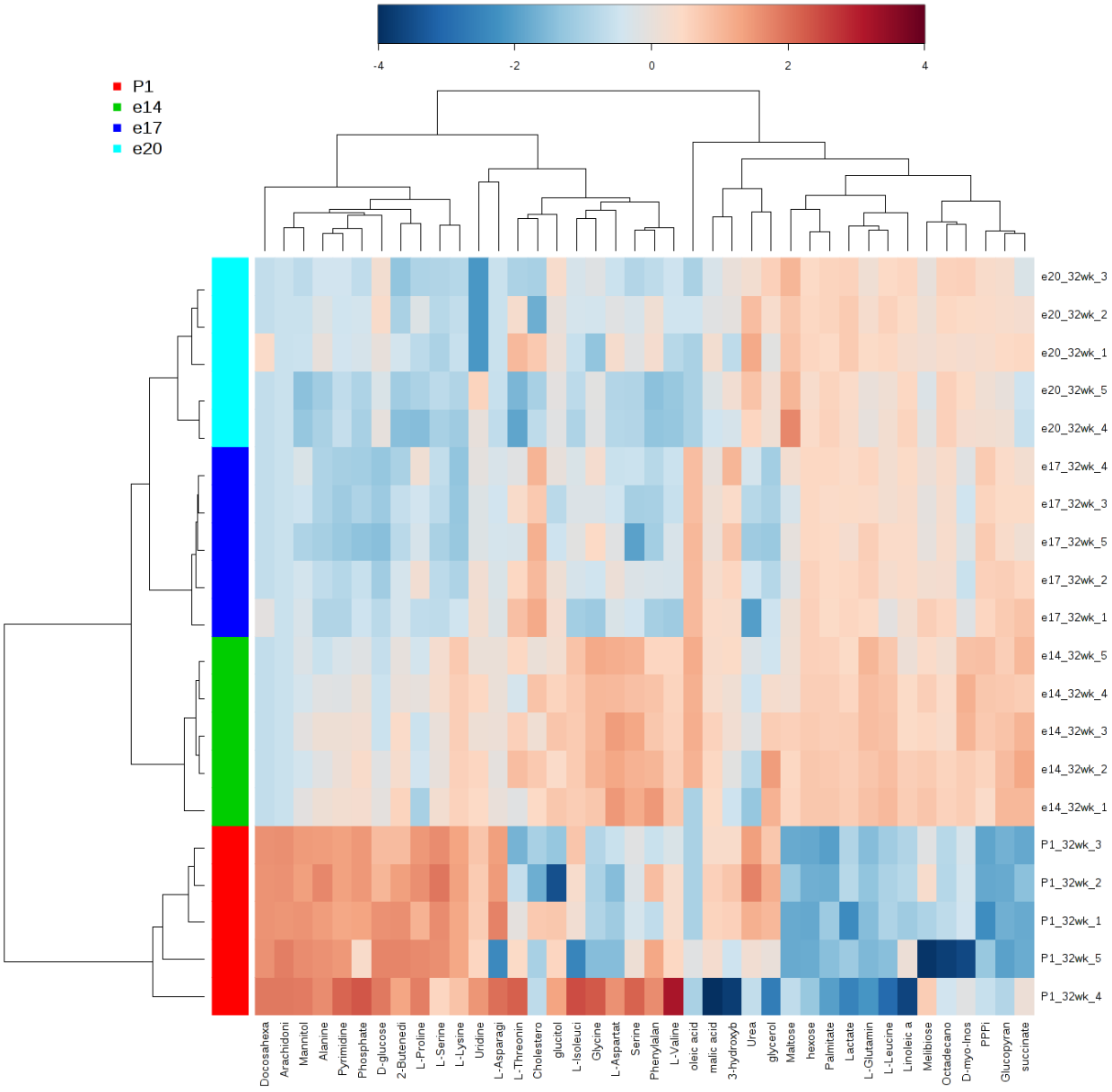

Figure 4.7 Hierarchical clustering analysis (HCA) for liver metabolites in embryos from 32 wk-old hens on e14, e17, e20 and posthatch day 1 (P1) (Exp. 1). The pattern of each parameter (shown in each column) was categorized by a Ward's linkage hierarchical clustering method. The bars indicate the normalized metabolite fold change, with dark red boxes denoting a ratio greater than the mean and dark blue boxes denoting a ratio below the mean. The tree clusters and the shorter Euclidean distance indicate higher similarities. Similarity within two samples or two metabolites is represented by branch height. The shorter the branch height, the more similar it's sub-tree.

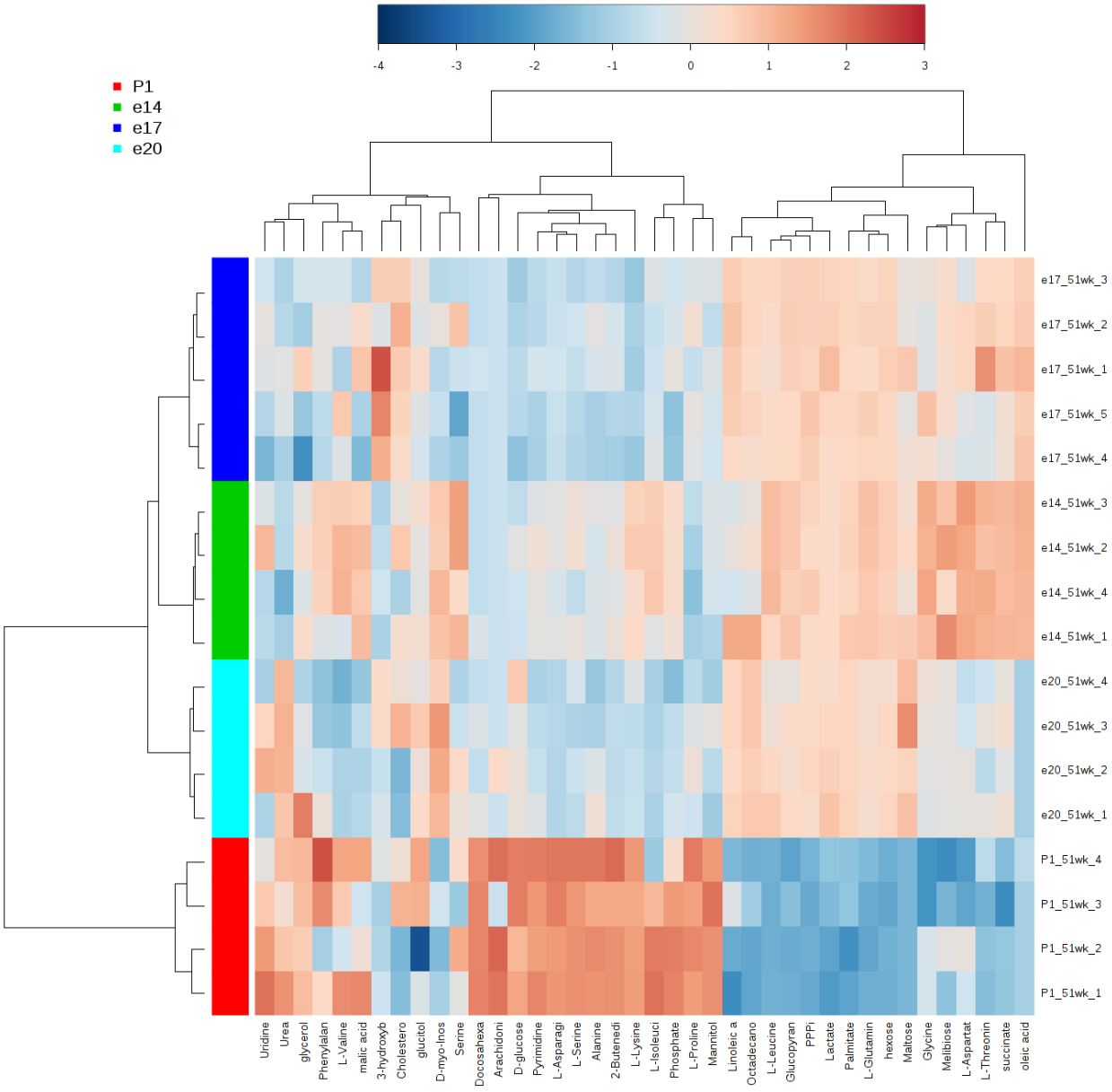

Figure 4.8 Hierarchical clustering analysis (HCA) for liver metabolites in embryos from 51 wk-old hens on e14, e17, e20 and posthatch day 1 (P1) (Exp. 1). The pattern of each parameter (shown in each column) was categorized by a Ward's linkage hierarchical clustering method. The bars indicate the normalized metabolite fold change, with dark red boxes denoting a ratio greater than the mean and dark blue boxes denoting a ratio below the mean. The tree clusters and the shorter Euclidean distance indicate higher similarities. Similarity within two samples or two metabolites is represented by branch height. The shorter the branch height, the more similar its sub-tree.

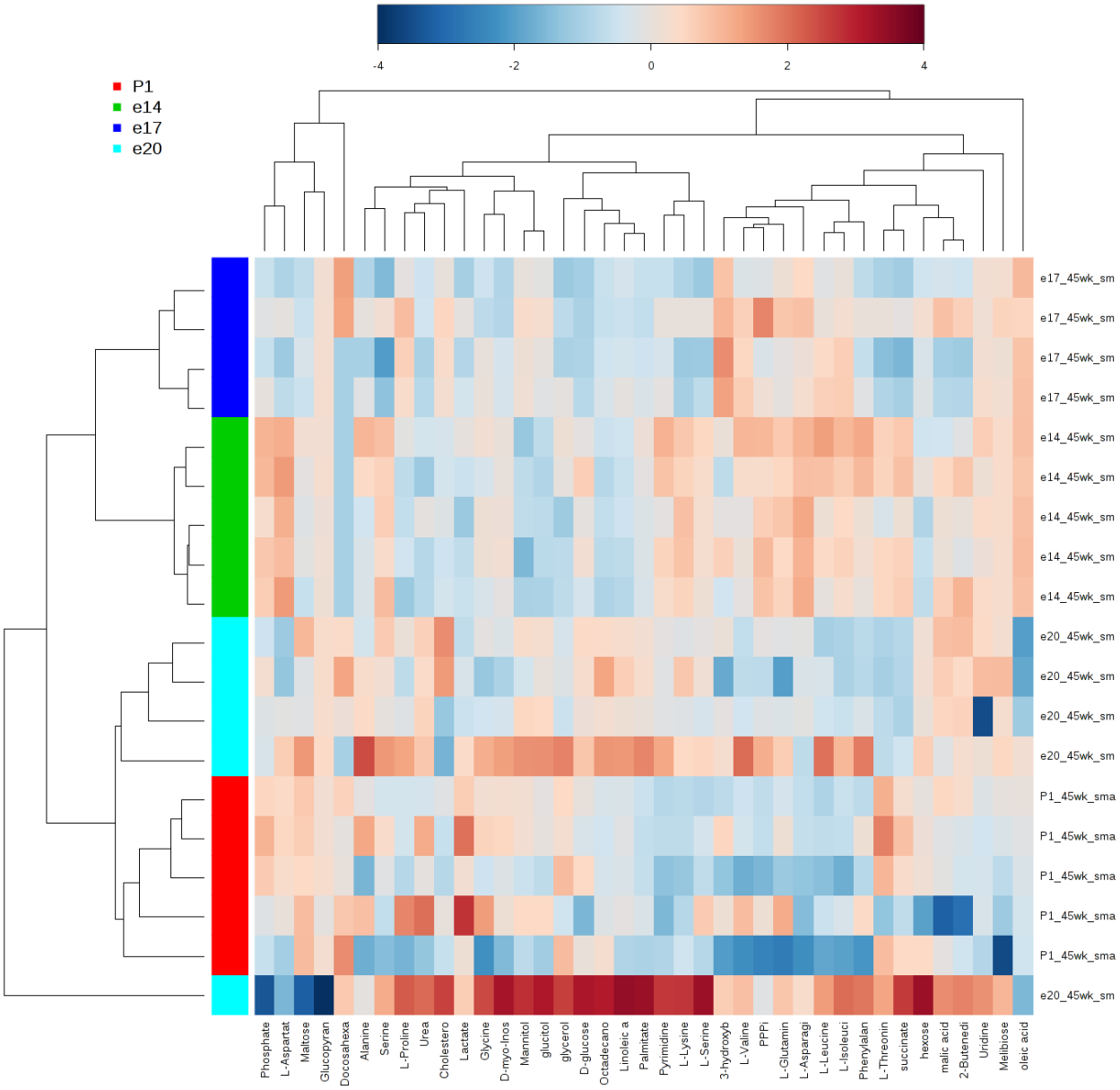

Figure 4.9 Hierarchical clustering analysis (HCA) for liver metabolites in embryos from small eggs from 45 wk- old hens on e14, e17, e20 and posthatch day 1 (P1) (Exp. 2). The pattern of each parameter (shown in each column) was categorized by a Ward's linkage hierarchical clustering method. The bars indicate the normalized metabolite fold change, with dark red boxes denoting a ratio greater than the mean and dark blue boxes denoting a ratio below the mean. The tree clusters and the shorter Euclidean distance indicate higher similarities. Similarity within two samples or two metabolites is represented by branch height. The shorter the branch height, the more similar its sub-tree.

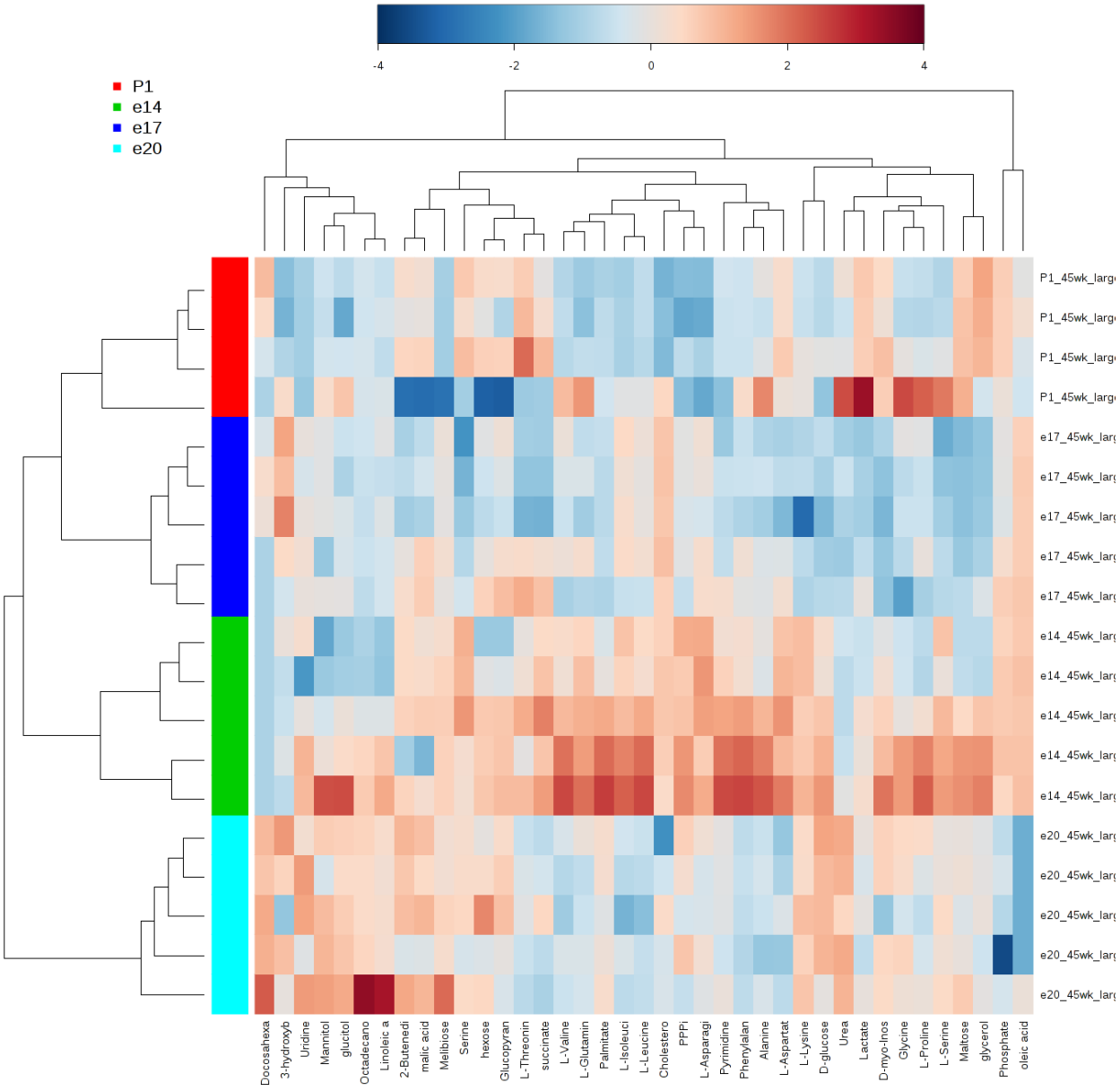

Figure 4.10 Hierarchical clustering analysis (HCA) of liver metabolites in embryos from large eggs from 45 wk- old hens on e14, e17, e20 and posthatch day 1 (P1) (Exp. 2). The pattern of each parameter (shown in each column) was categorized by a Ward's linkage hierarchical clustering method. The bars indicate the normalized metabolite fold change, with dark red boxes denoting a ratio greater than the mean and dark blue boxes denoting a ratio below the mean. The tree clusters and the shorter Euclidean distance indicate higher similarities. Similarity within two samples or two metabolites is represented by branch height. The shorter the branch height, the more similar its sub-tree.

Table 4.6 Liver metabolic pathways that were significantly different during development of embryos from 32 wk-old hens (Exp. 1)[1].

Pathway Name	Metabolites[2]	*P* value	FDR[3]
Starch and sucrose metabolism	Glucose, Maltose	< 0.0001	< 0.0001
Aminoacyl-tRNA biosynthesis	Aspargine, Phenylalanine, Glutamine, Glycine, Aspartate, Lysine, Serine, Leucine, Isoleucine, Threonine, Proline	< 0.0001	< 0.0001
Arachidonic acid metabolism	Arachidonic acid	< 0.0001	< 0.0001
Amino sugar and nucleotide sugar metabolism	Hexose	< 0.0001	< 0.0001
Galactose metabolism	Glucose, Hexose, Melibiose, Glycerol	< 0.0001	< 0.0001
Fatty acid elongation	Palmitic acid	< 0.0001	< 0.0001
Fatty acid metabolism	Palmitic acid	< 0.0001	< 0.0001
Biosynthesis of unsaturated fatty acids	Palmitic, Oleic, Stearic, Linoleic, Arachidonic acid	< 0.0001	< 0.0001
Glycolysis or Gluconeogenesis	Glucose, Lactate	< 0.0001	< 0.0001
Arginine and proline metabolism	Glutamine, Aspartate, Proline	< 0.0001	< 0.0001
Valine, leucine and isoleucine metabolism	Valine, Leucine, Isoleucine, Threonine	< 0.0001	< 0.0001
Purine metabolism	Glutamine	< 0.0001	< 0.0001
D-Glutamine and D-glutamate metabolism	Glutamine	< 0.0001	< 0.0001
Methyl group metabolism	Glycine, Serine	< 0.0001	< 0.0001
Glycine, serine and threonine metabolism	Glycine, Serine, Threonine	< 0.0001	< 0.0001
Alanine, aspartate and glutamate metabolism	Succinate, Aspartate, Aspargine, Glutamine	< 0.0001	< 0.0001
Fatty acid biosynthesis	Palmitic, Oleic, Stearic acid	< 0.0001	< 0.0001
Cysteine and methionine metabolism	Serine	< 0.0001	< 0.0001
Sphingolipid metabolism	Serine	< 0.0001	< 0.0001
Lysine degradation	Lysine	< 0.0001	0.000134
Pyruvate metabolism	Lactate, Malate	0.000118	0.000215

Pathway Name	Metabolite	*P* value	FDR
Propanoate metabolism	Succinate	0.000188	0.000329
Linoleic acid metabolism	Linoleic acid	0.000402	0.000675
Butyric acid metabolism	Succinate, β-hydroxybutyric acid	0.00061	0.000985
Pyrimidine metabolism	Uridine	0.00133	0.00207
Pantothenate and CoA biosynthesis	Valine	0.00363	0.00544
Steroid biosynthesis	Cholesterol	0.00404	0.00548
Primary bile acid biosynthesis	Cholesterol	0.00404	0.00548
Steroid hormone biosynthesis	Cholesterol	0.00404	0.00548
Histidine metabolism	Aspartate	0.00554	0.00706
beta-Alanine metabolism	Aspartate	0.00554	0.00706
Phenylalanine, tyrosine and tryptophan metabolism	Phenylalanine	0.00668	0.00789
Citrate cycle (TCA cycle)	Malate, Succinate	0.00676	0.00789

[1] Metabolic pathways that are different based on normalized liver metabolite data in eggs from 32 wk-old hens on e14, e17, e20 and posthatch day 1.
[2] Metabolites that were involved in the listed metabolic pathways are shown.
[3] False discovery rate (FDR) = the rate that significant features are truly null.

Table 4.7 Liver metabolic pathways that were significantly different during development of embryos from 51 wk-old hens (Exp. 1)[1].

Pathway Name	Metabolites[2]	*P* value	FDR[3]
Aminoacyl-tRNA biosynthesis	Aspargine, Phenylalanine, Glutamine, Glycine, Aspartate, Lysine, Serine, Leucine, Isoleucine, Threonine, Proline	< 0.0001	< 0.0001
Valine, leucine and isoleucine metabolism	Valine, Leucine, Isoleucine, Threonine	< 0.0001	< 0.0001
Starch and sucrose metabolism	Glucose, Maltose	< 0.0001	< 0.0001
Glycine, serine and threonine metabolism	Glycine, Serine, Threonine	< 0.0001	< 0.0001
Alanine, aspartate and glutamate metabolism	Succinate, Aspartate, Aspargine, Glutamine	< 0.0001	< 0.0001
Amino sugar and nucleotide sugar metabolism	Hexose	< 0.0001	< 0.0001
Pyruvate metabolism	Lactate, Malate	< 0.0001	< 0.0001
Glycolysis or Gluconeogenesis	Glucose, Lactate	< 0.0001	< 0.0001
Methyl group metabolism	Glycine, Serine	< 0.0001	< 0.0001
Biosynthesis of unsaturated fatty acids	Palmitic, Oleic, Stearic, Linoleic, Arachidonic acid	< 0.0001	< 0.0001
Fatty acid elongation	Palmitic acid	< 0.0001	< 0.0001
Fatty acid metabolism	Palmitic acid	< 0.0001	< 0.0001
Galactose metabolism	Glucose, Hexose, Melibiose, Glycerol	< 0.0001	< 0.0001
Purine metabolism	Glutamine	< 0.0001	< 0.0001
D-Glutamine and D-glutamate metabolism	Glutamine	< 0.0001	< 0.0001
Fatty acid biosynthesis	Palmitic, Oleic, Stearic acid	< 0.0001	< 0.0001
Butyric acid metabolism	Succinate, β-hydroxybutyric acid	< 0.0001	< 0.0001
Arginine and proline metabolism	Glutamine, Aspartate, Proline	< 0.0001	< 0.0001
Citrate cycle (TCA cycle)	Malate, Succinate	< 0.0001	< 0.0001
Sphingolipid metabolism	Serine	0.000107	0.000205
Cysteine and methionine metabolism	Serine	0.000107	0.000205

Pathway Name	Metabolites	*P* value	FDR
Lysine degradation	Lysine	0.000118	0.000206
Biotin metabolism	Lysine	0.000118	0.000206
Propanoic acid metabolism	Succinate	0.000189	0.000318
Synthesis and degradation of ketones	β-hydroxybutyric acid	0.000766	0.00124
Linoleic acid metabolism	Linoleic acid	0.00146	0.00228
Arachidonic acid metabolism	Arachidonic acid	0.00188	0.00282
Glutathione metabolism	Glycine	0.00218	0.00305
Histidine metabolism	Aspartate	0.00355	0.00466
beta-Alanine metabolism	Aspartate	0.00355	0.00466
Pantothenate and CoA biosynthesis	Valine	0.0132	0.0169
Glyoxylate and dicarboxylate metabolism	Malate	0.0243	0.0301
Glycerolipid metabolism	Glycerol	0.0337	0.0404

[1] Metabolic pathways that are different based on normalized liver metabolite data in embryos from 51 wk-old hens on e14, e17, e20 and posthatch day 1.
[2] Metabolites that were involved in the listed metabolic pathways are shown.
[3] False discovery rate (FDR) = the rate that significant features are truly null.

Table 4.8 Liver metabolic pathways that were significantly different during development of small egg embryos from 45 wk-old hens (Exp. 2)[1]

Pathway Name	Metabolites[2]	*P* value	FDR[3]
Galactose metabolism	Glucose, Hexose, Melibiose, Glycerol	< 0.0001	< 0.0001
Biosynthesis of unsaturated fatty acids	Palmitic, Oleic, Stearic, Linoleic, Arachidonic acid	< 0.0001	< 0.0001
Fatty acid biosynthesis	Palmitic, Oleic, Stearic acid	< 0.0001	< 0.0001
Alanine, aspartate and glutamate metabolism	Succinate, Aspartate, Aspargine, Glutamine	0.000165	0.001691
Linoleic acid metabolism	Linoleic acid	0.000453	0.003708
Fatty acid elongation	Palmitic acid	0.000633	0.003708
Fatty acid metabolism	Palmitic acid	0.000633	0.003708
Arginine and proline metabolism	Glutamine, Aspartate, Proline	0.00144	0.00672
Pyruvate metabolism	Lactate, Malate	0.00148	0.00672
Fructose and mannose metabolism	Glucitol	0.00218	0.00893
Aminoacyl-tRNA biosynthesis	Aspargine, Phenylalanine, Glutamine, Glycine, Aspartate, Lysine, Serine, Leucine, Isoleucine, Threonine, Proline	0.00275	0.00893
Histidine metabolism	Aspartate	0.00283	0.00893
beta-Alanine metabolism	Aspartate	0.00283	0.00893
Lysine degradation	Lysine	0.00396	0.01083
Biotin metabolism	Lysine	0.00396	0.01083
Valine, leucine and isoleucine Metabolism	Valine, Leucine, Isoleucine, Threonine	0.0186	0.0478
Starch and sucrose metabolism	Glucose, Maltose	0.0242	0.0584
Butyric acid metabolism	Succinate, β-hydroxybutyric acid	0.0264	0.0602
Synthesis and degradation of ketone bodies	β-hydroxybutyric acid	0.0384	0.0788
Amino sugar and nucleotide sugar metabolism	Hexose	0.0489	0.0954

[1] Metabolic pathways that are different based on normalized liver metabolites data in small eggs on e14, e17, e20 and posthatch day 1.
[2] Metabolites that were involved in the listed metabolic pathways are shown.
[3] False discovery rate (FDR) = the rate that significant features are truly null.

Table 4.9 Liver metabolic pathways that were significantly different during development of large egg embryos from 45 wk-old hens (Exp. 2)[1]

Pathway Name	Metabolites[2]	*P* value	FDR[3]
Aminoacyl-tRNA biosynthesis	Aspargine, Phenylalanine, Glutamine, Glycine, Aspartate, Lysine, Serine, Leucine, Isoleucine, Threonine, Proline	< 0.0001	< 0.0001
Fatty acid biosynthesis	Palmitic, Oleic, Stearic acid	< 0.0001	0.000142
Biosynthesis of unsaturated fatty acids	Palmitic, Oleic, Stearic, Linoleic, Arachidonic acid	< 0.0001	0.000142
Alanine, aspartate and glutamate metabolism	Succinate, Aspartate, Aspargine, Glutamine	< 0.0001	0.000151
Arginine and proline metabolism	Glutamine, Aspartate, Proline	< 0.0001	0.000223
Starch and sucrose metabolism	Glucose, Maltose	< 0.0001	0.000409
Galactose metabolism	Glucose, Hexose, Melibiose, Glycerol	0.000155	0.000703
Phenylalanine, tyrosine and tryptophan metabolism	Phenylalanine	0.000176	0.000703
Lysine degradation	Lysine	0.000215	0.000703
Biotin metabolism	Lysine	0.000215	0.000703
Histidine metabolism	Aspartate	0.000226	0.000703
beta-Alanine metabolism	Aspartate	0.000226	0.000703
Valine, leucine and isoleucine metabolism	Valine, Leucine, Isoleucine, Threonine	0.000240	0.000703
Fatty acid elongation	Palmitic acid	0.000996	0.00240
Fatty acid metabolism	Palmitic acid	0.000996	0.00240
Pantothenate and CoA biosynthesis	Valine	0.00357	0.00762
Cysteine and methionine metabolism	Serine	0.00372	0.00762
Sphingolipid metabolism	Serine	0.00372	0.00762
Glycolysis or Gluconeogenesis	Glucose, Lactate	0.00531	0.0104
Steroid biosynthesis	Cholesterol	0.00616	0.0105
Primary bile acid biosynthesis	Cholesterol	0.00616	0.0105

Pathway Name	Metabolites	*P* value	FDR
Purine metabolism	Glutamine	0.00929	0.0141
D-Glutamine and D-glutamate metabolism	Glutamine	0.00929	0.0141
Glycine, serine and threonine metabolism	Glycine, Serine, Threonine	0.00988	0.0145
Methyl group metabolism	Glycine, Serine	0.0125	0.0177
Propanoate metabolism	Succinate	0.0190	0.0260
Glycerolipid metabolism	Glycerol	0.0199	0.0263
Butyric acid metabolism	Succinate, β-hydroxybutyric acid	0.0212	0.0271
Pyrimidine metabolism	Uridine	0.0334	0.0415
Synthesis and degradation of ketones	β-hydroxybutyric acid	0.0469	0.0566

[1] Metabolic pathways that are different based on normalized liver metabolites data in large eggs on e14, e17, e20 and posthatch day 1.
[2] Metabolites that were involved in the listed metabolic pathways are shown.
[3] False discovery rate (FDR) = the rate that significant features are truly null.

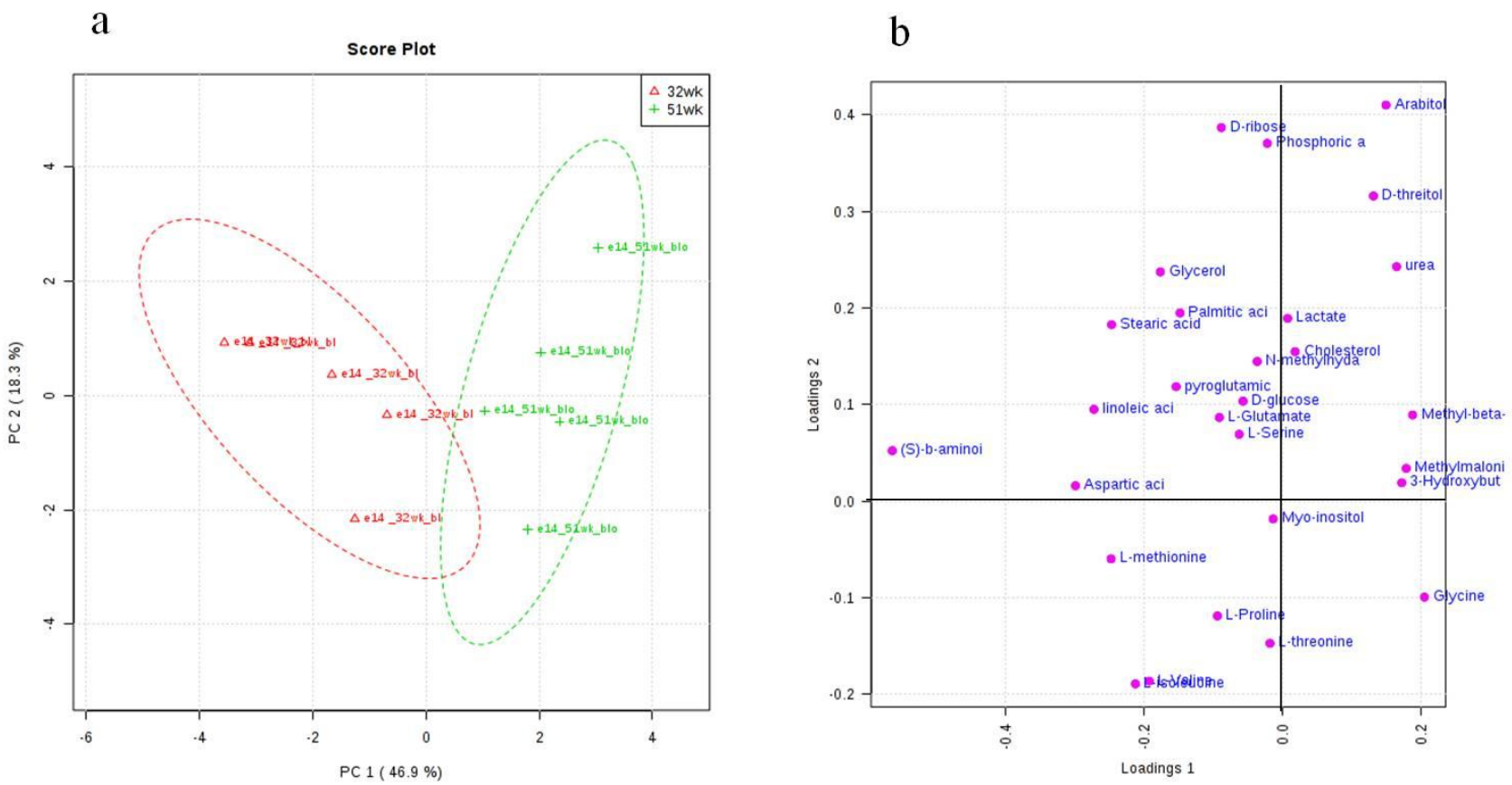

Figure 4.11 Principal component analysis (PCA) of e14 blood metabolomic profile. **a** The PCA score plot distinguishes the metabolic profiles of blood metabolites in eggs from 32 wk (Δ) *vs* 51 wk (+) old hens on e14 (Exp. 1). The first three characters represent the embryo developmental age (e14) followed by age (32 wk, 51 wk) and replicates (1-5 samples). **b** Loading plot shows the correlations among individual blood metabolite of PC1 and PC2 (eigenvalues). Variables (metabolite) with the same distance from zero with similar positions are positively correlated. Those in the opposite direction are negatively correlated.

Table 4.10 Metabolic pathways based on blood metabolites that were significantly different in e14 embryos from 32 wk *vs* 51 wk old hens (Exp. 1)[1]

Pathway Name	Metabolites[2]	*P* value	FDR[3]
Valine, leucine and isoleucine metabolism	Valine, Leucine, Isoleucine, Threonine	0.000369	0.00603
Linoleic acid metabolism	Linoleic acid	0.000389	0.00603
Biosynthesis of unsaturated fatty acids	Palmitic, Oleic, Stearic, Linoleic, Arachidonic acid	0.00218	0.0226
Aminoacyl-tRNA biosynthesis	Asparagine, Phenylalanine, Glutamine, Glycine, Aspartate, Lysine, Serine, Leucine, Isoleucine, Threonine, Proline	0.00362	0.0281
Fatty acid biosynthesis	Palmitic, Oleic, Stearic acid	0.00940	0.0583
Pantothenate and CoA biosynthesis	Valine	0.0177	0.0725
Alanine, aspartate and glutamate metabolism	Succinate, Aspartate, Aspargine, Glutamine	0.0189	0.0725
Cysteine and methionine metabolism	Serine	0.0210	0.0725
Glycerolipid metabolism	Glycerol	0.0349	0.0982
Fatty acid elongation	Palmitic acid	0.0380	0.0982
Fatty acid metabolism	Palmitic acid	0.0380	0.0982
Galactose metabolism	Glucose, Hexose, Melibiose, Glycerol	0.0422	0.100

[1] Metabolic pathways that are different based on normalized e14 blood metabolites data in eggs from 32 wk *vs* 51 wk old hens.
[2] Metabolites that were involved in the listed metabolic pathways are shown.
[3] False discovery rate (FDR) = the rate that significant features are truly null.

Discussion

In Chapter 3, the energy-sensing mechanism in embryos from small compared to large eggs was investigated. Although AMPK activity was observed to be higher in the liver of large egg embryos and egg nutrient supply was greater for the embryos from large eggs, it was not clear what egg and embryo factors lead to these differences. In that study, small eggs were from young hens (26 wk) whereas large eggs were laid by older hens (42 wk). Thus, hen age may have confounded the effects due to egg size and possibly egg composition. Therefore, in this study, we investigated the influences of hen age and egg size separately on chicken embryo growth and development by exploring embryo metabolism during later development (e14-posthatch day 1).

The initial yolk to albumen ratio was higher in eggs of the same weight but from different ages of hens (32 wk *vs* 51 wk). Thus, embryos from 51 wk-old hens had a more energy-dense nutrient supply. However, we did not observe any embryo or liver weight difference from e11 to posthatch day 1 in this group of eggs, which was not in agreement with the study by Shanawany (1984). In that study, e18 embryo weights were reported to be greater in eggs from older hens than younger hens given the same egg weight category. The reason for this inconsistency is unclear. One possibility is that the sample size was not large enough in the current study to detect embryo weight difference. The weights of yolk and albumen were lower in small eggs than in large eggs, and the initial yolk to albumen ratio tended to be higher in small compared to large eggs, although this ratio differed by 0.3 units (the same as in Exp. 1). We noticed that the insignificance may be attributed to one sample that introduced large variation after further evaluating the original data. If the data from this sample were taken out, the ratio was significant between small versus large eggs, and consistent with the literature. Thus, we believe that yolk to albumen ratio was greater in the small eggs relative to large eggs in the current study, which is

consistent with an earlier study where small eggs had a higher proportion of yolk than large eggs from the same clutch (Vieira and Moran, 1998). The embryo, hatchling and liver weights differed on e20 and posthatch day 1, which we anticipated because nutrient supply was greater for embryos from large eggs.

As the yolk to albumen ratio was greater in eggs from 51 wk-old hens, and yolk contains 45% lipid (DM basis, Sato et al., 2006) that provides important fatty acids necessary for embryo development, we measured fatty acid composition in the yolk at set (e0) and on e11, e14, e17, e20 and posthatch day 1 to determine rates and patterns of fatty acid utilization during development. The proportions of oleic and linolenic acids were higher in eggs from 51 wk-old hens at each developmental age whereas palmitic and palmitoleic acids accounted for a higher proportion of fatty acids in yolks from 32 wk-old hens. The latter has also been observed by Latour et al. (1998). However, these fatty acids proportions were not different in yolk from eggs of different sizes from 45 wk-old hens. This may indicate that the yolk fatty acid profile is influenced by hen age but not egg size.

From the above results, it appears that hen age affects the yolk to albumen ratio whereas egg size determines egg nutrient content. Although there are studies reporting the effects of both hen age and egg size on hatchling quality and broiler performance (Shanawany, 1984; Applegate and Lilburn, 1999a, b; Ulmer-Franco et al., 2010), none of these studies reported quantitative information about egg nutrient utilization and the metabolic pathways that resulted in the growth difference. Therefore, it prompted us to investigate whether hen age and egg size would influence embryo metabolism and substrate utilization during later development. A GC-MS-based metabolomics profiling approach was applied to systematically evaluate whether hen age and egg size alter embryo metabolism. We chose the embryo liver and blood to measure

metabolite differences because the liver is the central and most metabolically active organ in the developing embryo while blood reflects ongoing metabolic pathway activities in the entire embryo.

To our knowledge, this is the first study that has employed a metabolomics profiling approach to investigate embryo metabolism. Our results clearly showed that e14 and e20 embryo liver metabolism differed in eggs from 32 wk *vs* 51 wk-old hens. The two metabolite clusters featured higher concentrations of palmitic, stearic and linoleic acids, BCAA, phenylalanine, glutamine, β-hydroxybutyric acid, glycerol and lactate but lower concentrations of succinate, glycine, threonine and oleic acid in e14 embryo livers from 32 wk compared to 51 wk-old hens. Similarly, the e14 blood metabolite profile of embryos from 32 wk-old hens reflected higher concentrations of BCAA, phenylalanine, glutamine and lactate as well as lower levels of glycine. The e20 liver had similar patterns of metabolites when compared to e14 embryos. Fatty acids are known to affect lipid utilization. For instance, oleic acid has a greater stimulatory effect on very low density lipoprotein (VLDL) secretion than palmitic acid in chicken liver cells (Mooney and Lane, 1981). VLDL is released into the circulation *in ovo* from the yolk sac membrane (Latour et al., 1998). The higher concentrations of oleic acid in embryo livers from 51 wk-old hens suggested that these embryos utilized yolk lipid to a greater extent compared to the embryos from 32 wk-old hens.

BCAA are essential nutrients that are required specifically for protein synthesis (Harper et al., 1984), and especially leucine act as a regulator for protein synthesis (Escobar et al., 2006). However, a recent study in human obesity patients showed elevated BCAA may result in incomplete oxidation of fatty acids, and excess carbon from BCAA catabolism may contribute to higher rates of lipogenesis and gluconeogenesis (Newgard, 2012). The present results showed a

difference in terms of BCAA metabolism in both e14 and e20 embryo livers from different ages of hens. Higher BCAA concentration in the liver may suggest a greater demand for protein synthesis in the embryos from 32 wk-old hens. Higher liver β-hydroxybutyric acid indicated the lower liver glycogen supply in embryos from 32 wk-old hens which may trigger the utilization of fatty acids for supply of energy. Hamidu et al., (2007) showed less O_2 consumption by developing embryos from young hens (29 wk) compared to older hens (55 wk), which indicates a shift from fatty acid oxidation to oxidation of amino acids, glycerol and glucose. Indeed, liver lactate was higher in embryos from 32 wk-old hens, which would be expected under conditions of reduced oxygen permeability of the eggshell membrane leading to greater glucose metabolism to lactate (anaerobic metabolism).

It is noteworthy that concentrations of glycine and threonine were higher in embryos from 51 wk-old hens. Glycine, threonine and serine metabolism was also found to be different in the pathway analysis for both e14 and e20 embryos. Glycine, sarcosine, serine and threonine and related metabolic pathways have been identified as pivotal substrates and pathways for cellular transformation (Locasale et al., 2011; Possemato et al., 2011) and murine embryonic stem cell proliferation (Wang et al., 2009). Higher glycine, threonine and serine metabolism in embryos from 51 wk-old hens may have facilitated embryo development. And, we did observe an embryo weight difference in the small compared to large eggs. We did not, however, observe differences in embryo metabolism between the two egg sizes by multivariate analysis on liver and blood metabolite data.

PCA and HCA were performed to investigate developmental changes in embryo metabolism. Our results clearly showed that the four developmental ages could be easily distinguished on the basis of liver metabolites for embryos from 32 wk and 51 wk-old hens and

from the two sizes of eggs. Chicken embryos on e14, e17 and e20 fell into one large sub-tree regardless of whether they were from 32 wk or 51 wk-old hens, and this sub-tree clustered apart from posthatch day 1 chicks. This implies that metabolism in posthatch day 1chicks has changed dramatically in 1 to 2 days compared to the developing embryos. Pathway analysis displayed similar metabolic shifts in embryos from 32 wk and 51 wk-old hens that contributed to differences observed between developmental ages. However, pathways involving synthesis and degradation of ketones, glycerolipid and glutathione metabolism were unique to embryos from 51 wk-old hens. This also reflected the fact that the proportion of yolk in eggs from older hens is higher, and hence reactions related to lipid metabolism would be more active.

In summary, GC-MS based metabolmoics and multivariate analysis were used to provide information on liver and blood metabolites in embryos from two ages of breeders and from two sizes of eggs. With increasing hen age, the proportion of yolk poly-unsaturated fatty acids, in particular oleic acid and the essential fatty acid linolenic acid were higher. Metabolism was different in e14 and e20 embryos from different ages of breeders. The PCA and HCA of liver data showed four distinct clusters of metabolites that corresponded to the four distinct developmental ages. Liver metabolite fold changes corresponding to e14, e17 and e20 were similar and mapped closely together, while the cluster of posthatch day1chicks clustered separately. Thus, maternal age influences embryo metabolism, and certain pathways of interest (i.e., BCAA metabolism, glycine, serine and threonine metabolism) could be further interrogated to establish the functions of these pathways in embryo development and growth. This study also demonstrated the potential of GC-MS based metabolomics as a tool to characterize metabolic pathways and to discover potential biomarkers of embryo development that correlate with optimal growth of chickens.

CHAPTER 5: EXPERIMENT 3

GLUCONEOGENESIS AND SUBSTRATE UTILIZATION IN CHICKEN EMBRYOS DURING LATER DEVELOPMENT[1]

[1] Hu, Q., U. Agarwal, B. J. Bequette. 2013. An *in ovo* ^{13}C-tracer approach to explore liver intermediary metabolism in developing chicken embryos. Will be presented in part at 4th International symposium on energy and protein metabolism and nutrition: September 9-12, 2013. Sacramento, CA, USA

Abstract

We aimed to investigate gluconeogenesis and substrate partitioning in the Krebs cycle, and related metabolic pathways, in embryonic (e) day e14 and e19 chicken embryos. This was accomplished by employing a constant tracer infusion approach *in ovo*. The hypotheses were that glucose and non-essential amino acid (NEAA) synthesis would increase from e14 to e19 embryos. A syringe pump was used to continuously infuse [U-^{13}C] glucose or [U-^{13}C] glycerol for 8 h into the chorio-allantoic compartment of eggs on e14 and e19 to attain a high level of incorporation of ^{13}C into metabolites of intermediary metabolism. Based on [U-^{13}C] glucose infusion, the glucose entry rate, Cori cycling and gluconeogenesis (non-Cori cycle flux) were higher ($P < 0.05$) in e19 compared to e14 embryos, presumably to support glycogen deposition in liver and muscle. Consistent with this finding, the contribution of glucose to alanine, aspartate, and glutamate synthesis was greater ($P < 0.05$) in e14 than in e19 embryos. Although the contribution of glycerol to gluconeogenesis by e19 embryos was greater ($P < 0.05$) than in e14 embryos, overall, glycerol made a small contribution (1.3-6.0%) to glucose synthesis. NEAA synthesis derived from glycerol was higher ($P < 0.05$) in e19 compared to e14 embryos. Based on infusion of [U-^{13}C] glucose, the activity of pyruvate carboxylase (PC) versus pyruvate dehydrogenase (PDH) was relatively higher ($P < 0.05$) in e14 compared to e19 embryos, indicating increased anaplerotic flux into the Krebs cycle for NEAA synthesis by e14 embryos. In conclusion, the constant tracer infusion approach developed in this study allowed for the measurement of embryo metabolism during a shorter window of developing embryos compared to the previous approach of dosing tracer for 3 to 4 days. Lastly, this study provided quantititave information on the developmental (e14 and e19) shifts in gluconeogenesis, lipolysis and NEAA

synthesis, as well as qualitative estimates of the activity of enzymes central to glucose and fatty acid metabolism and the Krebs cycle in chicken embryos.

Key words: [U-^{13}C] glucose, [U-^{13}C] glycerol, gluconeogenesis, NEAA synthesis, chicken embryo

Introduction

Metabolism in the chicken embryo during later development (e1-posthatch day 1) undergoes dramatic changes to adjust to the different physiological and metabolic needs for growth. As the embryo develops and O_2 diffusion across the air-cell membrane increases, the substrates that the embryo metabolizes for energy must shift from carbohydrates (respiratory quotient ~1.0) to fatty acids (respiratory quotient ~0.7) (Rahn et al., 1974; Moran, 2007; De Olivera et al., 2008). Although the egg nutrient composition features 45% lipids, 47% protein and less than 3% carbohydrates on a dry matter basis (Romanoff and Romanoff, 1967), glucose is an essential nutrient not only for energy supply, but also for brain and immune system development (Humphrey and Rudrappa, 2008). Plasma glucose was detected as early as embryonic (e) day e4 and increased steadily throughout development (Hazelwood, 1971; Savon et al., 1993). High rates of gluconeogenesis and glycogenesis occur after e13 (Pearce, 1977; Picardo and Dickson, 1982). The upregulation of gluconeogenesis is crucial in the later term developing chicken embryo to ensure blood glucose supply for development, and for muscle and liver glycogen storage for pipping and hatching.

In this study, quantifications of gluconeogenesis and substrate partition were particularly of interest as well as the composition of substrates utilized in the Krebs cycle and related metabolic pathways in e14 and e19 embryos. Based on the earlier studies (Chapters 3 and 4), e14

is a critical time point in embryo development. At this stage, liver AMPK activity is at its highest, and embryo metabolism differs on e14 when comparing eggs from young *vs* old hens. From e14 onwards to e19, the rate of embryo development and growth (2.5-fold increase in weight) is most dramatic with enhanced oxygen consumption, hormonal changes and storage of glycogen for pipping and emergence. Because this is a critical and dynamic period of embryo development, the rate of gluconeogenesis and substrate partition through the Krebs cycle must be finely balanced. It also represents the period when egg nutrient composition will be most influential to embryo growth, physiology and survival.

[U-^{13}C] glucose has been used as a tracer to investigate the regulation of glucose metabolism in human infants and adults, piglets, sheep and in developing chicken embryos in the laboratory (Sunny and Bequette, 2010). There are several advantages of using uniformly ^{13}C-labeled glucose and mass isotopomer distribution analysis (MIDA) rather than radio-isotopes. First, the enrichment of [M+6] glucose, i.e. the infused [U-^{13}C] glucose, reflects the rate of glucose entry rate resulting from glucose absorption, glucose carbon recycling and gluconeogenesis from non-glucose sources (i.e., amino acids and glycerol) (Pascual et al., 1997). Employing MIDA, ^{13}C recycling, Cori cycling and gluconeogenesis can be quantified from the appearance of glucose with less than six carbons labeled. Second, when ^{13}C-skeletons from glucose enter intermediary metabolism, the labeling patterns in intermediates and products downstream of glucose catabolism reflect the activity of the pathways the carbon skeletons traversed and as well as unequivocal evidence that these end-products are synthesized in the cell, tissue or whole body (Berthold et al., 1994; Pascual et al., 1997; Wykes et al., 1998). In relationship to the developing chicken embryo, Sunny and Bequette, (2010) have previously demonstrated that the embryo is capable of synthesizing so-called non-essential amino acids

(NEAA), which raises the question "What are the substrates that are metabolized for NEAA synthesis?"

Glycerol is a well-known glucogenic substrate. In the liver, glycerol is phosphorylated and subsequently converted to glyceraldehyde phosphate and dihydroxyacetone phosphate. Thus, glycerol enters the Krebs cycle, gluconeogenesis, or pentose phosphate pathway through the 3-carbon pool. [U-^{13}C] Glycerol has been used to quantify the contribution of glycerol to glucose synthesis in healthy term and preterm infants (Patel and Kalhan, 1992; Sunehag et al., 1999). And, the turnover of ^{13}C of glycerol reflects the rate of lypolysis as well as the contribution of glycerol to the syntheses of other intermediates. A diagram showing [U-^{13}C] glucose and [U-^{13}C] glycerol metabolism and stable isotope distribution in the intermediates and final products is presented in **Figure 5.1**.

Previously, a daily injection protocol was employed for dosing stable isotope tracers into the chorio-allantoic compartment of eggs in the laboratory (Sunny and Bequette, 2010, 2011). Though steady state labeling was often achieved, the method was time-consuming (3-4 days of dosing), embryo losses were common, and there were such large variations in the enrichment of the dosed tracer in the blood that necessitated elimination of observations. Moreover, the contribution of glycerol to glucose synthesis was not determined due to the large variations in blood glycerol enrichment. Therefore, to overcome the variation and shorten the period of tracer administration so that smaller windows in embryo development could be investigated, a constant tracer infusion protocol was developed (8-h infusion) in the current study to improve steady state labeling of intermediates and improve the accuracy of estimating gluconeogenesis, glycerol turnover and substrate utilization by e14 and e19 chicken embryos.

Materials and Methods

Egg Incubation and Stable Isotope Tracer Infusion

The experimental protocol was approved by the University of Maryland Institutional Animal Care and Use Committee.

Fertile eggs from layers (~50 wk-old, White leghorn) (61.2 ± 3.2 g, n = 51) were acquired from B & E eggs (York Springs, PA). Eggs were incubated under the standard condition of 65% relative humidity and 37.5°C. On embryonic (e) day 9, eggs were candled and undeveloped eggs removed. A tracer infusion protocol was developed for continuous infusion of [U-^{13}C] glucose (Exp.1) or [U-^{13}C] glycerol (Exp. 2) (99 atom percent ^{13}C, Cambridge Isotope Laboratories, Inc., Andover, MA) into chorio-allantoic fluid. Mass spectrometry analysis confirmed isotopomer purity of 93.7% $^{13}C_6$ and 6.1% $^{13}C_5$ for [U-^{13}C] glucose tracer, and isotopomer purity of 96.6% $^{13}C_3$ and 3.3% $^{13}C_2$ for [U-^{13}C] glycerol.

On e14 and e19, the air cell end of the egg was sterilized with 70% ethanol before piercing of the egg shell. A 27-gauge blunted needle was introduced 2-3 mm through the air-cell membrane into the chorio-allantoic compartment and glued in place to the egg shell. The needle was then connected to a 1m polyethylene infusion line (I.D. 0.38mm; O.D. 1.09mm, Becton Dickinson and Co., Sparks, MD) with a 0.5mL syringe attached. [U-^{13}C] Glucose (0.15 g/g saline) or [U-^{13}C] glycerol (0.14 g/g saline) was continuously (8 h) infused into the eggs using a speed adjustable syringe pump (NE-300, New Era Pump Systems, Inc., Farmingdale, NY) (**Figure 5.2**). The pump speed was set at 47.49 µL/h for [U-^{13}C] glucose and 50 µL/h for [U-^{13}C] glycerol to deliver a total of 50 mg [U-^{13}C] glucose or [U-^{13}C] glycerol over the 8-h infusion period. The initial and final weights of the tracer infusion syringe and time of infusion were recorded for calculation of the rate of isotope infusion.

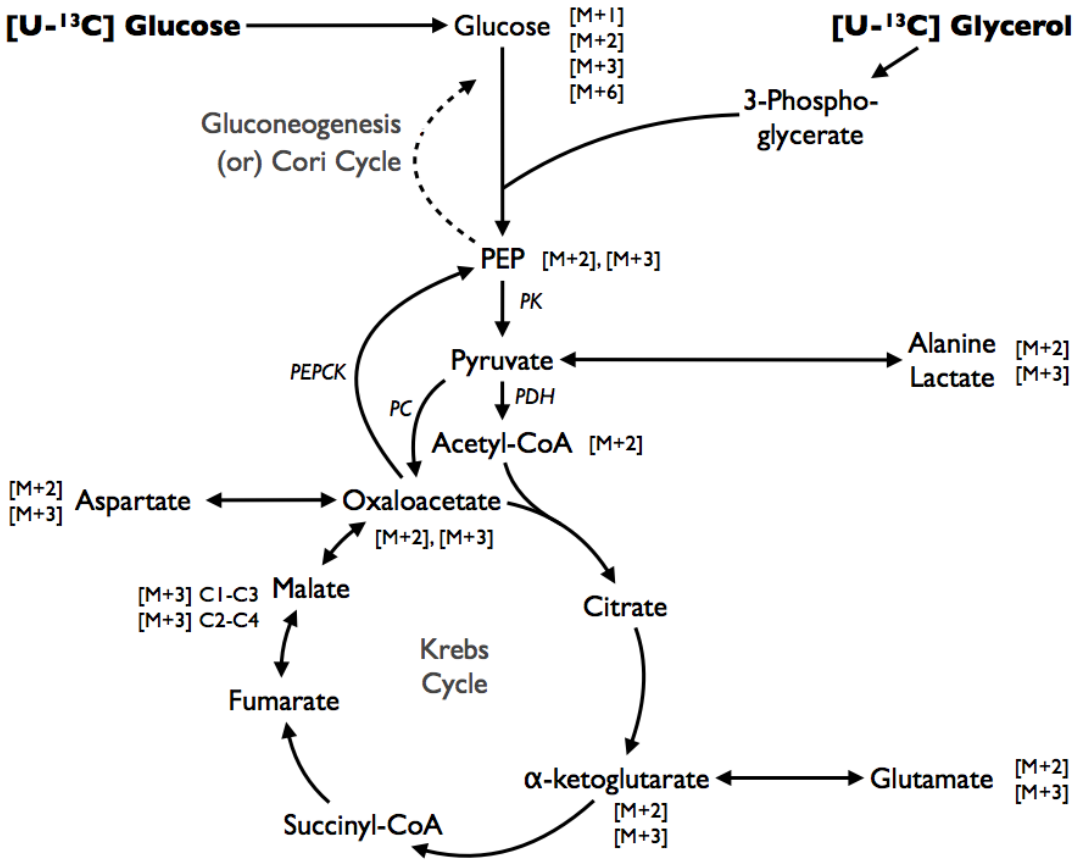

Figure 5.1 [U-^{13}C] Glucose and [U-^{13}C] glycerol metabolism and stable isotope distribution in the intermediates and final products in glyceolysis and the Krebs cycle.

Sample Collection and Analysis

At the end of infusion, eggs were dissected for collection of blood and liver. After removing the infusion line, a hole was made into the large end of the egg with scissors, the crown removed, and whole egg contents were carefully transferred to a petri-dish on ice. The vitelline vessels (artery and vein) were exposed on the top and clearly visible. Blood was drawn using a 0.5mL syringe equipped with a 27-gauge needle (Becton Dickinson and Co.) piercing into the blood vessels. The blood was transferred into a 1 mL blood collection tube (Multivette®, Sarstedt AG & Co) with a solid lithium heparin ring to prevent blood clotting and immediately frozen at -20 °C. The weights of embryos were recorded, and the whole liver was immediately wrapped in aluminum foil before being stored at -20 °C for later analysis.

Glucose Enrichments

For determination of blood glucose enrichments, samples (50 µL) were extracted with 0.5 mL of ice-cold methanol, vortex mixed and centrifuged for 10 min at 13,000 × *g* at room temperature. The supernatant was transferred to a 2mL v-vial and reduced to dryness under N_2 gas at room temperature. The di-O-isopropylidene acetate (IPAc) derivative of glucose was formed prior to GC-MS analysis. The derivative was separated by GC using a fused silica capillary column (ZB-50; 30 m × 0.25 mm× 0.50 µm, Phenomenex, Torrance, CA) with helium as the carrier gas. For liver free glucose enrichment, 1 mL of ice-cold 10% sulpho-salicylic acid (w/v) was added to samples (60 mg) and homogenized on ice. The homogenates were centrifuged for 10 min at 13, 000 ×*g* at room temperature. The supernatant was applied to cation-exchange resin (AG 50W-X8 resin, 100-200 mesh; Bio-Rad Laboratories, Hercules, CA), and glucose was eluted from the resin with 2 mL of distilled H_2O and frozen prior to being lyophilized to dryness. The IPAc derivative of glucose was formed as above. Ions with mass-to-

charge (m/z) 287-293 were monitored using selective ion monitoring (SIM) with the MS operated in electron ionization mode (Hannestad and Lundblad, 1997).

Blood Lactate and Alanine Enrichments

Lactate and alanine in the blood were extracted using ice-cold methanol. Briefly, 0.5 mL of ice-cold methanol was added to 50 µL of blood, vortexed briefly and then samples were centrifuged at 13,000 ×*g* for 10 min at room temperature. The supernatant was reduced to dryness under N_2 gas. The tert-butyl dimethylsilyl (t-BDMS) derivatives were separated by GC on a fused silica capillary column (ZB-50; 30m × 0.25mm × 0.50µm) with helium as the carrier gas. Selective ion monitoring of ions with m/z 261-264 for lactate and m/z 260-263 for alanine was performed with the MS operated under electron ionization mode.

Glycerol Enrichments

Blood glycerol (50 µL) was extracted with 0.5 mL of ice-cold methanol, vigorously vortexed and centrifuged at 13,000 ×*g* for 10 min. The supernatant was transferred to a 1-mL v-vial and reduced to dryness under N_2 gas. A mixture of acetic anhydride: pyridine (v/v, 2:1) was added to the dried sample and heated at 60°C for 30 min. The sample was reduced to dryness under N_2 gas and reconstituted in ethyl acetate (100 µL) before GC-MS analysis. The glycerol triacetate derivative was separated by GC using a fused silica capillary column (HP-5; 30m × 0.25mm ×0.25µm, Hewlett-Packard, Palo Alto, CA) with helium as the carrier gas. The MS was operated in methane positive chemical ionization mode, and ions of m/z 159-163 were monitored for glycerol enrichment (Kalhan et al., 2001).

Amino Acid Enrichments

For determination of NEAA enrichment, liver samples (60 mg) were deproteinized by the addition of ice-cold 10% sulpho-salicylic acid (w/v) and homogenized on ice. The homogenates were centrifuged for 10 min at 13, 000 ×*g* at room temperature, and the acid supernatant applied to cation-exchange (AG 50W-X8 resin, 100-200 mesh; Bio-Rad Laboratories). Amino acids were eluted from resin with 2 mL of 2*M* NH_4OH followed by 1 mL of H_2O. The eluate was frozen and lyophilized to dryness. Amino acids were derivatized with a mixture of N-methyl-N-[tert-butyldimethyl-silyl] trifluoroacetimide (MTBSTFA) containing 1% tert-butyldimethylchlorosilane (TBDMCS) and dimethylformamide (DMF) (v/v, 1:1). After heating by microwave (200 watts for 2 min), the amino acid t-BDMS derivatives were separated by GC with a fused silica capillary column (ZB-50; 30 m × 0.25 mm × 0.50 µm, Phenomenex) and the MS operated in electron ionization mode. The following ions of m/z were monitored: lactate 261-264, alanine 260-263, glycine 246-248, proline 286-290, serine 390-393, aspartate 418-422, glutamate 330-334, and glutamine 431-436. The fragment ions monitored (e.g., 261 for alanine) contained all of the carbons for that amino acid.

Calculations

Throughout this chapter, isotopomers of glucose, glycerol and their metabolites containing 1, 2, 3,…*n* ^{13}C atoms were denoted as [M+1], [M+2], [M+3], … [M+*n*]. The crude ion abundances of analytes were corrected for the natural abundance of isotopes (e.g., ^{13}C, ^{2}H, ^{15}N) present in the molecule and in the derivative employing a matrix approach (Fernandez et al., 1996). Natural isotopomer distributions in unlabelled glucose, glycerol, lactate and amino acids were quantified using unlabelled pure standards. Corrected enrichments of precursors, intermediates and products are reported as moles of tracer [M+*n*] per 100 moles of tracee [M+0] for all calculations.

Calculation of glucose entry rate, recycling (Cori cycle) and gluconeogenesis were based on the dilution of [M+6] glucose (Katz et al., 1989) and ^{13}C isotopomer recycling derived from glycolytic metabolism of [U-^{13}C (Tayek et al., 1996, 1997). The assumption of the calculation of gluconeogenesis is that glucose synthesis via pyruvate results in ^{13}C recycling to glucose (Wykes et al., 1998). The calculation in this chapter was also based on the assumption that the labeling of alanine, aspartate and glutamate is a direct reflection of the labeling of their respective transamination partners pyruvate, oxaloacetate and α-ketoglutarate when [U-^{13}C] glucose or [U-^{13}C] glycerol was infused (Berthold et al., 1994).

Apparent glucose entry rate was calculated according to Wykes et al. (1998):

$$[\text{U-}^{13}\text{C}]\ \text{glucose infused (mg/h)} \times \left(\frac{\text{P}}{[\text{M+6}]\ \text{glucose}} - 1\right) \quad (1)$$

where P is the isotopic purity of [U-^{13}C] glucose tracer (93.7%).

Glucose carbon ^{13}C recycling was calculated according to Pascual et al. (1997):

$$\frac{\sum_1^3(\text{glucose})3}{\sum_1^6(\text{glucose})6} \quad (2)$$

where

$$\sum_1^6(\text{glucose})6 = ([\text{M}+1]) + ([\text{M}+2]\times 2) + ([\text{M}+3]\times 3) + ([\text{M}+6]\times 6) \quad (3)$$

$$\sum_1^3(\text{glucose})3 = ([\text{M}+1]) + ([\text{M}+2]\times 2) + ([\text{M}+3]\times 3). \quad (4)$$

Cori cycling, as a fraction of glucose entry rate, was based on [U-^{13}C] glucose infusion and calculated as:

$$\frac{[M+1]+[M+2]+[M+3]}{[M+1]+[M+2]+[M+3]+[M+6]} \quad (5)$$

Equation (5) calculates the fraction of labeled glucose molecules that result from carbon recycling without consideration of the dilution of unlabeled molecules arisen from the entry of amino acid and fatty acid carbons into the 3-carbon and Krebs cycle intermediate pools (Tayek and Katz, 1996). Metabolism of [M+6] glucose and glucose carbon recycling leads to the production of [M+6] and [M+3] glucose isotopomers. Hence, [M+3] pyruvate can only be synthesized from these two glucose isotopomers. [M+3] pyruvate yields [M+3] alanine via transamination, whereas metabolism of [M+3] pyruvate in the Krebs cycle leads to the synthesis of [M+3] oxaloacetate and, thus, [M+3] aspartate via transamination (Pascual et al., 1998). The fractional contribution of glucose to alanine or aspartate fluxes was calculated as:

$$\frac{[M+3]\text{alanine or } [M+3]\text{aspartate}}{[M+6]\text{glucose}+(0.5\times[M+3]\text{glucose})} \quad (6)$$

Furthermore, metabolism of [M+3] pyruvate introduces [M+3] oxaloacetate via pyruvate carboxylase (PC) into the Krebs cycle. Alternatively, decarboxylation of [M+3] pyruvate via pyruvate dehydrogenase (PDH) leads to the synthesis of [M+2] acetyl-CoA. Subsequently, concurrent metabolism of [M+3] pyruvate via PC and PDH activity leads to the synthesis of [M+2] and [M+3] α-ketoglutarate isotopomers and via transamination [M+2] and [M+3] glutamate isotopomers (Pascual et al., 1998). The contribution of glucose to glutamate synthesis via oxalacetate is calculated as:

$$\frac{2\times[M+3]\text{glutamate}}{[M+6]\text{glucose}+(0.5\times[M+3]\text{glucose})} \quad (7)$$

and the contribution of 3-carbon pool precursors to glutamate synthesis is calculated as:

$$\frac{2\times[\mathrm{M+3}]\mathrm{glutamate}}{[\mathrm{M+3}]\mathrm{alanine}} \quad (8)$$

Here, [M+3] glutamate was multiplied by a factor of 2 because of fumarate-oxaloacetate cycling which leads to an equilibrium mixture of two isomers of [M+3] oxaloacetate. One isomer will be labeled in carbons 1-3 while the other isomer is labeled in carbons 2-4. When citrate is metabolized to α-ketoglutarate, carbon 1 of citrate that arises from oxaloacetate is lost. Therefore, only [M+3] oxaloacetate labeled in carbons 2-4 can lead to the synthesis of [M+3] glutamate. If [M+3] glutamate enrichment was used in the equation (8) without multiplying by the factor of 2, the true contribution of [M+3] oxaloacetate would be underestimated by 100% (Pascual et al., 1998). Pyruvate carboxylase and pyruvate dehydrogenase activities can also be estimated by:

$$\frac{[\mathrm{M+3}]\mathrm{aspartate}}{[\mathrm{M+3}]\mathrm{alanine}} \quad (9)$$

$$\frac{[\mathrm{M+2}]\mathrm{acetyl-CoA}}{[\mathrm{M+3}]\mathrm{alanine}} \quad (10)$$

In Equation (10), [M+2] acetyl-CoA enrichment was calculated as:

$$[\mathrm{M+2}]\ \mathrm{glutamate} - \left(1 - \frac{[\mathrm{M+3}]\mathrm{glutamate}}{[\mathrm{M+3}]\mathrm{aspartate}}\right) \times [\mathrm{M}+3]\mathrm{aspartate} - [\mathrm{M}+3]\mathrm{aspartate} \quad (11)$$

And, the measurement of PC versus PDH activity was calculated from the ratio:

$$\frac{[\mathrm{M+3}]\mathrm{glutamate}}{[\mathrm{M+2}]\mathrm{acetyl-CoA}} \quad (12)$$

The basis of this calculation is that [M+2] fumarate with ^{13}C at carbons 3 and 4 will be produced when [M+3] oxaloacetate is metabolized during the first turn in the Krebs cycle, regardless of the position of ^{13}C in the oxaloacetate. Hence, the enrichment of [M+2] oxaloacetate should be equal to [M+3] oxaloacetate after the first turn in the Krebs cycle. The enrichment of [M+2] glutamate synthesized from [M+2] oxaloacetate will be the same as the enrichment of [M+3] oxaloacetate after the second turn if we do not consider the entry of other sources of ^{13}C. In fact, of the final enrichment of [M+2] glutamate, part of it will be generated in the Krebs cycle on the first turn metabolism of [M+3] oxaloacetate with ^{13}C at carbons 1-3. A portion of the [M+2] glutamate enrichment is ascribed to the metabolism of [M+2] oxaloacetate in the second turn of the Krebs cycle. The differences between [M+2] glutamate and these two parts of [M+2] glutamate enrichment should be contributed by the entry of [M+2] acetyl-CoA from [M+3] pyruvate (Berthold et al., 1994). Thus, the contribution of the 3-carbon pool to [M+2] acetyl-CoA synthesis is calculated as:

$$\frac{[\mathrm{M+2}]\mathrm{acetyl-CoA}}{[\mathrm{M+3}]\mathrm{alanine\ or\ [M+3]lactate}} \tag{13}$$

When [U-^{13}C] glycerol was infused into embryos, glycerol entry rate was calculated as:

$$[\text{U-}^{13}\text{C}]\ \text{glycerol infused (mg/h)} \times \left(\frac{\mathrm{P}}{\mathrm{G}} - 1\right) \tag{14}$$

Where P is the isotopic purity (96.6%) of the [U-^{13}C] glycerol tracer, and where G is:

$$\frac{[\mathrm{M+3}]\mathrm{glycerol}}{[\mathrm{M+0}]\mathrm{glycerol} + [\mathrm{M+3}]\mathrm{glycerol}} \tag{15}$$

The fractional contributon of glycerol to gluconeogenesis was estimated as:

$$\frac{[M+3]\text{glucose}}{[M+3]\text{glycerol}} \quad (16)$$

The contributions of glycerol to the syntheses of alanine, aspartate and glutamate were calculated as:

$$\frac{[M+3]\text{alanine or } [M+3]\text{ aspartate}}{[M+3]\text{glycerol}} \quad (17)$$

$$\frac{2\times[M+3]\text{glutamate}}{[M+3]\text{glycerol}} \quad (18)$$

As stated above, [M+3] glutamate enrichment was multiplied by 2 due to oxaloacetate and fumarate cycling and equilibrium.

Statistical Analysis

All data were verified to meet assumptions of normality and homogeneity of variance. Results were analyzed by Student's *t*-test procedure of SAS 9.2 (SAS Institute Inc., Cary, NC). Results are presented as mean ± SEM. A probability of $P < 0.05$ was considered statistically significant.

Results

Embryo Growth

The initial egg weights were not different between e14 and e19 embryos in the experiments where [U-^{13}C] glucose (Exp. 1) or [U-^{13}C] glycerol (Exp. 2) were infused (**Table 5.2** and **Table 5.3**). The weights of embryos on e14 differed ($P < 0.0001$) from those of e19 embryos in both experiments. Overall, embryo weight increased by 210 to 250% between e14 and e19 in both experiments.

Glucose Metabolism

When [U-^{13}C] glucose was infused (Exp.1), the tracer:tracee ratios of the ^{13}C isotopomers, ^{13}C recycling of glucose (%) and glucose molecule recycling (%) in blood and liver glucose in the e14 and e19 chicken embryos were as shown in **Table 5.1**. The tracer:tracee ratios of blood [M+3] and [M+6] glucose were substantially higher ($P < 0.05$) in e14 than those of e19 embryos. Likewise, the tracer:tracee ratios of liver [M+3] and [M+6] glucose were higher ($P < 0.01$) in e14 versus e19 embryos. The lower enrichments in e19 embryos reflect greater dilution of glucose as a result of higher rates of glucose entry. Irrespective of glucose pool, glucose ^{13}C recycling and glucose molecule recycling did not change with the day of development. Values for apparent glucose entry rate, Cori cycling and gluconeogenesis on an absolute (g of glucose per embryo^{-1} • d^{-1}) and body weight (BW)-adjusted basis (g of glucose per 100 g BW^{-1} • d^{-1}) in e14 and e19 chicken embryos are presented in **Table 5.2**. For this calculation, blood and liver glucose enrichments were considered as precursors. Apparent glucose entry rate based on blood and liver enrichment was higher ($P < 0.05$) in e19 than in e14 embryos, except for BW-adjusted glucose entry rate when blood glucose was the precursor pool where fluxes did not differ. Cori cycling and gluconeogenesis (non-Cori cycling) on an absolute basis were higher ($P < 0.05$) in e19 embryos for both precursor pools. When adjusted to a BW-basis, liver Cori cycling as well as gluconeogenesis increased ($P < 0.05$) as the embryo developed. However, these two fluxes on a BW-adjusted basis were not different between e14 and e19 embryos when blood was the precursor pool.

In Exp. 2 when [U-^{13}C] glycerol was infused, glycerol entry rate adjusted by BW tended to be higher ($P = 0.061$) in e14 (452.9 mg per 100 g BW^{-1} • d^{-1}) versus e19 (111.4 mg per 100 g BW^{-1} • d^{-1}) embryo, but statistical difference was not detected due to high variations within the

samples (**Table 5.3**). Although the fractional contribution of glycerol to gluconeogenesis was higher ($P < 0.05$) in e19 compared to e14 embryos when blood glucose was considered as the product pool, values were much lower than hypothesized. Overall, the contribution of glycerol to gluconeogenesis in e19 embryos averaged 2.1% when calculated using blood glucose as the product pool.

Glucose and 3-Carbon Pool Contribution to Liver NEAA Synthesis

The enrichments of [M+1], [M+2] and [M+3] of alanine, aspartate and glutamate in the liver free pool were markedly higher ($P < 0.01$) in e14 compared to e19 embryos when [U-^{13}C] glucose was infused (**Figure 5.3**). As a result, the contribution of blood glucose to liver alanine, aspartate and glutamate synthesis was greater ($P < 0.05$) in e14 versus e19 embryos (**Figure 5.4**). Unfortunately, due to the limited volumes of blood that could be collected from e14 and e19 embryos, the number of replicates was insufficient to perform statistical analysis on the contribution of the 3-carbon pool to liver [M+3] glutamate synthesis. Nonetheless, despite the limited number of observations (**Figure 5.5**), blood alanine and lactate contributions to [M+3] glutamate synthesis were numerically higher in e14 versus e19 embryos. By contrast, when liver alanine was considered as the 3-carbon precursor pool, [M+3] glutamate synthesis from alanine was numerically lower in e14 compared to e19 embryos.

When [U-^{13}C] glycerol was infused (Exp.2), the estimate of the contribution of blood glycerol to liver alanine and glutamate synthesis was greater ($P < 0.05$) in e19 embryos than in e14 embryos (**Figure 5.6**). Blood glycerol contribution to liver aspartate synthesis was not different due to high variation among samples. Compared to other 3-carbon substrates (10-50%), i.e., lactate and alanine in the blood, the contribution of glycerol (0.1-0.2%) to glutamate synthesis was much less.

Figure 5.2 Speed adjustable syringe pump system. The pump was connected to a polyethylene tubing infusion line and fitted to a 0.5-mL syringe. A 27-gauge blunted needle was inserted into the chorio-allantoic compartment, secured to the egg shell with glue and connected to the polyethylene infusion line.

Synthesis of Acetyl-CoA from the 3-Carbon Pool

When [U-^{13}C] glucose was infused, the calculated enrichment of liver [M+2] acetyl-CoA was higher ($P < 0.05$) in e14 versus e19 embryos (**Figure 5.7**). The latter suggests that glucose contributed more, or that other substrates (e.g., fatty acids, leucine and lysine) contributed less to acetyl-CoA flux and, thus, Krebs cycle oxidation. Unfortunately, the limited number of replicates precluded statistical evaluation of the contribution of the 3-carbon pool to acetyl-CoA synthesis. Despite this limitation, the contribution of blood lactate to acetyl-CoA synthesis was numerically similar in e14 and e19 embryos (**Figure 5.8**). When blood alanine was considered as the 3-carbon pool precursor, the contribution of alanine to acetyl-CoA synthesis was numerically higher in e19 compared to e14 embryos.

In Exp. 2 when [U-^{13}C] glycerol was infused, liver [M+2] acetyl-CoA enrichment was higher ($P < 0.05$) in e19 embryos than e14 embryos (**Figure 5.7**). The enrichment of [M+2] acetyl-CoA was similar in e19 embryos when comparing [U-^{13}C] glucose and [U-^{13}C] glycerol tracer infusions, although the enrichment in e14 embryos was lower when the eggs were infused with [U-^{13}C] glucose. This may indicate the possible differences in the extent that glucose and glycerol are metabolized to acetyl-CoA in e14 embryos.

PC and PDH Activity

The activities of PC and PDH largely determine the anaplerotic flux of 3-carbon pool substrates into the Krebs cycle and into the acetyl-CoA pool for oxidation or fatty acid synthesis. Herein, the activity of PC in the liver was estimated by the ratio of [M+3] aspartate to [M+3] alanine. PC activity increased ($P < 0.05$) from e14 to e19 in embryos (**Figure 5.9**), suggesting increased anaplerosis in the liver of e19 embryos for gluconeogenesis, NEAA synthesis, or both. PDH activity was calculated from the ratio of [M+2] acetyl-CoA to [M+3] alanine, and this ratio

was higher in e14 compared to e19 embryos. The ratio of PC to PDH activity reflects the balancing of 3-carbon pool fluxes into the Krebs cycle for anaplerosis versus oxidation and fatty acid synthesis, and it was estimated by the ratio of [M+2] acetyl-CoA to [M+3] glutamate. (**Figure 5.10**). In e14 embryos, the ratio of PC to PDH activity was greater ($P < 0.05$) compared to e19 embryos. When [U-^{13}C] glycerol was infused as the metabolic probe, liver PC activity in e14 embryos did not differ from that in e19 embryos. Moreover, the crude ratio of PC to PDH activity did not differ in e14 compared to e19 embryos (data not shown).

Table 5.1 Glucose ^{13}C enrichment, and ^{13}C and glucose molecular recycling in e14 and e19 chicken embryos infused with [U-^{13}C] glucose[1]

Precursor pool	Mass isotopomers (tracer:tracee ratio)				^{13}C isotopic enrichment		^{13}C recycling[4] (%)	Glucose molecule recycled[5] (%)
	M+1	M+2	M+3	M+6	M+1-M+3[2]	M+1-M+6[3]		
Blood glucose								
e14	10.9 ± 3.3	15.3 ± 4.6	7.6 ± 2.5	36.3 ± 14.3	64.3 ± 19.6	282.1 ± 100.7	23.3 ± 4.0	48.6 ± 5.7
e19	6.9 ± 3.3	9.1 ± 4.0	3.2 ± 1.6	16.7 ± 8.7	34.5 ± 15.7	134.8 ± 51.5	27.6 ± 12.8	53.6 ± 15.8
age effect	NS	$P < 0.05$	$P < 0.01$	$P < 0.05$	$P < 0.05$	$P < 0.01$	NS	NS
Liver glucose								
e14	12.9 ± 4.3	18.3 ± 6.3	8.5 ± 3.3	14.9 ± 9.3	39.6 ± 13.7	54.5 ± 21.0	73.5 ± 7.0	73.6 ± 7.0
e19	2.7 ± 1.1	3.7± 1.6	1.2 ± 0.6	2.1 ± 1.3	7.6 ± 3.21	9.7 ± 3.9	79.5 ± 5.6	79.5 ± 6.7
age effect	$P < 0.001$	$P < 0.001$	$P < 0.001$	$P < 0.01$	$P < 0.001$	$P < 0.001$	NS	NS

[1] Values are moles of tracer/100 moles of tracee (means ± SD, n=6).
[2] $\sum_1^3(\text{glucose})3$ in Equation (4)
[3] $\sum_1^6(\text{glucose})6$ in Equation (3)
[4] Calculated with Equation (2)
[5] Calculated with Equation (5)
NS: not significantly different ($P \geq 0.05$)

Table 5.2 Glucose entry rate, ^{13}C and Cori cycling, and gluconeogenesis (GNG) based on blood and liver glucose enrichment in e14 and e19 chicken embryos infused with [U-^{13}C] glucose.[1]

Precursor pool	Original egg wt (g)	Embryo wet wt (g)	Glucose entry rate[2] (g/embryo/d)	Glucose entry rate (g/100g BW/d)	Cori cycling[3] (g/embryo/d)	Cori cycling (g/100g BW/d)	GNG[4] (g/embryo/d)	GNG (g/100 g BW/d)
Blood glucose								
e14	60.8 ± 3.3	8.2 ± 0.5	0.23 ± 0.10	2.79 ± 1.10	0.11 ± 0.05	1.40 ± 0.60	0.11 ± 0.05	1.39 ± 0.53
e19	59.9 ± 3.5	25.5 ± 2.4	0.80 ± 0.36	3.23 ± 1.54	0.47 ± 0.28	1.87 ± 1.10	0.33 ± 0.12	1.36 ± 0.63
age effect		$P < 0.0001$	$P < 0.01$	NS	$P < 0.05$	NS	$P < 0.01$	NS
Liver glucose								
e14			0.87 ± 0.44	10.66 ± 5.37	0.66 ± 0.35	8.06 ± 4.27	0.21 ± 0.10	2.59 ± 1.18
e19			5.10 ± 1.48	19.67 ± 6.56	3.92 ± 1.22	15.09 ± 5.26	1.58 ± 0.76	4.58 ± 1.58
age effect			$P < 0.001$	$P < 0.05$	$P < 0.001$	$P < 0.05$	$P < 0.01$	NS

[1] Values are means ± SD (n=6).
[2] Calculated with Equation (2).
[3] Calculated with Equation (5) and multiplied with glucose entry rate.
[4] Calculated from the difference of glucose entry rate and Cori cycling.
NS: not significantly different ($P \geq 0.05$).

Table 5.3 Glycerol entry rate and contribution to gluconeogenesis (GNG) based on blood and liver glucose enrichment in e14 and e19 chicken embryos infused with [U-^{13}C] glycerol[1]

Product pool	Original egg wt (g)	Embryo wet wt (g)	Glycerol entry rate[2] (mg/embryo/d)	Glycerol entry rate (mg/100 BW/d)	GNG from glycerol[3] (%)
Blood glucose					
e14	61.3 ± 2.2	7.3 ± 0.8	32.5 ± 24.9	452.9 ± 345.2	0.4 ± 0.4
e19	63.4 ± 2.8	25.3 ± 1.6	28.1 ± 14.6	111.4 ± 57.9	2.1 ± 2.9
age effect		$P < 0.0001$	NS	NS	$P < 0.05$
Liver glucose					
e14					0.3± 0.3
e19					1.3 ± 1.2
age effect					NS

[1] Values are means ± SD (n = 5).
[2] Calculated with Equation (14).
[3] Calculated with Equation (16).
NS: not significantly different ($P \geq 0.05$).

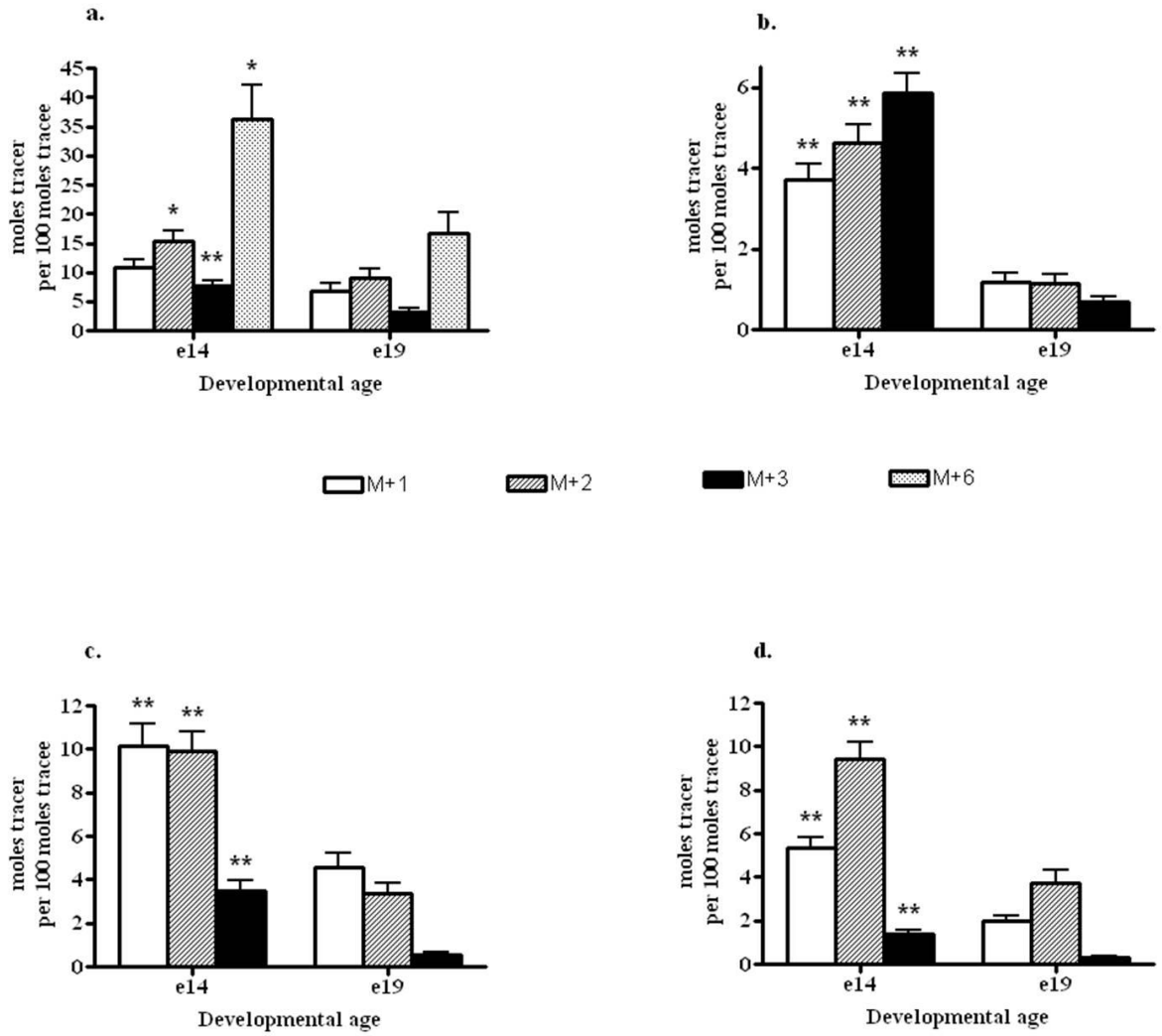

Figure 5.3 Enrichments of (**a**) blood glucose, (**b**) liver alanine, (**c**) liver aspartate and (**d**) liver glutamate isotopomers in e14 and e19 chicken embryos continuously infused (8 h) with [U-^{13}C] glucose. Enrichments are expressed as moles of [^{13}C] isotopomer per 100 moles of [^{12}C] isotopomer. Each bar represents the mean ± SEM (n = 6). *$P < 0.05$, ** $P < 0.01$.

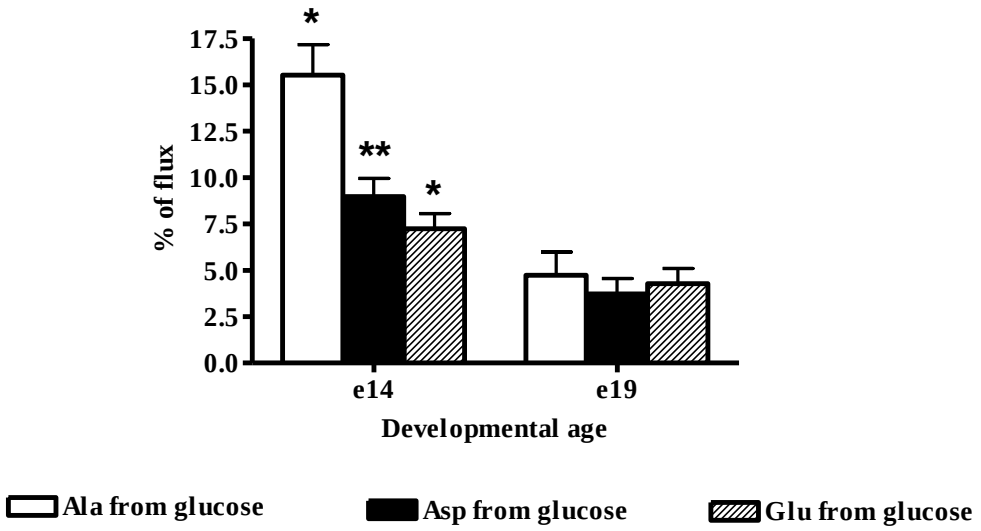

Figure 5.4 Contribution (% of flux) of blood glucose to liver alanine (Ala), aspartate (Asp) and glutamate (Glu) synthesis in e14 and e19 embryos infused (8 h) with [U-^{13}C] glucose. Values were calculated with Equations (6) and (7). Each bar represents the mean ± SEM (n = 6).*P < 0.05, ** P < 0.01.

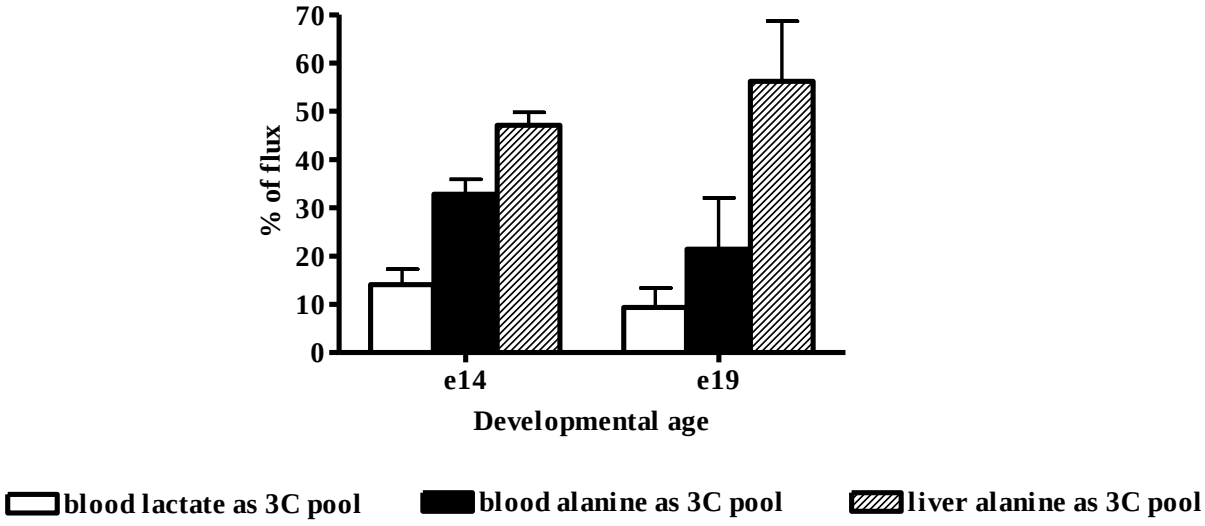

Figure 5.5 Glutamate synthesis in the liver from the 3-carbon (3C) pool via activity of pyruvate carboxylase. Blood lactate and alanine, and liver alanine were considered as precursors in in Equation (8). Bars represent the mean ± SEM (n = 2-3 when blood lactate and alanine were considered and n = 2-6 when liver alanine was considered. Statistical comparisons of e14 *vs* e19 embryos were not performed due to the limited number of replicates.

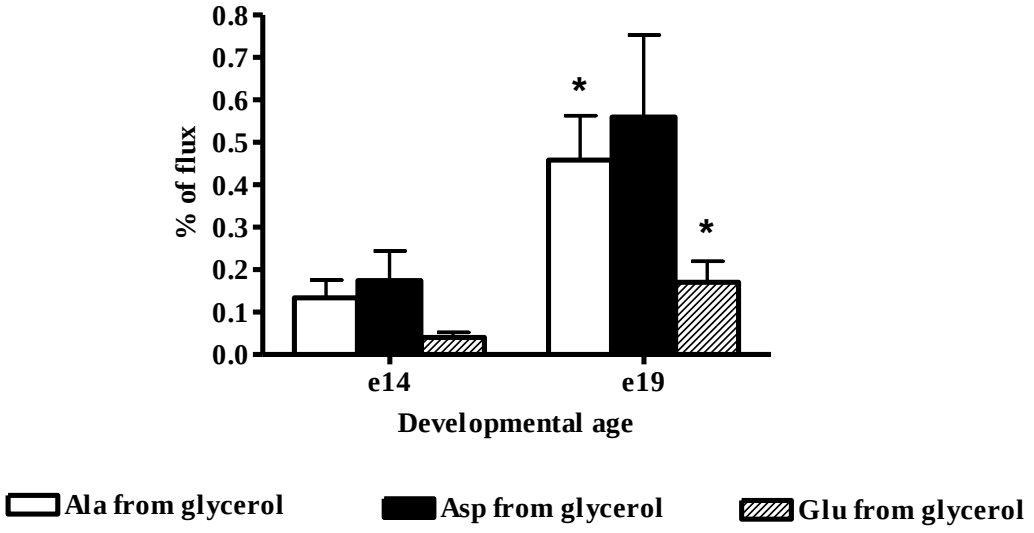

Figure 5.6 Contribution of blood glycerol to liver alanine (Ala), aspartate (Asp) and glutamate (Glu) synthesis in e14 and e19 embryos continuously infused (8 h) with [U-^{13}C] glycerol. Values were calculated with Equations (17) and (18). Each bar represents the mean ± SEM (n = 5). * P <0.05.

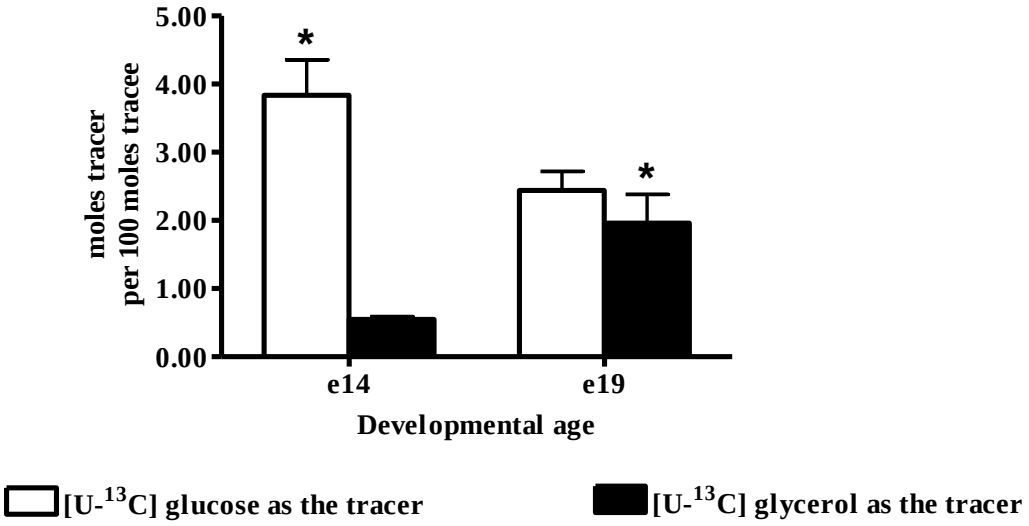

Figure 5.7 Liver [M+2] acetyl-CoA enrichment in e14 and e19 chicken embryos when infused with [U-^{13}C] glucose and [U-^{13}C] glycerol. [M+2] acetyl-CoA enrichment was calculated with Equation (11). Values are expressed as moles [M+2] acetyl-CoA per 100 moles of ^{12}C acetyl-CoA. Bars represent the mean ± SEM (n = 6 when infused with [U-^{13}C] glucose and n = 3-5 when infused with [U-^{13}C] glycerol). * $P < 0.05$.

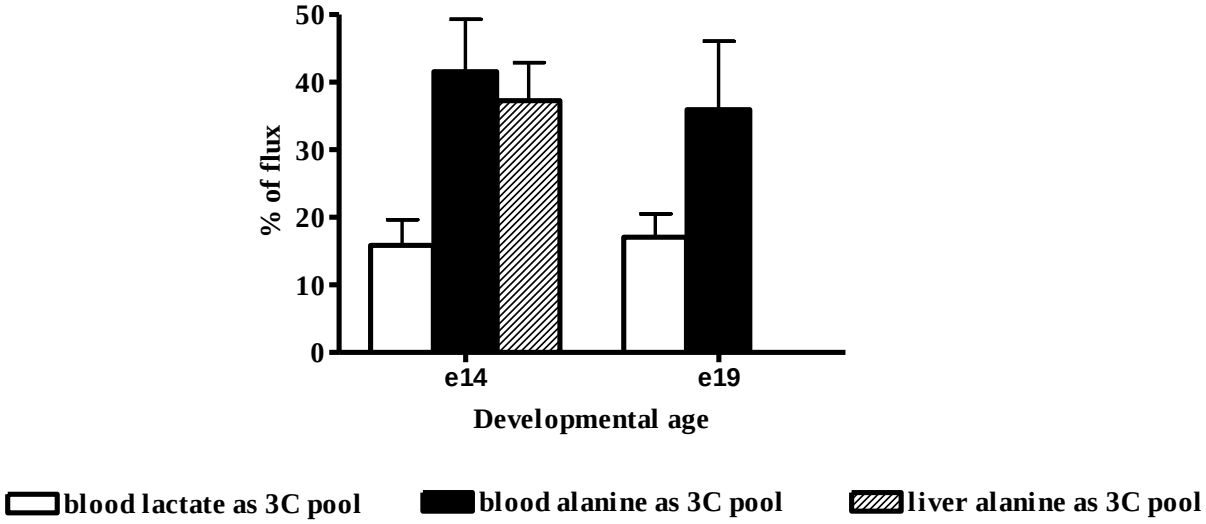

Figure 5.8 Contribution of the 3-carbon (3C) pool to acetyl-CoA flux via activity of pyruvate dehydrogenase when [U-^{13}C] glucose was infused. Values were calculated with Equation (13). Each bar represents the mean ± SEM (n = 2-3 for calculations with blood lactate or alanine as the 3-carbon precursor pool and n = 6 for calculations with liver alanine as the 3-carbon precursor pool. Values on e19 when liver alanine was considered as 3-carbon precursor pool are not shown as these values exceeded 100%, which suggests that at e19 this pool is not theoretically sound. Thus, statistical comparisons of e14 *vs* e19 were not possible.

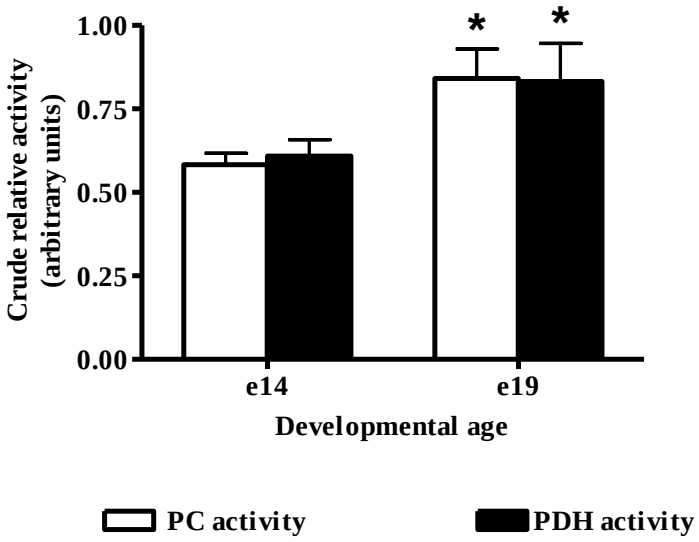

Figure 5.9 Pyruvate carboxylase (PC) and pyruvate dehydrogenase (PDH) activities in e14 and e19 chicken embryos when infused with [U-^{13}C] glucose. PC activity was calculated with Equation (9), and PDH activity was calculated with Equation (10). Each bar represents the mean ± SEM (n = 6). * $P < 0.05$, ** $P < 0.01$.

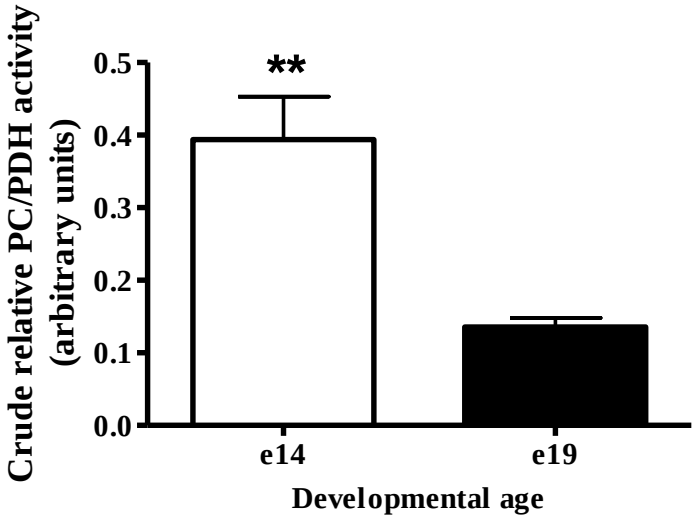

Figure 5.10 Crude relative activity of pyruvate carboxylase (PC) *vs* pyruvate dehydrogenase (PDH) in e14 and e19 chicken embryos when infused with [U-^{13}C] glucose. The ratio was calculated with Equation (11). Each bar represents the mean ± SEM (n = 6). ** $P < 0.01$.

Discussion

In the present study, a continuous infusion approach was employed for delivery of stable isotope tracers into the embryo for quantification of glucose and glycerol metabolism and general substrate utilization by e14 and e19 chicken embryos. [U-^{13}C] Glucose and [U-^{13}C] glycerol were chosen as metabolic probes to investigate developmental changes in gluconeogenesis and the contribution of 3-carbon pool substrates to the synthesis of NEAA. It was aimed to evaluate the two metabolic probes in studying Krebs cycle metabolism and related pathway activities. In this regard, this study was particularly interested in the comparative shifts in the fluxes of substrates through glycolysis and the Krebs cycle, and the activities of central enzymes (PC and PDH) as the embryo develops. It was expected that this evaluation would further reflect that as the embryo develops and grows, the metabolism of the macronutrients supplied from the yolk and albumen would shift from carbohydrate to fatty acid metabolism.

The weights e19 chicken embryos differed remarkably from e14 embryos, featuring a two-fold increase in both experiments. Based on the previous experiments (Chapters 3 and 4), we specifically selected the period between e14 and e19 because e14 is a critical developmental age when we observed enhancement of the energy-sensing mechanism of AMPK and embryo metabolism (e14 and e20) that also differed between small and large eggs and their different nutrient environments. The period between these two development ages represents the most dynamic period of embryo metabolism and hormonal changes (Wise and Frye, 1973; Scott et al., 1981; Moran, 2007), and the most rapid rate of embryo growth. [U-^{13}C] Glucose and [U-^{13}C] glycerol were constantly delivered into the chorio-allantoic compartment of the eggs for three reasons. Firstly, it was technically challenging to insert a catheter into the vitelline or other vessels of the embryo without causing hemorrhage. Secondly, direct uptake of the infused tracers

into the blood circulation was possible because of the extensive capillary network surrounding the embryo at these stages. And, lastly, the tracers were infused at a constant, but very slow rate, during 8 h compared to the previous approach of daily bolus dosing of tracers in the laboratory. By the end of the constant infusion period, about 50 mg of tracer was delivered into the eggs and this is less likely to have caused a substrate response by the embryo compared to the single daily dosing approach. This amount was infused to ensure high rates of ^{13}C incorporation into intermediates and products, and thus not only more accurate estimations of substrate fluxes but also greater distribution of ^{13}C-skeletons in downstream pathways to allow for a more global assessment of pathway fluxes and enzyme activities.

The two metabolic probes were delivered at a constant rate into the eggs and this has advantages. Firstly, the tracer was continuously delivered at a slow rate over an 8-h window to provide a better picture of the short-term changes in the developing embryos. Compared to daily injections of tracer for three to four consecutive days in the previous studies in the laboratory (Sunny and Bequette, 2010, 2011), the constant infusion protocol shortened the time course of the study. Secondly, frequent handling of the eggs was necessary when tracer was injected daily and this lends itself to greater possibility of damaging the structural integrity of the shell membranes and potentially disturbing embryo development. The latter approach often resulted in the death of the embryos before the tracer dosing period was complete. Herein, the implantation of needle in the egg for constant tracer infusion was accomplished with only one puncture of the egg and eggshell membrane. Thirdly, the tracer was delivered continuously into the egg to attain a steady state enrichment and a high level of ^{13}C incorporation into intermediates, after which the embryo was immediately sampled. With the daily bolus injection of tracer, it was unknown at the time of embryo sampling (3-5 h after dosing) whether tracer enrichment had remained steady. In

fact, in our previous work, large variations in substrate enrichments existed among embryos and resulted in elimination of data. And, lastly, the amount of tracer continuously infusion was administrated at a rate typically employed in humans and animals, Herein, the amount of tracer glucose infused represented about 18% of the blood glucose pool.

When [U-^{13}C] glucose was infused (Exp. 1), both blood and liver [M+3] and [M+6] glucose enrichments were lower in e19 embryos. This suggests an increased synthesis of glucose from other sources (i.e., unlabelled), which resulted in greater dilution of the [M+3] and [M+6] glucose enrichments. Higher glucose entry and greater Cori cycling and gluconeogenesis on both an absolute (blood and liver precursor pools) and body weight (liver precursor pool)-adjusted basis were observed in e19 compared to e14 embryos in Exp.1. This pattern of change in gluconeogenesis is consistent with known changes in corticosterone, an activator of gluconeogenesis. In the study of Scott et al. (1981), corticosterone increased rapidly from e10-e14 until e16, and remained at a higher level through to e18, with a tendancy to increase up to e20. Further, the ratio of insulin to glucagon also increases during this period, which serves to promote the deposition of glucose into tissue glycogen (Lu et al., 2007). In consequence, higher gluconeogenesis in later developmental age leads to greater supply of glucose for glycogen accumulation in the liver and muscles. These observations are also in agreement with the earlier study (Chapter 3) where AMPK activity was highest on e14. Higher AMPK activity is expected to reduce the activity of energy consuming pathways, e.g., gluconeogenesis, while enhancing energy generating pathways. Moreover, the increased glucose entry rate on an absolute basis also suggested more glucose and glycogen synthesis as embryo weight increased.

In Exp.2, when eggs were infused with [U-^{13}C] glycerol, a higher contribution of glycerol to gluconeogenesis was observed in e19 compared to e14 embryos. The appearance of ^{13}C from

glycerol in glucose has been used to estimate the contribution of glycerol to gluconeogenesis (Kalhan and Parimi, 2000). However, current estimates of the contribution of glycerol to glucose synthesis are variable. Studies in healthy term infants during the first 48 h after birth found that the contribution of glycerol accounted for 10-20% of glucose synthesized (Bougneres et al., 1982; Pater et al., 1992; Sunehag et al., 1996a). In extremely preterm infants on the first day after birth, gluconeogenesis from glycerol was much lower and ranged from 1.7-37.6%, with a median value of 5% (Sunehag et al., 1996b). The e19 chicken embryo might be considered to be at a similar physiological state as the preterm infant. In this respect, the finding in the e19 chicken embryo that glycerol contributes only 2.1% (1.3-6.0%) to gluconeogenesis would appear to be consistent with that of the preterm infant. In addition, these results further demonstrate that other substrates, such as amino acids and lactate, make a more substantial contribution to gluconeogenesis at this stage of embryo development.

In young and adult animals, glucose is an important contributor to NEAA synthesis (Pascual et al., 1998). Metabolism of glucose leads to significant distribution of its carbon skeletons throughout the glycolytic pathway and in the Krebs cycle where carbon skeletons are used for NEAA synthesis. In the estimate of blood glucose to liver NEAA synthesis in Exp.1, the contribution of glucose to alanine, aspartate and glutamate synthesis decreased as the embryo developed. Although the proportional contribution of glucose to NEAA synthesis was comparable to another study (Sunny and Bequette, 2010), this observation is not consistent with the original hypothesis that NEAA synthesis would be promoted as the embryo grows. The possible explanation is that by e14, the embryo is structurally completed (Moran, 2007). The embryos require a large amount of amino acids for tissue protein gain whereas by e19, embryo protein mass reaches the maximum. More NEAA for protein synthesis would be demanded for

the rapid growth of e14 embryos. The contribution of blood glucose to NEAA synthesis was higher in e14 embryos demonstrated that glucose was spared for glycogen accumulation in e19 embryos. In fact, the isotopic profiles of [M+1], [M+2], and [M+3] liver alanine, aspartate and glutamate also showed a higher incorporation of glucose carbon by e14 embryos.

The synthesis of glutamate from 3-carbon substrates (i.e., lactate and pyruvate) arises from oxaloacetate. Thus, pyruvate is converted to oxaloacetate via PC for entry into the Krebs cycle. The contribution of blood lactate and alanine to the synthesis of [M+3] glutamate was found to be higher in e14 than e19 embryos, whereas the ratio was lower in e14 embryos when considering liver alanine as the 3-carbon pool (Exp. 1). Although this needs to be further confirmed due to limited replicates, it certainly provides preliminary information on the contribution of 3-carbon substrates to the synthesis of NEAA.

In Exp. 2 when [U-^{13}C] glycerol was the tracer, the proportions of alanine, aspartate and glutamate derived from the 3-carbon pool was relatively smaller compared to Exp.1, where the contribution of other 3-carbon sources to NEAA production was estimated. The contribution of glycerol to alanine, aspartate and glutamate synthesis was higher in e19 versus e14 embryos. A higher contribution of glycerol to glucose synthesis was also observed in e19 embryos. One explanation is that on e14, when there is a large demand for energy for embryo development, glycerol that is liberated from yolk triglycerides is metabolized in the Krebs cycle to produce energy.

The synthesis of [M+2] glutamate arises primarily via decarboxylation of [M+3] substrates (pyruvate) by action of PDH to form [M+2] acetyl-CoA. While [M+3] glutamate can only be derived from [M+3] pyruvate via PC, the ratio of [M+3] glutamate and [M+2] acetyl-

CoA gives a direct measure of PC versus PDH activity. The ratio of PC to PDH activity was higher in e14 embryos regardless of whether the estimation employed glucose or glycerol as the tracer. Relatively lower activity of PDH in e14 embryos indicated less production of acetyl-CoA from 3-carbon substrates. Therefore, the acetyl-CoA pool must derive from other sources, such as via fatty acid β-oxidation. The latter conclusion is consistent with calorimetric measurements of developing chicken embryos. Hamidu et al. (2007) measured respiratory quotient (RQ) of developing eggs and observed the RQ to be lower for e14 compared to e19 embryos. A low RQ (e.g., 0.7) represents a high level of fatty acid oxidation compared to a high RQ (e.g., 1.0) where carbohydrates are predominately oxidized, as the former requires a greater O_2 supply.

In summary, higher glucose entry rate, Cori cycling, and gluconeogenesis were observed in e19 compared to e14 embryos. The contribution of glucose to NEAA synthesis was higher in e14 than in e19 embryos. These metabolic shifts are consistent with the rapid development of the embryo at e14 and the high demands for glycogen accumulation in e19 embryos. The higher rate of lipolysis (glycerol turnover) and contribution of glycerol to both gluconeogenesis and NEAA synthesis in e19 embryos indicates that glycerol is an important anaplerotic substrate in the Krebs cycle at this stage. The two metabolic probes employed in this study, i.e., [U-^{13}C] glucose and [U-^{13}C] glycerol, provided rich information about the developmental adaptations in gluconeogenesis, the Krebs cycle and activities of related pathways. Results based on [U-^{13}C] glucose infusion highlighted the importance of glucose carbon recycling and the utilization of several substrates that contribute to the 3-carbon precursor pool for synthesis of NEAA and acetyl-CoA. The results based on the [U-^{13}C] glycerol tracer provide strong evidence of the changing role of lipolysis in provision of fatty acids for energy, and the utilization of triglyceride glycerol for gluconeogenesis and NEAA synthesis. The constant tracer infusion approach

developed in this study is also valuable for investigating other aspects of embryo metabolism and pathway activities. For example, glycine, serine and threonine metabolism that differed in the liver metabolism in eggs from young versus old hens using [U-^{13}C] threonine.

Summary and Conclusions

This thesis research aimed to determine the influences of egg size and hen age on embryo development, and whether metabolic events are altered accordingly to allow for adaptations at different developmental ages and nutrient environments. Three experiments were conducted with the objective to investigate embryo metabolism and substrate partition in response to nutrient (egg yolk and albumen) availability and physiological stage. Western blot and ELISA were used to determine AMPK activity, and metabolomic profiling was applied to compare embryo metabolism in eggs of two sizes and from different ages of hens. A constant stable isotope infusion approach was employed for delivery of [U-^{13}C] glucose and [U-^{13}C] glycerol into the chorio-allantoic fluid of e14 and e19 embryos to quantify gluconeogenesis and substrate partition and utilization in the Krebs cycle and related pathways.

The results demonstrated that activity of the energy-sensor, AMPK, was higher in large compared to small eggs, and activity peaked on e14 in both size eggs. This suggests greater energy demand in embryos from large eggs to support their more rapid growth during later term development. Liver metabolism differed in e14 and e20 embryos from 32 wk compared to 51wk-old hens, but was not found to be different in embryos from small versus large eggs. The residual yolk contained a higher proportion of oleic acid and linolenic acid in eggs from older hens. This suggests that hen age influences the deposition of fatty acids into the yolk which subsequently affects embryo development and nutrient utilization. Moreover, embryo metabolism underwent dramatic changes as the embryo developed and displayed an interesting pattern with respect to different developmental ages. For example, metabolism was distinctly different between posthatch day 1hatchlings and embryos on e14, e17 and e20. This observation supported our hypothesis that embryo metabolism adapts to different egg nutrient compositions (yolk and

albumen) and physiological stages that enables normal and maximum embryo growth *in ovo*. In consequence, chicks would be prepared metabolically to face different nutrient environments at hatch.

During later development, the ability of the embryo to utilize substrates derived from 3-carbon sources or from amino acids to synthesize glucose increased as the embryo developed. This is consistent with the observations that gluconeogenesis increased from e14 to e19. These observations are also consistent with other studies that glucose synthesis is promoted for glycogen storage close to the time of hatching. Mass isotopomer distribution patterns of NEAA in liver indicated that glucose carbon made a larger contribution to NEAA synthesis in e14 compared to e19 embryos. At this critical developmental age, the embryo is structurally complete but requires a significant supply of amino acids for tissue protein expansion. Glycerol's contribution to glucose synthesis was only ~5%, and the contribution of glycerol to glutamate synthesis was relatively small compared to other 3-carbon substrates, e.g. lactate, alanine. The comparative activities of pyruvate carboxykinase (PC) and pyruvate dehydrogenase (PDH) in the liver determine the partition of 3-carbon substrates to produce either oxaloacetate or acetyl-CoA, respectively. Our observation that the ratio of PC to PDH was higher in e14 than in e19 embryos suggests that a greater proportion of acetyl-CoA flux in the e14 embryo liver derives from fatty acid metabolism rather than from 3-carbon substrates.

Although previous studies have assessed the effects of egg size or maternal age on embryo development and hatchability, the two factors were often confounding. It was not clear from these studies the actual influence of egg size, and hen age *per se* on embryo metabolism and development. Hence, the experiments in this thesis were specifically designed to study the separate effects of egg size and hen age on embryo metabolism and growth. To our knowledge,

quantitative information on embryo metabolism still remains limited, especially the lack of data on the metabolic adaptations of the developing embryo. In addition, there is a lack of information on substrate utilization by developing chicken embryos when egg nutrient composition is different, i.e. higher yolk to albumen ratio in eggs from old hens. The results from this thesis allow for a better understanding of which of the two, hen age or egg size, has a greater influence on embryo development. Knowledge of nutrient partition and utilization in developing chicken embryos will provide a better view of how and whether the embryos adapts to changing nutrient environments and physiological states. The metabolomic profiling and *in ovo* constant stable isotope infusion approaches employed in this thesis could also be applied using alternative metabolic probes to better understand embryo metabolism *in vivo*. For example, [U-^{13}C] threonine can be used to study glycine, serine and threonine metabolism. This metabolic pathway is known to be central in support of embryonic stem cell proliferation, and glycine metabolism is essential to support purine nucleotide biosynthesis *de novo*.

Appendix a, b

a.

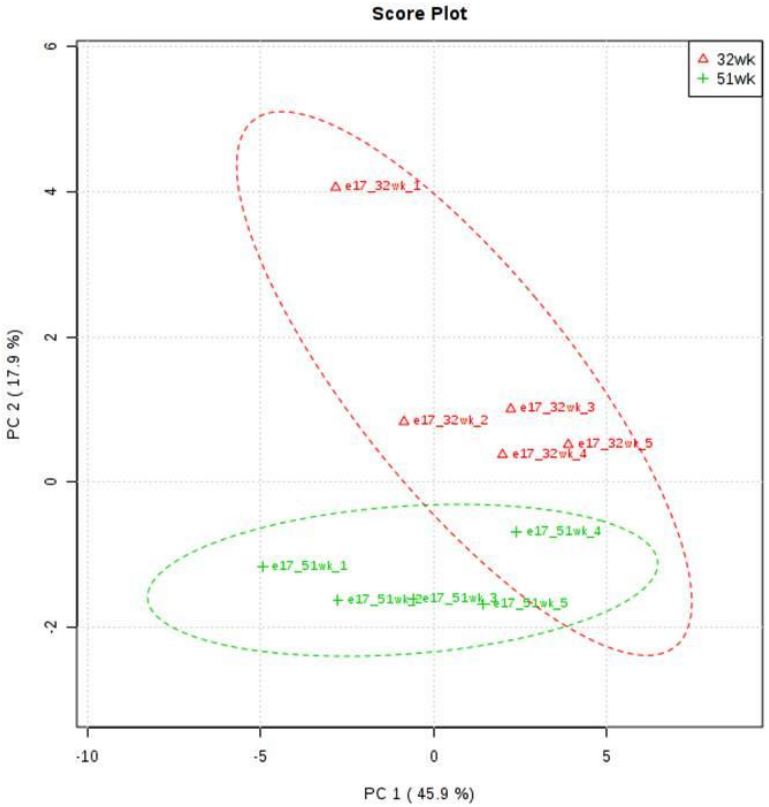

b.

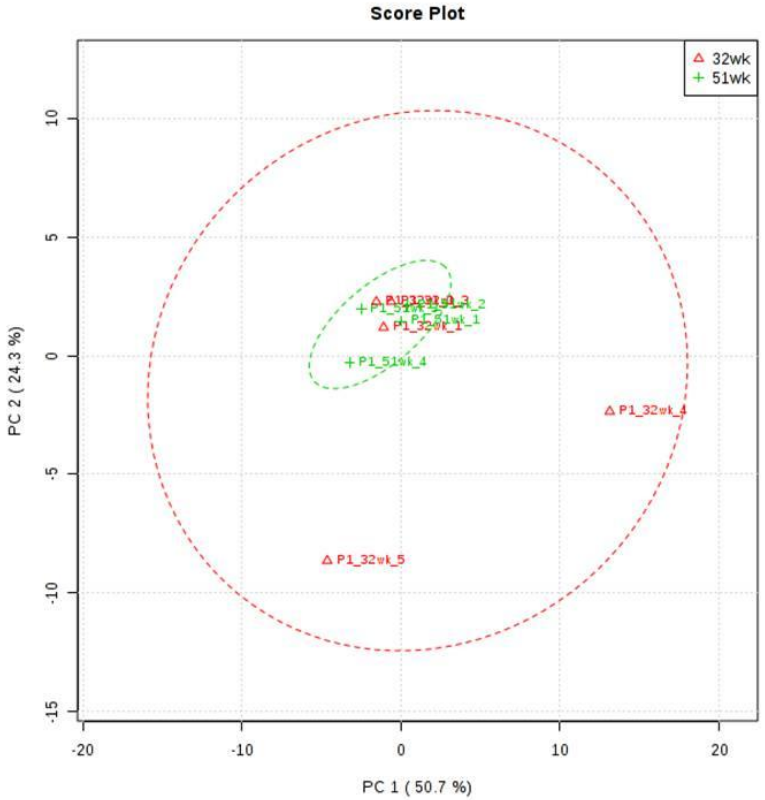

a. Principal component analysis (PCA) of e17 metabolomic profile (Exp. 1). The first three characters represent the embryo developmental age (e17) followed by age (32 wk-, 51 wk-) and replicates (1-5 samples). **b.** PCA of posthatch day 1 metabolomic profile (Exp. 1). The first three characters represent the embryo developmental age (P1) followed by age (32 wk-, 51 wk-) and replicates (1-5 samples). PCA score plot cannot distinguish the metabolic profiles of liver metabolites in eggs from 32 wk (Δ) *vs* 51 wk (+) old hens on e17 and posthatch day 1.

Appendix c, d

c.

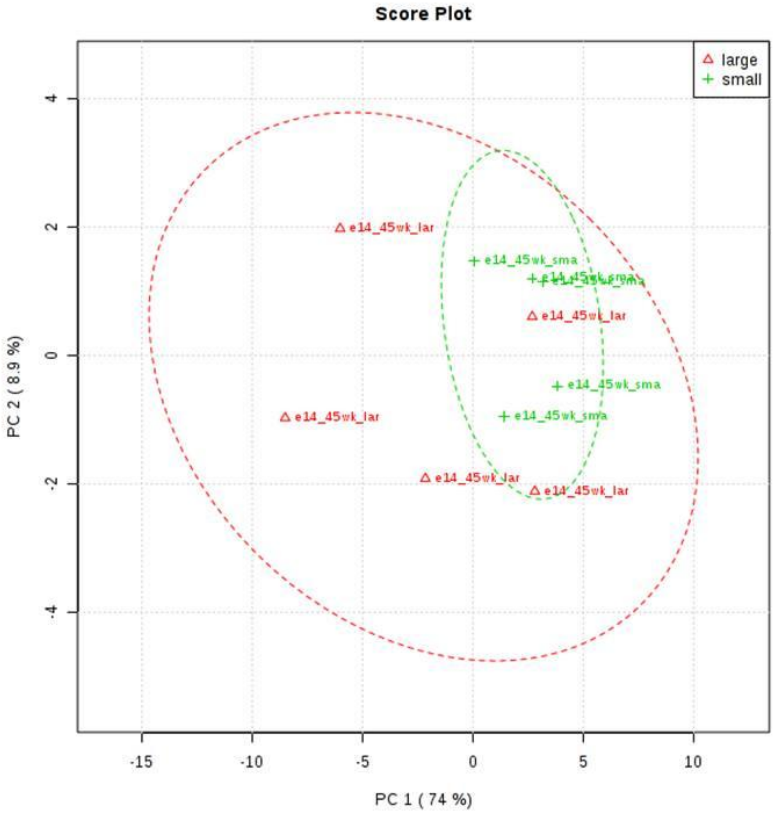

d.

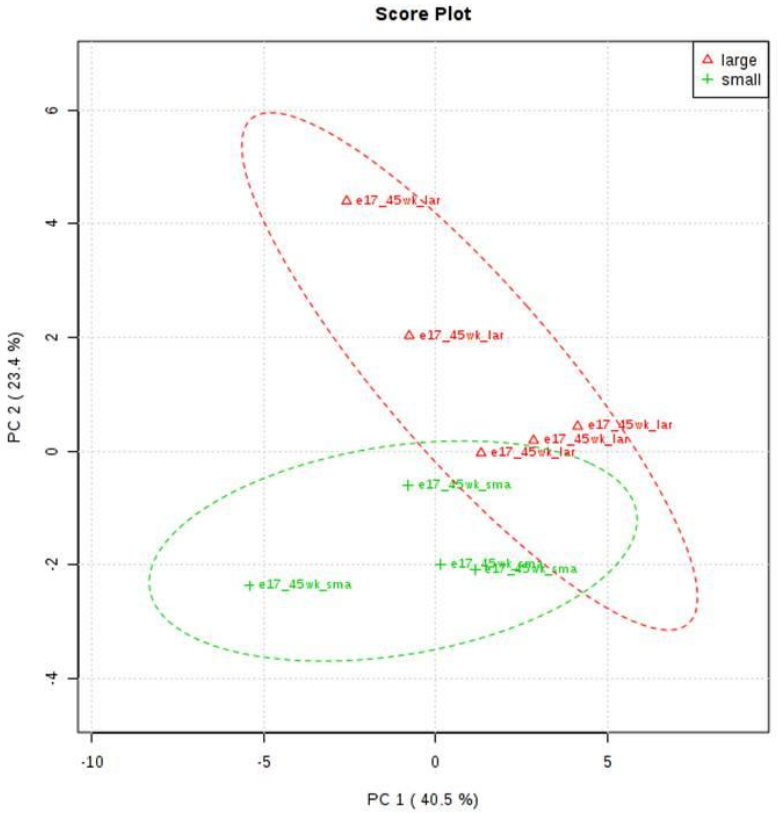

c. Principal component analysis (PCA) of e14 liver metabolomic profile (Exp. 2). The first three characters represent the embryo developmental age (e14) followed by age (45 wk-) and size and replicates (small, large, 1-5 samples). **d.** PCA of e17 liver metabolomic profile (Exp. 2). The first three characters represent the embryo developmental age (e17) followed by age (45 wk-) and size and replicates (small, large, 1-5 samples). PCA score plot cannot distinguish the metabolic profiles of liver metabolites in eggs of small (+) *vs* large (Δ) on e14 and e17.

Appendix e, f

e.

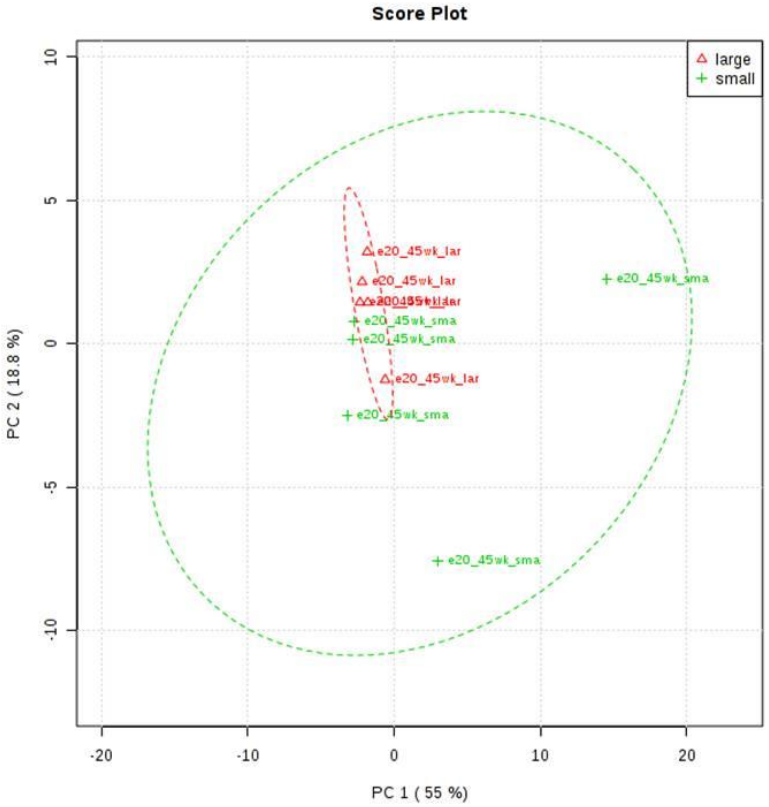

f.

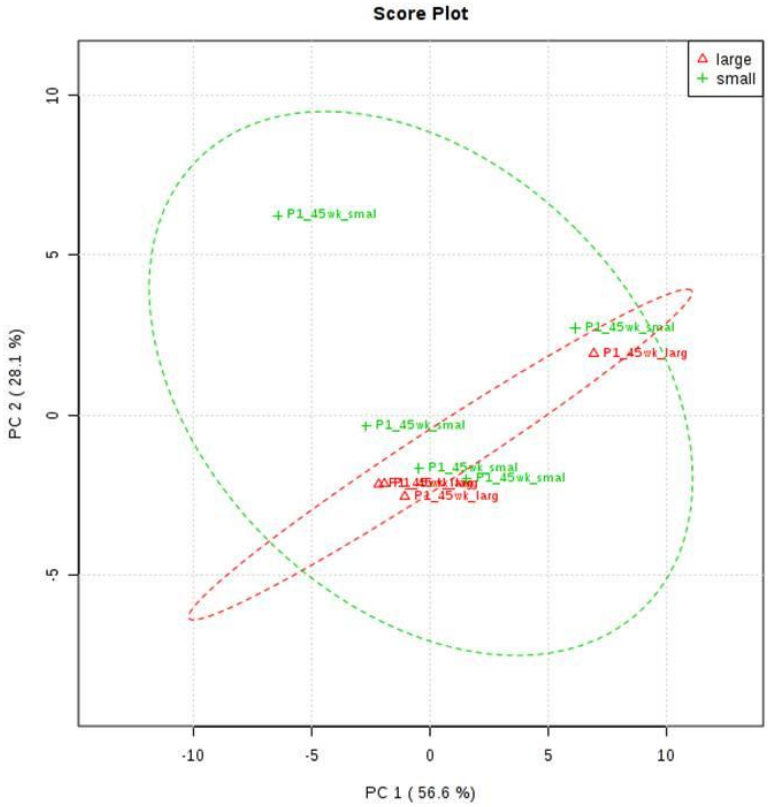

e. Principal component analysis (PCA) of e20 liver metabolomic profile (Exp. 2). The first three characters represent the embryo developmental age (e20) followed by age (45 wk) and size and replicates (small, large, 1-5 samples). **f.** PCA of posthatch day 1 liver metabolomic profile (Exp. 2). The first three characters represent the embryo developmental age (e17) followed by age (45 wk) and size and replicates (small, large, 1-5 samples). PCA score plot cannot distinguish the metabolic profiles of liver metabolites in eggs of small (+) *vs* large (Δ) on e20 and posthatch day 1.

Appendix g, h

g. **h.**

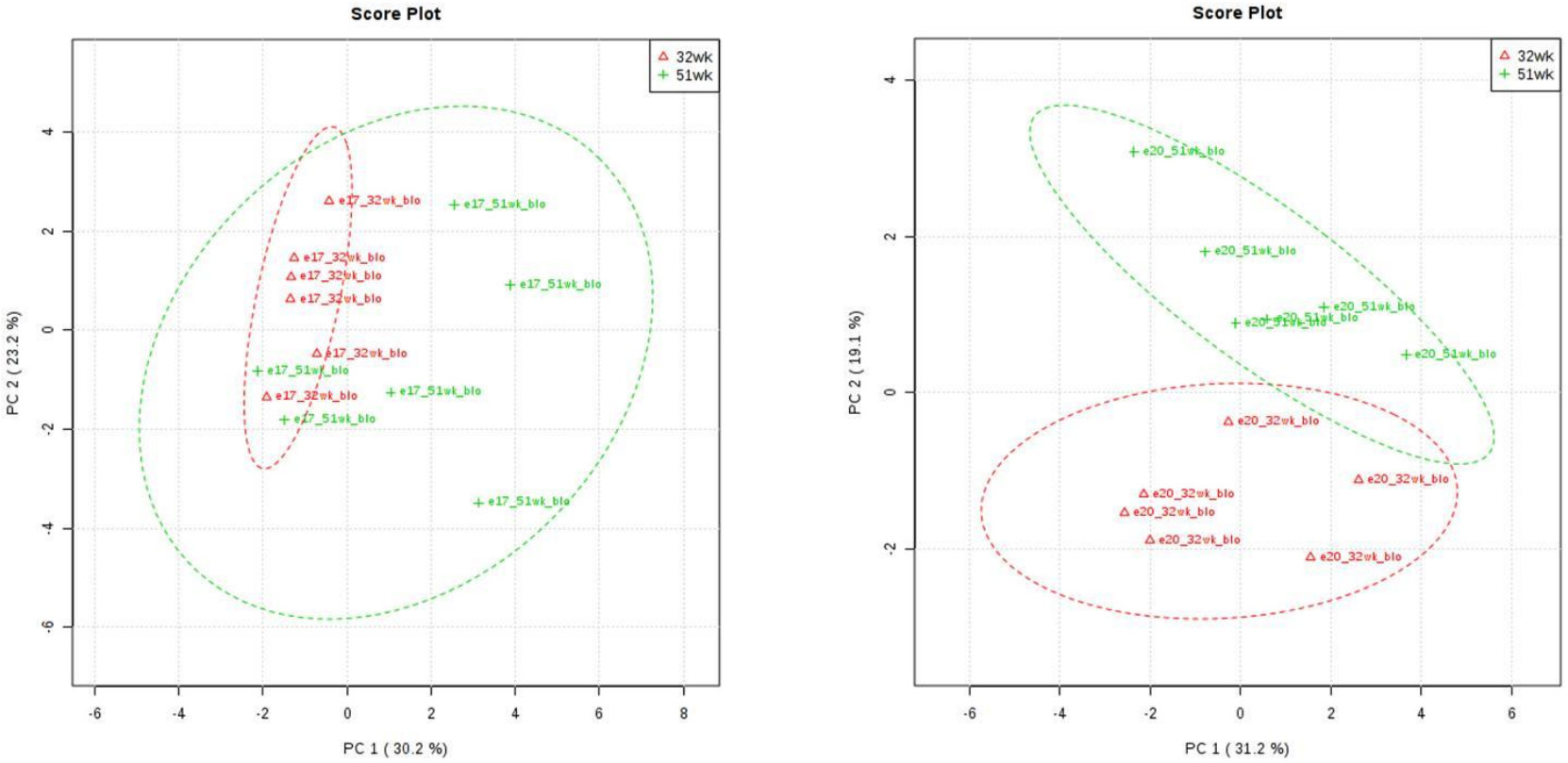

g. Principal component analysis (PCA) of e17 blood metabolomic profile (Exp. 1). The first three characters represent the embryo developmental age (e17) followed by age (51 wk, 32 wk) and replicates (1-5 samples). **h.** PCA of e20 blood metabolomic profile (Exp. 1). The first three characters represent the embryo developmental age (e20) followed by age (51 wk, 32 wk) and replicates (1-5 samples). PCA score plot cannot distinguish the metabolic profiles of liver metabolites in eggs from 32 wk (Δ) *vs* 51 wk (+) on e17 and e20.

Appendix i

i.

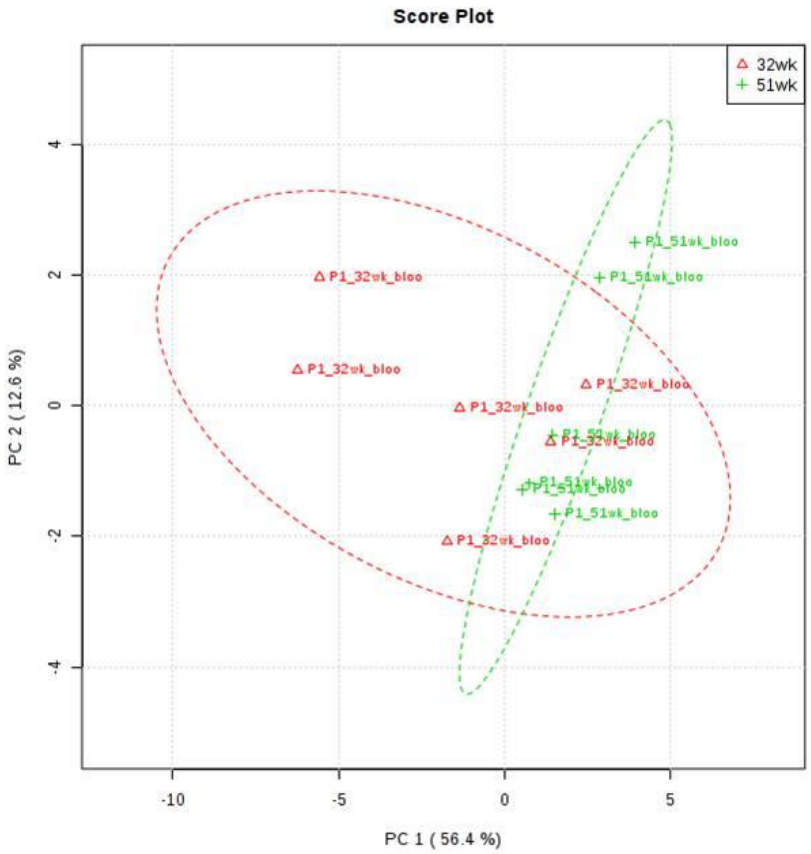

i. Principal component analysis (PCA) of posthatch day 1 blood metabolomic profile (Exp. 1). The first three characters represent the embryo developmental age (P1) followed by age (51 wk, 32 wk) and replicates (1-5 samples). PCA score plot cannot distinguish the metabolic profiles of liver metabolites in eggs from 32 wk (Δ) *vs* 51 wk (+) on posthatch day 1.

Appendix j, k

j. **k.**

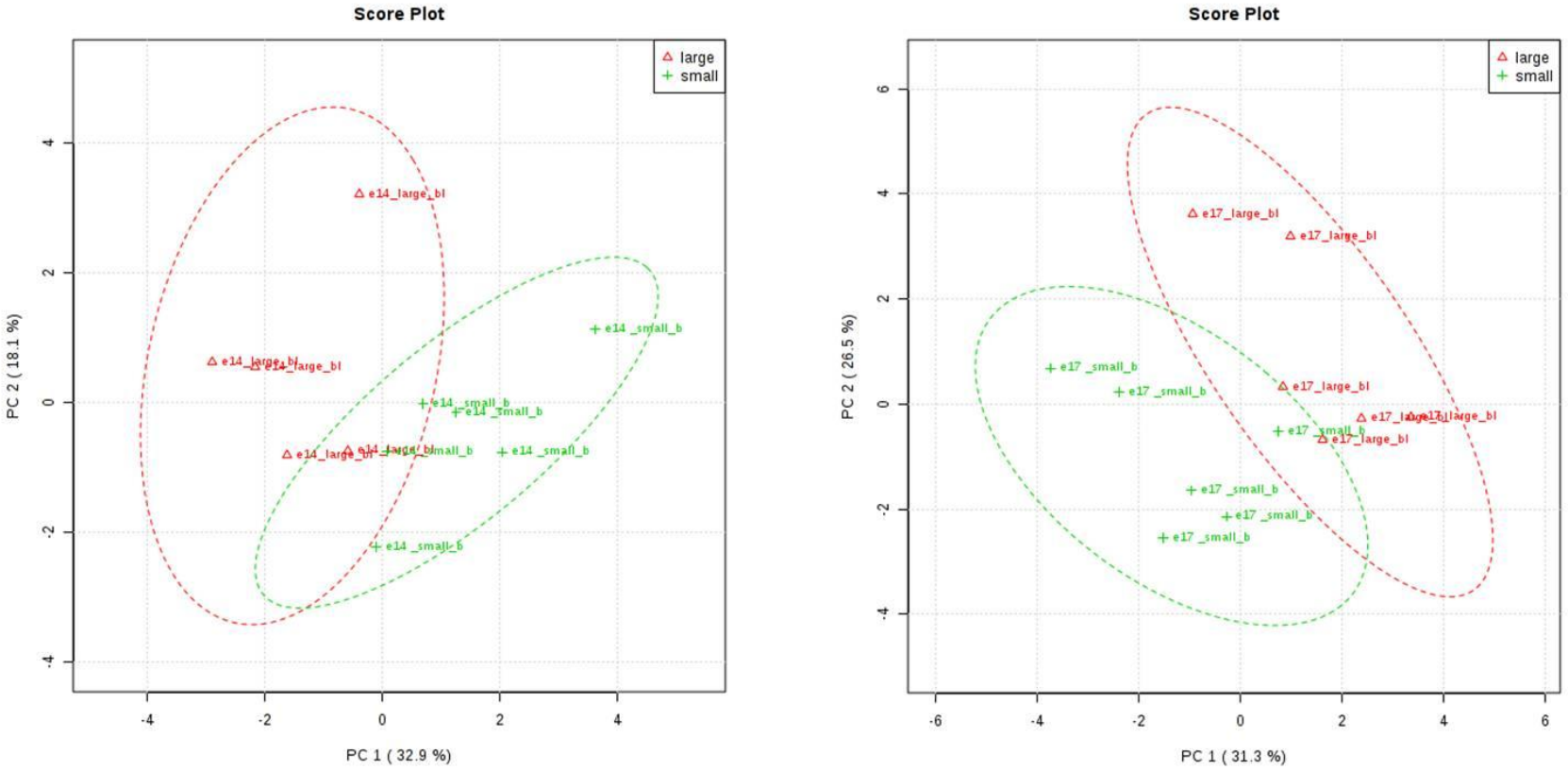

j. Principal component analysis (PCA) of e14 blood metabolomic profile (Exp. 2). The first three characters represent the embryo developmental age (e14) followed by size (small, large) and replicates (1-5 samples). **k.** PCA of e17 blood metabolomic profile (Exp. 2). The first three characters represent the embryo developmental age (e17) followed by size (small, large) and replicates (1-5 samples). PCA score plot cannot distinguish the metabolic profiles of blood metabolites in eggs of small (+) *vs* large (Δ) on e14 and e17.

Appendix l, m

l.

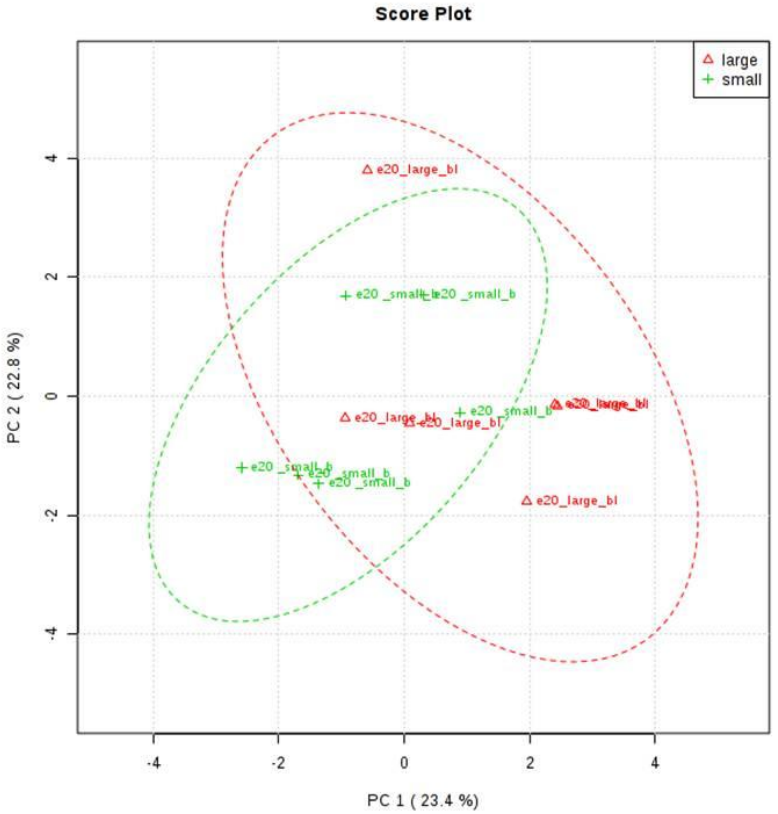

m.

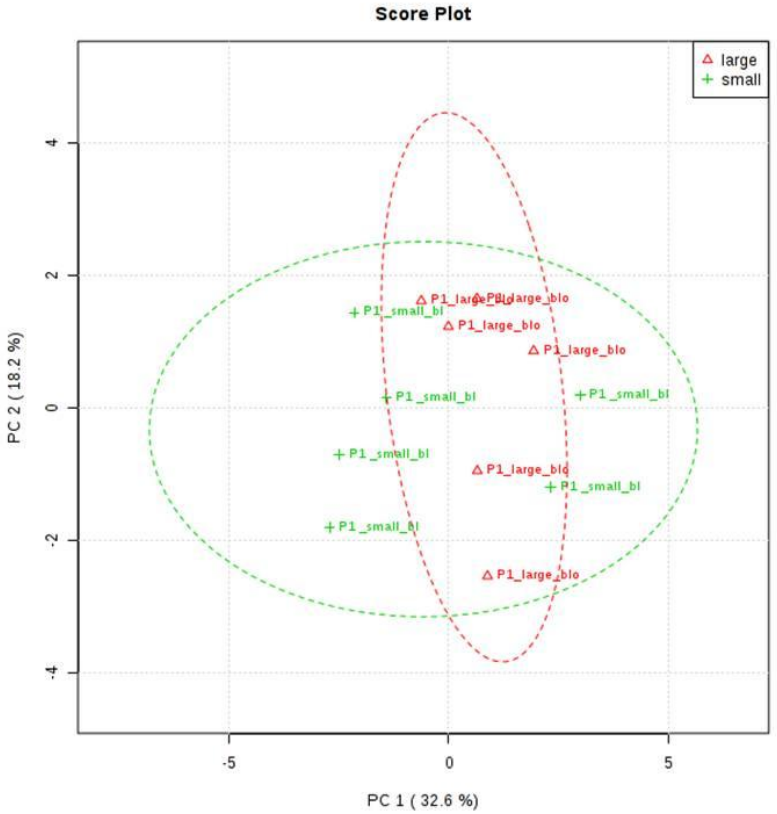

l. Principal component analysis (PCA) of e20 blood metabolomic profile (Exp. 2). The first three characters represent the embryo developmental age (e20) followed by size (small, large) and replicates (1-5 samples). **m.** PCA of posthatch day 1 blood metabolomic profile (Exp. 2). The first three characters represent the embryo developmental age (P1) followed by size (small, large) and replicates (1-5 samples). PCA score plot cannot distinguish the metabolic profiles of blood metabolites in eggs of small (+) *vs* large (Δ) on e20 and posthatch day 1.

Bibliography

Anderson, G. J., W. E. Connor, and J. D. Corliss. 1990. Docosahexaenoic acid is the preferred dietary n-3 fatty acid for the development of the brain and retina. Pediatr. Res. 27: 89-97.

Applegate, T. J., and M. S. Lilburn, 1996. Independent effects of hen age and egg size on incubation and poult characteristics in commercial turkeys. Poult. Sci. 75: 1210-1216.

Alton, G., M. Hasilik, R. Niehues, K. Panneerselvam, J.R. Etchison, F. Fana, and H. H. Freeze. 1997. Direct utilization of mannose for mammalian glycoprotein biosynthesis. Glycobiol. 8(3): 285-295.

Baumann, R., and H. J. Meuer. 1992. Blood oxygen transport in the early avian embryo. Physiol. Rev. 72: 941-965.

Becker, D., and J. B. Lowe. 2003. Fucose: biosynthesis and biological function in mammals. Glycobiol. 13(7): 41R-53R.

Bellabarba, D., S. Belisle, N. Gallo-Payet, and J.G. Lehoux, 1988. Mechanism of action of thyroid hormones during chick embryogenesis. Am. Zool. 28: 389-399.

Bequette, B. J., N.E. Sunny, S.W. El-Kadi, and S.L. Owens. Application of stable isotopes and mass isotopomer distribution analysis to the study of intermediary metabolism of nutrients. J. Anim. Sci. 2006;84(E. Suppl.): E50-E59.

Berasi, S. P., C. Huard, D. Li, H. H. Shih, Y. Sun, W. Zhong, J. E. Paulsen, E. L. Brown, R. E. Gimeno, and R. V. Martinez, 2006. Inhibition of gluconeogenesis through transpcriptional activation of EGR1 and DUSP4 by AMP-activated kinase. J. Biol. Chem. 281(37): 27167-27177.

Berthold, H. K., L.J. Wykes, F. Jahoor, P. D. Klein, and P. J. Reeds, 1994. The use of uniformly labeled substrates and mass isotopomer analysis to study intermediary metabolism. Pro. Nutr. Soc. 53: 345-354.

Berthold, K.H., P.F. Crain, I.Gouni, P.J. Reeds, and P.D. Klein. 1995. Evidence for incorporation of intact dietary pyrimidine (but not purine) nucleosides into hepatic RNA. Proc. Natl. Acad. Sci. 92: 10123-10127.

Bougnères, P. F., I. E. Karl, L. S. Hillman, and D. M. Bier, 1982. Lipid transport in the human newborn: palmitate and glycerol turnover and the contribution of glycerol to neonatal hepatic glucose output. J. Clin. Invest. 70: 262-270.

Brady, L. J., D. R. Romsos, and G. A. Leveille. 1979. Gluconeogenesis in isolated chicken (*Gallus domesticus*) liver cells. Comp. Biochem. Physiol. B 63: 193-198.

Brunengraber, H., J. K. Kelleher, and C. Des Rosiers. 1997. Applications of mass isotopomer analysis to nutrition research. Annu. Rev. Nutr. 17: 559-96.

Bryk, S. G., and Z. G. Gheri. 1990. On the development of the chick embryo colon: A computerized morphometric study. Z. Mikrosk. Anat. Forsch. 104: 97-118.

Burley, R.W., and D. V. Vadehra. 1989. The avian egg: Chemistry and Biology. John Wiley & Sons.

Burton, F.G., and Tullett, S.G., 1985. Respiration of avian embryos. Comp. Biochem. Physiol. 82: 735-744.

Carsia, R.V., M. E. Morin, H. D. Rosen, and H. Weber 1987 Ontogenic corticosteroidogenesis of the domestic fowl: response of isolated adrenocortical cells. Proc. Soc. Exp. Biol. Med., 184: 436-445.

Cherian, G., and J. S. Sim. 1992. Preferential accumulation of n-3 fatty acids in the brain tissue of chicks from n-3 fatty acid enriched eggs. Poult. Sci. 71: 1658-1668.

Christensen, V. L., W. E. Donaldson, and J. P. McMurtry, 1996. Physiological differences in late embryos from turkey breeders at different ages. Poult. Sci. 75:172-178.

Christensen, V. L., J. L. Grimes, W. E. Donaldson, and S. Lerner. 2000. Correlation of body weight with hatchling blood glucose concentration and its relationship to embryonic survival. Poult. Sci., 79:1817-1822.

Christensen, V. L., M. J. Wineland, G. M. Fasenko, and W. E. Donaldson. 2001. Egg storage effects on plasma glucose and supply and demand tissue glycogen concentrations of broiler embryos. Poult. Sci. 80: 1729–1735.

Cogburn, L. A., S. S. Liou, C. P. Alfonso, M. C. McGuinness, and J. P. McMurtry. 1989. Dietary thyrotropin-releasing hormone stimulates growth rate and increases the insulin: Glucagon molar ratio of broiler chickens. Proc. Soc. Exp. Biol. Med. 192: 127-134.

Connolly, C. C., K. E. Steiner, R. W. Stevenson, D. W. Neal, P. E. Williams, K. G. M. M. Alberti, and A. D. Cherrington, 1991. Regulation of glucose metabolism by norepinephrine in conscious dogs. Am. J. Physiol. Endocrinol. Metab. 261:E764–E772.

Davison, J. M., and G. A. Cheyne. 1974. History of the measurement of glucose in urine: a cautionary tale. Med. Hist. 18: 194-197.

Deeming, D. C. 1989. Importance of sub-embryonic fluid and albumen in the embryo's response to turning of the egg during incubation. Br. Poult. Sci. 30: 591-606.

Deeming, D. C., and M. W. Ferguson. 1991. Egg incubation: Its effects on embryonic development in birds and reptiles. Cambridge University Press.17-28.

De Oliveira, J. E., Z. Uni, and P. R. Ferket. 2008. Important metabolic pathways in poultry embryos prior to hatch. World's Poult. Sci. 64: 488-499.

De Pablo, F., L. A. Scott, and J. Roth. 1990. Insulin and insulin-like growth factor I in early development: peptides, receptors and biological event. Endocr. Rev. 11: 558-577.

Dickson, A. J., and D. R. Langslow. 1978. Hepatic gluconeogenesis in chickens. Mol. Cell. Biochem. 22:167–181.

Donaldson, W. E., and V. L. Christensen. 1991. Dietary carbohydrate level and glucose metabolism in turkey poults. Comp. Biochem. Physiol. A 98: 347-350.

Dunn, W. B., D. Broadhurst, P. Begley, E. Zelena, S. Francis-McIntyre, N. Anderson, M. Brown, J. D. Knowles, A. Halsall, J. N. Haselden, A. W. Nicholls, I. D. Wilson, D. B. Kell, R. Goodacre, and The human serum metabolome (HUSERMET) Consortium, 2011. Procedures for large-scale metabolic profiling of serum and plasma using gas chromatography and liquid chromatography coupled to mass spectrometry. Nat. Prot. 6 (7): 1060-1083.

Dunn, W.B., A. Erban, R.J.M. Weber, D. J. Darren, M. Brown, R. Breitling, T. Hankemeier, R. Goodacre, S. Neumann, J. Kopka, and M.R. Viant. 2013. Mass appeal: metabolite identification in mass spectrometry-focused untargeted metabolomics. Metabolomics. 9: S44-S66.

Escobar, J., J. W. Frank, A. Suryawan, H. V. Nguyen, S. R. Kimball, L. S. Jefferson, and T. A. Davis. 2006. Regulation of cardiac and skeletal muscle protein synthesis by individual branched-chain amino acids in neonatal pigs. Am. J. Physiol. 290: E612-E621.

Farkas, K., I. A. J. Ratchford, R. C. Noble, and B. J. Speake. 1996. Changes in the size and docosahexaenoic acid content of adipocytes during chick embryo development. Lipids. 31: 313-321.

Fazeka, S., G. Feher, L. Kondics, I. Ovary, and V. Szekessy-Hermann. 1985. Purification and properties of myosin from the “haching mucscle” (*M. complexus*) of geese. Acta. Physiol. Hung. 66: 5-25.

Fernandez, C. A., C. Des Rosiers, S. F. Previs, F. David, and H. Brunengraber, 1996. Correction of ^{13}C mass isotopomer distributions for natural stable isotope abundance. J. Mass. Spectrom. 31: 255-262.

Fiehn, O., and J. Spranger. 2002. Can metabolomics be used for assessing nutritive-dependent human diseases? Phytochem. Rev. 1: 223-230.

Freeman, B. M. 1969. The mobilization of hepatic glycogen in Gallus domesticus at the end of incubation. Comp. Biochem. Physiol. 28: 1169-1176.

Freeze, H. H., and Sharma, V. 2010. Metabolic manipulation of glycosylation disorders in humans and animal models. Semin.Cell Dev. Biol. 21 (6): 655–662.

Garcia, F. J., A. Pons, M. Alemany, and A. Palout. 1986. Tissue glycogen and lactate handling by the developing domestic fowls. Comp. Biochem. Physiol. A 85: 155-159.

Getty, C. M., A. A. Baratta, and R. N. Dilger. 2013. Metabolomic profiling of the small for gestational age piglet. FASEB. J. 27: 1073. 15.

Goodridge, A. G. 1973. Regulation of fatty acid synthesis in the liver of prenatal and early postnatal chicks. J. Biol. Chem. 248: 1939-1945.

Hamidu, J. A., G. M. Fasenko, J. J. R. Feddes, E. E. O'Dea, C. A. Ouellette, M. J. Wineland, and V. L. Christensen, 2007. The effect of broiler breeder genetic strain and parent flock age on eggshell conductance and embryonic metabolism. Poult. Sci. 86: 2420-2432.

Hall, J.E. 2012. Guyton and Hall textbook of medical physiology. Unit 14: Endocrinology and reproduction. 12th edition, Publisher: Elsevier. Available from https://www.inkling.com/read/textbook-of-medical-physiology-guyton-hall-12th/chapter-77/functions-of-the-glucocorticoids

Hardie, D.G. 2007a. AMP-activated / SNF1 protein kinases: conserved guardians of cellular energy. Nature Rev. Mol. Cell Biol. 322: 37-42.

Hardie, D.G. 2007b. AMPK and Raptor: matching cell growth to energy supply. Mol. Cell 30: 263-265.

Harper, A. E., R. H. Miller, and K. P. Block, 1984. Branched-chain amino acid metabolism. Ann. Rev. Nutr. 4: 409-454.

Harvey, S., C. D. M. Johnson, and E. J. Sanders. 2001. Growth hormone in neural tissue of the chick embryo. J. Endocrinology 169: 487-498.

Havenstein, G. B., P. R. Ferket, and M. A. Qureshi. 2003a. Growth, Livability and Feed Conversion of 1957 *vs* 2001 Broilers when fed representative 1957 and 2001 Broiler diets1 Poult. Sci 82: 1500-1508.

Havenstein, G. B., P. R. Ferket, and M. A. Qureshi. 2003b. Carcass composition and yield of 1957 *vs* 2001 broilers when fed representative 1957 and 2001 broiler diets. Poult. Sci 82: 1509-1518.

Havenstein, G. B., P. R. Ferket, J. L. Grimes, M. A. Qureshi, and K. E. Nestor. 2007. Comparison of the performance of 1966- versus 2003-type turkeys when fed representative

1966 and 2003 turkey diets: growth rate, livability, and feed conversion. Poult. Sci. 86: 232-40.

Hawley, S. A., M. Davison, A. Woods, S. P. Davies, R. K. Beri, D. Carling, and D. G. Hardie. 1996. Characterization of the AMP-activated protein kinase kinase from rat liver and identification of threonine 172 as the major site at which it phosphorylates AMP-activated protein kinase. J. Biol. Chem. 271: 27879-27887.

Hayward, L.S., and J. C. Wingfield. 2004. Maternal corticosterone is transferred to avian yolk and may alter offspring growth and adult phenotype. Gen. Comp. Endo., 135(3): 365-371.

Hazelwood, R. L.1971. Endocrine control of avian carbohydrate metabolism. Poult. Sci. 50: 9-18.

Hazelwood, R.L. 1986. Carbohydrate metabolism. In: Avian Physiology (Ed. P. D. Sturkie) pp.303-325. ISBN-13: 9780387961958, Springer Verlag, New York.

Heffron, C. M. Metallo, T. Muranen, H. Sharfi, A.T. Sasaki , D. Anastasiou, E. Mullarky , N. I. Vokes, M, Sasaki, R. Beroukhim, G. Stephanopoulos, A. H. Ligon, M. Meyerson, A. L. Richardson, L. Chin, G. Wagner, J. M. Asara, J. S. Brugge, L. C. Cantley, and M.G. Vander Heiden, 2011. Phosphoglycerate dehydrogenase diverts glycolytic flux and contributes to oncogenesis. Nat. Genet. 43 (9): 869-874.

Heitmann, R. N., W. H. Hoover, and C. J. Sniffen. 1973. Gluconeogenesis from amino acids in mature wether sheep. J. Nutr.103:1587-93.

Hellerstein, M. K., and R. A. Neese. 1999. Mass isotopomer distribution analysis at eight years: theoretical, analytic, and experimental considerations. Am. J. Physiol. 276: E1146-E1170.

Hoiby, M., A. Aulie, and P. O. Bjonnes. 1987. Anaerobic metabolism in fowl embryos during normal incubation. Comp. Biochem. Physiol. A 86: 91-94.

Humphery, B. D., and S. G. Rudrappa, 2008. Increased glucose availability activates chicken thymocyte metabolism and survival. J. Nutr. 138: 1153-1157.

Jain, M., R. Nilsson, S. Sharma, N. Madhusudhan, T. Kitami, A. L. Souza, R. Kafri, M. W. Kirschner, C. B. Clish, and V. K. Mootha. 2012. Metabolite profiling identifies a key role for glycine in rapid cancer cell proliferation. Science. 336: 1040-1044.

Joseph, N. S., and E. T. Moran, Jr. Effect of flock age and postemergent holding in the hatcher on broiler liver performance and further processing yield. J. Appl. Poult. Sci. 14: 512-520.

Jiang, G., and B. B. Zhang. 2003. Glucagon and regulation of glucose metabolism. Am. J. Physiol. Endocrinol. Metab. 284: E671-678.

Jiye A, J. Trygg, J.Gullberg, A. I. Johansson, P. Jonsson, H. Antti, S. L. Marklund, and T. Moritz, 2005. Extraction and GC/MS analysis of the human blood plasma metabolome. Anal. Chem. 77: 8086-8094.

Kahn, B. B., T. Alquier, D. Carling, and D. G. Hardie. 2005. AMP-activated protein kinase: Ancient energy gauge provides clues to modern understanding of metabolism. Cell Metab. 1: 15-25.

Kalhan, S.C., S. Mahajan, E. Burkett, L. Reshef, and R. W. Hanson. 2001. Glyceroneogenesis and the souce of glycerol for hepatic triacylglycerol synthesis in human. J. Biol. Chem. 276(16): 12928-12931

Kallecharan R., and B. K. Hall. 1974. A developmental study of the levels of progesterone, coritcosterone, cortisol, and cortisone circulating in plasma of chick embryos. Gen. Comp. Endocrinol. 24: 364-372.

Kalhan , S.C., 2001. Stable isotopic tracers for studies of glucose metabolism. J. Nutr. 126: 362S-368S.

Kalhan, S., and P. Parimi, 2000. Gluconeogenesis in the fetus and neonate. Semin. Perinatol. 24: 94-106.

Katz, J., W.-N. P. Lee, P. A. Wals, and E. A. Bergner. 1989. Studies of glycogen synthesis and the Krebs cycle by mass isotopomer analysis with [U-^{13}C] glucose in rats. J. Biol. Chem. 264 (22): 12994-13001.

Katz, J., and W.-N. P. Lee. 1991. Application of mass isotopomer analysis for determination of pathways of glycogen synthesis. Am. J. Physiol. Endocrinol. Metab. 261: E332-E336.

Koal, T., and H. P. Deigner. 2010. Challenges in mass spectrometry based targeted metabolomics. 2010. Curr. Mol. Med. 10(2): 216-226.

Kouremenos, K. A., J. J. Harynuk, W. L. Winniford, P. D. Morrison, and P. J. Marriott, 2010. One-pot microwave derivatization of target compounds relevant to metabolomics with comprehensive two-dimensional gas chromatography. J. Chromatogr. B, 878: 1761-1770.

Krebs, H.A. 1972. Some aspects of the regulation of fuel supply in omnivorous animals. Adv. Enzyme Regul. 10: 397-420.

Kubrusly, R.C.C, A. L. M. Ventura, R.A. de Melo Reis, G. C. F. Serra, E. N. Yamasaki, P.F.Gardino, M. C. F. de Mello, and F. G. de Mello, 2007. Norepinephrine acts as D1-dopaminergic agonist in the embryonic avian retina: Late expression of β1-adrenergic receptor shifts norepinephrine specificity in the adult tissue. Neurochem. Inter. 50: 211-218.

Kucera, P., E. Raddatz, and A. Baroffio. 1984. Oxygen and glucose uptake in the early chick embryo. Pages 299-309 in Respiration and Metabolism of Embryonic Vertebrates. R.S. Seymour, ed. W. Junk, Dordrecht, the Netherlands.

Kurland, I. J., A. Alcivar, S. Bassilian, and W-N. P. Lee, 2000. Loss of [^{13}C] glycerol carbon via the pentose cycle. J. Biol. Chem. 275: 36787-36793.

Lage, R., C. Diéguez, A. Vida-Puig, and M. López. 2008. AMPK: a metabolic gauge regulating whole-body energy homeostasis. Trends Mol. Med. 14 (12): 539-549.

Langslow, D. R., and R. J. Lewis. 1972. The compositional development of adipose tissue in *Gallus domesticus*. Comp. Biochem. Physiol. B 43: 681-688.

Langslow, D. R., G. Cramb, and K. Siddle. 1979. Possible mechanisms of the increased sensitivity to glucagon and catecholamines of chicken adipose tissue during hatching. Gen. Comp. Endocr. 39: 527-533.

Latour, M. A., E. D. Peebles, C. R. Boyle, S. M. Doyle, T. Pansky, and J. D. Brake. 1996. Effects of breeder hen age and dietary fat on embryonic and neonatal broiler serum lipids and glucose. Poult. Sci. 75:695–701.

Latour, M.A., E. D. Peebles, S. M. Doyle, T. Pansky, T. W. Smith, and C. R. Boyle, 1998. Broiler breeder age and dietary fat influence the yolk fatty acid profiles of fresh eggs and newly hatched chicks. Poult. Sci. 77: 47-53.

Leclercq, B. 1984. Adiposet tissue metabolism and its control in birds. Poult. Sci. 63: 2044-2054.

Levenberg, B., S. C. Hartman, and J. M. Buchanan. 1956. Biosynthesis of the purines. X. Further studies *in vitro* on the metabolic origin of nitrogen atoms 1 and 3 of the purine ring. J. Biol. Chem. 220: 379-390.

Levinsohn, E. M., D. S. Packard Jr., E. M. West, and D. R. Hootnick. 1984. Arterial anatomy of chicken embryo and hatchling. Am. J. Anat. 169: 377-405.

Lilburn, M. S. 1998. Practical aspects of early nutrition for poultry. J. Appl. Poult. Res. 7:420-424.

Lin, G., C. Liu, C. Feng, Z. Fan, Z. Dai, C. Lai, Z. Li, G. Wu, and J. Wang. 2012. Metabolomic analysis reveals differences in umbilical vein plasma metabolites between normal and growth-restricted fetal pig during late gestation. J. Nutr. 142: 990-998.

Litke, L. L., and F. N. Low. 1975. Scanning electron microscopy of yolk absorption in early chick embryos. Am. J. Anat. 142: 527-531.

Lobley, G. E. 1992. Control of the metabolic fate of amino acids in ruminants: a review. J. Anim. Sci. 70: 3264-3275.

Locasale, J.W., A. R. Grassian, T. Melman, C. A. Lyssiotics, K. R. Mattaini, A.J. Bass, G. Heffron, C. M. Metallo, T. Muranen, H. Sharfi H, A.T. Sasaki , D. Anastasiou, E. Mullarky, N. I. Vokes, M, Sasaki, R. Beroukhim, G. Stephanopoulos, A. H. Ligon, M. Meyerson, A. L. Richardson, L. Chin, G. Wagner, J. M. Asara, J. S. Brugge, L. C. Cantley, and M.G. Vander Heiden, 2011. Phosphoglycerate dehydrogenase diverts glycolytic flux and contributes to oncogenesis. Nat. Genet. 43 (9): 869-874.

Lochhead, P. A., I. P. Salt, K. S. Walker, D. G. Hardie, and C. Sutherland. 2000. 5-aminoimidazole-4-carboxamide riboside mimics the effects of insulin on the expression of the 2 key gluconeogenic genes PEPCK and glucose-6-phosphatase. Diabetes 49: 896–903.

Lourens, A., R. Molenaar, H. van den Brand, M. J. Heetkamp, R. Meijerhof, and B. Kemp. 2006. Effect of egg size on heat production and the transition of energy from eggs to hatchling. Poult. Sci. 85: 770-776.

Lowe, P. C., and V. A. Garwood. 1977. Chick embryo development rate in response to light stimulus. Poult. Sci. 56: 218-222.

Lu, J.W., J. P. McMurtry, and C. N. Coon. 2007. Developmental changes of plasma insulin, glucagon, insulin-like growth factors, thyroid hormones, and glucose concentrations in chick embryos and hatched chicks. Poultry Sci. 86: 673-683.

Marie, C. 1981. Ontogenesis of the adrenal glucocorticoids and of the target function of the enzymatic tyrosine transaminase activity in the chick embryo. J. Endocrinol. 98: 193-200.

Matthews, C. K., and K. E. Holde. 1990. Carbohydrate metabolism I: anaerobic processes in generating metabolic energy. In: Biochemistry. 670-703 (The Benjamin/Cummings Publishing Company, Inc., Redwood City, CA).

McBride, A., S. Ghilagaber, A. Nikolaev, and D. G. Hardie. 2009. The glycogen-binding domain on the AMPK β subunit allows the kinase to act as a glycogen sensor. Cell. Metab. 9: 23-34.

McKay, L. I., and J. A. Cidlowski. 2003. Physiologic and pharmacologic effects of corticosteroids. In: Kufe DW, Pollock RE, Weichselbaum RR, et al., editors. Holland-Frei Cancer Medicine. 6th edition. Hamilton (ON): BC Decker; 2003.Available from: http://www.ncbi.nlm.nih.gov/books/NBK13780/

McNabb, F. M. A. 2000. Thyroids. Pages 461–471 in Sturkie's Avian Physiology. G. Whittow, ed. Academic Press, New York, NY.

McNaughton, J. L., J. W. Deaton, and F. N. Reece, 1978. Effect of age of parents and hatching egg weight on broiler chick mortality. Poult. Sci. 57: 38-44.

Metabolomics data analysis http://link.springer.com.proxy-um.researchport.umd.edu/journal/11306/8/1/suppl/page/1

Michelhill, K. I., D. Stapleton, G. Gao, C. House, B. Michell, F. Katsis, L. A. Witters, and B. E. Kemp. 1994. Mammalian AMP-activated protein kinase shares structural and functional homology with the catalytic domain of yeast Snf1 protein kinase. J. Biol. Chem. 269: 2361-2364.

Mooney, R. A., and M. D.Lane, 1981. Formation and turenover of triglyceride-rich vesicles in the chick liver cells. Effects of cAMP and carnitine on triglyceride mobilization nd conversion to ketones. J. Biol. Chem. 256: 11724-11733.

Moran Jr., E. T. 2007. Nutrition of the developing embryo and hatchling. Poult. Sci. 86:1043-1049.

Mortola, J. P., and K. Al Awam. 2010. Growth of the chicken embryo: implication of egg size. Comp. Biochem. Physiol. A 156: 373-379.

Nakamura T, Y. Tanabe, and H. Hirano. 1978. Evidence of the in vitro formation of cortisol by the adrenal gland of embryonic and young chickens (*Gallus domesticus*). Gen. Comp. Endocrinol. 35: 302-308.

Newgard, C. B. 2012. Interplay between lipids and branched-chain amino acids in development of insulin resistance. Cell Metab. 15: 606-614.

Noble, R. C., M. Cocchi. 1990. Lipid metabolism and the neonatal chicken. Prog. Lipid. Res. 29: 107-140.

Noble, R. C., F. Lonsdale, K. Connor, and D. Brown. 1986. Changes in the lipid metabolism of the chick embryo with parental age. Poul. Sci. 65: 409-416.

Ohta, Y., N. Tsushima, K. Koide, M. T. Kidd, and T. Ishibashi. 1999. Effect of amino acid injection in broiler breeder eggs on embryonic growth and hatchability of chicks. Poult. Sci. 78: 1493-1498.

O'Sullivan, N. P., E. A. Dunnington, and P. B. Siegel. 1991. Relationships among age of the dam, egg components, embryo lipid transfer, and hatchability of broiler breeder eggs. Poult. Sci. 70: 2180-2185.

Owen, O. E., S. C. Kalhan, and R.W. Hanson. 2000. The key role of anaplerosis and cataplerosis for citric acid cycle function. J. Biol. Chem. 277: 30409-30412.

Pascual, M., F. Jahoor, and P. J. Reeds, 1997. Dietary glucose is extensively recycled in the splanchnic bed of fed adult mice. J. Nutr. 127: 1480-1488.

Pascual, M., F. Jahoor, and P. J. Reeds, 1998. In vivo glucose contribution to glutamate synthesis is maintained while its contribution to acetyl CoA is lowed in adult mice fed a diet with a hight fat:conbohydrate ratio. J. Nutr. 128: 733-739.

Pasikanti, K. K., P.C. Ho, and E. C. Y. Chan, 2008. Gas chromatography/mass spectrometry in metabolic profiling of biological fluids. J. Chromatogr. B, 871: 201-211.

Patel, D. G., and S. C. Kalhan, 1992. Glycerol metabolism and triglyceride/fatty acid cycling in the human newborn: effect of maternal diabetes and intrauterine growth retardation. Pediatr Res. 31: 52-58.

Patti, G. J., O. Yanes, and G. Siuzdak. 2012. Metabolomics: the apogee of the omics trilogy. Mol. Cell. Biol. 13: 263-269.

Pearce, J., 1977. Some differences between avian and mammalian biochemistry. Int. J. Biochem. 8: 269-275.

Peebles, E. D., and J. Brake. 1987. Eggshell quality and hatchability in broiler breeder eggs. Poult. Sci. 66: 596–604.

Peebles, E. D., C. D. Zumwalt, S. M. Doyle, P. D. Gerard, M. A. Latour, C. R. Boyle, T. W. Smith, 2000. Effects of breeder age and dietary fat source and level on broiler hatching egg characteristics. Poult. Sci., 79(5):698-704.

Peebles, E. D. S. M. Doyle, C. D. Zumwalt, P. D. Gerard, M. A. Latour, C. R. Boyle, and T. W. Smith. 2001. Breeder age influences embryogenesis in broiler hatching eggs. Poult. Sci. 80: 272-277.

Peebles, D. 2007. Optimizing the performance of early nutrient restricted offspring from young broiler breeders. Mississippi State University Department of Poultry Science Newsletter 1: 3-4.

Picardo, M., and A. J. Dickson, 1982. Hormonal regulation of glycogen metabolism in hepatcyte suspensions isolated from chicken embryos. Comp. Biochem. Physiol. 71B: 689-693.

Possemato, R., K. M. Marks, Y. D. Shaul, M. E. Pacold, D. Kim, K. Birsoy, S. Sethumadhavan , H.K. Woo, H. G. Jang, A. K. Jha, W. W. Chen, F. G. Barrett , N. Stransky, Z. Y. Tsun, G. S. Cowley, J. Barretina, N. Y. Kalaany, P. P. Hsu, K. Ottina, A. M. Chan , B. Yuan, L. A. Garraway, D. E. Root, M, Mino-Kenudson, E. F. Brachtel, E. M. Driggers, and D. M. Sabatini, 2011. Functional genomics reveal that the serine synthesis pathway is essential in breast cancer. Nature. 476 (7630): 346-350.

Proszkowiec-Weglarz, M., M. P. Richards, and J. P. McMurtry. 2006a. Molecular cloning, geneomic organization, and expression of three chicken 5’-AMP-activated protein kinase gamma subunit genes. Poult. Sci. 85: 2031-2041.

Proszkowiec-Weglarz, M., M. P. Richards, R. Ramachandran, and J. P. McMurtry. 2006b. Characterization of the AMP-activated protein kinase pathway in chickens. Comp. Biochem. Physiol. B Biochem. Mol. Biol. 143:92-106.

Proszkowiec-Weglarz, M., and M. P. Richards. 2009. Expression and acitivity of the 5'-adenosine monophosphate-activated protein kinase pathway in selected tissues during chicken embryonic development. Poult. Sci. 88:159-178.

Rahn, H., C. V. Paganelli, and A. Ar. 1974. The avian egg: air-cell gas tension, metabolism and incubation time. Res. Physiol. 22: 297-309.

Reddy, D. V., M. E. Lombardo, and L. R. Cerecedo. 1952. Nucleic acid changes during the development of the chick embryo. J. Biol. Chem. 198: 267-270.

Reeds, P.J., H. K. Berthold, J. J. Boza, D. G. Burrin, F. Jahoor, T. Jaksic, P. D. Klein, T. Keshen, R. Miller, B. Stoll, and L. J. Wykes. 1997. Intergration of amino acid and carbon intermediary metabolism: studies with uniformly labeled tracers and mass isotomper analysis. Eur. J. Pediatr. 156 [Suppl 1]: S50-S58.

Reidy, R. R., J. L. Atkinson, and S. Leeson, 1994. Strain comparisons of turkey egg components. Poult. Sci. 73: 388-395.

Reinhart, B. S., and E. T. Moran, 1979. Incubation characteristics of eggs from older small white turkeys with emphasis on the effects due to egg weight. Poult. Sci. 58: 1599-1605.

Reis, L. H. L. T. Gama, and M. C. Soares. 1997. Effects of short storage condictions and broiler breeder age on hatchability, hatching time, and chick weight. Poult. Sci. 76: 1459-1466.

Reyns, G. E., K. Venken, G. M. de Escobar, E. R. Kühn, and V. M. Darras. 2003. Dynamics and regulation of intracellular thyroid hormone concentrations in embryonic chicken liver, kidney, brain, and blood. Gen. Comp. Endocrinol. 134: 80–87.

Ricklef, R. E. 1987. Comparative analysis of avian embryonic growth. J. Exp. Zool. Suppl. 1: 309-323.

Roberts, L. D., A. L. Souza, R. E. Gerszten, and C. B. Clish. 2012. Unit 30.2 Targeted metabolomics. Curr. Protoc. Mol. Biol. 98: 30.2.1-30.2.24.

Romanoff, A. L. 1939. Cornell Rural School Leaflet: figure 9.

Romanoff, A. L. 1960. The avian embryo structural and functional development. MacMillan Co., New York, NY.

Romanoff, A. L., and A. J. Romanoff. 1967. The biochemistry of the avian embryo: a quantitative analysis of prenatal development. John Wiley & Sons.

Sato, M., T. Tachibana, and M. Furuse. 2006. Heat production and lipid metabolism in broiler and layer chickens during embryonic development. Comp. Biochem. Physiol. A 143: 382–388.

Savon, S., P. Hakimi, and R. W. Hanson. 1993. Expression of the genes for the mitochondrial and cytosolic forms of phosphoenolpyruvate carboxykinase in avian liver during development. Biol. Neonate. 64: 62-68.

Scalbert, A., L. Brenna, O. Fiehn, T. Hankemeier, B. S. Kristal, B. Ommen, E. Pujos-Guillot, E. Verheij, D. Wishart, and S. Wopereis. 2009. Mass-spectrometry-based metabolomics: limitations and recommendations for future progress with particular focus on nutrition research. Metabolomics: 5: 435-458.

Schaal, T., and G. Cherian. 2007. A survey on the hatchability of broiler and turkey eggs in the United States from 1985 through 2005. Poult. Sci. 86: 598-600.

Scott, T. R., W. A. Johnson, D. G. Satterlee, and R. P. Gildersleeve, 1981. Circulating levels of corticosterone in the serum of developing chick embryos and newly hatched chicks. Poult. Sci. 60: 1314-1320.

Shaham, O., R. Wei, T. J. Wang, C. Ricciardi, G. D. Lewis, R. S. Vasan, S. A. Carr, R. Thadhani, R. E. Gerszten, and V. K. Mootha. 2008. Metabolic profiling of the human response to a glucose challenage reveals distinct axes of insulin sensitivity. Mol. Syst. Biol. 4: 214.

Shanawany, M. M. 1987. Hatching weight in relation to egg weight in domestic birds. World´s Poult. Sci. J. 43:107-115.

Shand, J. H, D. W. West, R. J. McCartney, R. C. Noble, and B. J. Speake. 1993. The esterificaiton of cholesterol in the yolk sac membrane of the chick embryo. Lipids. 28: 621-625.

Simon, J., P. Freychet and G. Rosselin. 1974. Chicken insulin: Radioimmunological characterization and enhanced activity in rat fat cells and liver plasma membranes. Endocrinology. 95:1439-1449.

Sonne, J. C., I. Lin, and J. M. Buchanan. 1956. Biosynthesis of the purines: IX. Precursors of the nitrogen atoms of the purine ring. J. Biol. Chem. 220: 369-378.

Speake, B. K., A. M. Murray, and R. C. Noble. 1998. Transport and transformations of yolk lipids during the development of the avian embryo. Prog. Lipid Res. 37: 1-32.

Speak. B. K., R. C. Noble, and R. McCartney. 1992. Lipoprotein lipase activity in tissues of the developing embryo. Biochem. Soc. Trans. 20: 295S.

Stapleton, D., K. I. Mitchelhill, G. Gao, J. Widmer, B. J. Michell, T. Teh, C. M. House, C. S. Fernandez, T. Cox, L. A., Witters, B. E. Kemp. 1996. Mammalian AMP-activated protein kinase subfamily. J. Biol. Chem. 271: 611-614.

Stevenson, R.W., K. E. Steiner, C. C. Connolly, H. Fuchs, K. George, M. M. Alberti, P. E. Williams, and A. D. Cherrington. 1991. Dose-related effects of epinephrine on glucose production in conscious dogs. Am. J. Physiol. Endocrinol. Metab. 260: E363–E370.

Sugimoto, Y., S. Sanuki, S. Ohsako, Y. Higashimoto, M. Kondo, J, Kurawaki, H. R. Ibrahim, T. Aoki, T. Ksusakeabe, and K. Koga. 1999. Ovalbumin in developing chicken eggs migrates from egg white to embryonic organs while changing its conformation and thermal stability. J. Biol. Chem. 274: 11030-11037.

Sundekilde, U. K., L. B. Larsen, and H. C. Bertram. 2013. NMR-based milk metabolomics. Metabolites. 3: 204-222. Savon, S, P. Hakimi and R. W. Hanson. 1993. Expression of the genes for the mitochondrial and cytosolic forms of phosphoenolpyruvate carboxykinase in avian liver during development. Biol. Neonate. 64 (1): 62-68.

Sunehag, A. L., M. W. Haymond, R. J. Schanler, P.J. Reeds, and D. M. Bier, 1999. Gluconeogenesis in very low birth weight infants receiving total parenteral nutrition. Diabetes: 48: 791-800

Sunehag, A. L., J. Gustafesson, and U. Ewald, 1996 a. Glycerol carbon contributes to hepatic glucose production during the first eight hours in healthy term infants. Acta. Paediatr. 85: 1339-1343.

Sunehag, A. L., U. Ewald, and J. Gustafesson, 1996 b. Extremely preterm infants (<28 weeks) are capable of gluconeogenesis from glycerol on their first day of life. Pediatr Res. 40: 553-557.

Sunny, N. E. and B. J. Bequette. 2010. Gluconeogenesis differs in developing chick embryos derived from small compared with typical size broilder breeder eggs. J. Anim. Sci. 88:912-921.

Sunny, N. E. and B. J. Bequette. 2011. Glycerol is a major substrate for glucose, glycogen, and nonessential amino acid synthesis in late-term chicken embryos. J. Anim. Sci. 89:3945-3953.

Surez, M. E., H. R. Wilson, F. B. Mather, C. J. Wilcox, and B. N. McPherson. 1997. Effect of strain and age of the broiler breeder female on incubation time and chick weight. Poult. Sci. 76: 1029-1036.

Tanabe Y., N Saito, and T. Nakamura. 1986. Ontogenetic steroidogenesis by testes, ovary, and adrenals of embryonic and postembryonic chickens (*Gallus domesticus*). Gen. Comp. Endocrinol. 63: 456-463.

Tayek, J. A., and J. Katz, 1996. Glucose production, recycling, and gluconeogenesis in normals and diabetics: a mass isotopomer [U-^{13}C] glucose study. Am. J. Physiol. 270 (Endocrinol. Metab. 33): E707-E717.

Tayek, J. A., and J. Katz, 1997. Glucose production, recycling, and gluconeogenesis in humans: relationship to serum cortisol. Am. J. Physiol. 272 (Endocrinol. Metab. 35): E476-E484.

Tazawa, H., A. H. J. Visschedijk, J. Wittmann, and J. Piiper. 1983. Gas exchange, blood gases and acid-base status in the chick before, during and after hatching. Respir. Physiol. 53: 173-185.

Tazawa, H., Hashimoto, Y., Nakazawa, S., and Whittow, G.C., 1992. Metabolic responses of chicken embryos with naturally varying egg shell conductance. Respir. Physiol. 54, 137-144.

Towler, M. C. and D. G. Hardie. 2007. AMP-activated protein kinase in metabolic control and insulin signaling. Circ. Res. 100: 328-341.

t'Kindt R, Scheltema RA, Jankevics A, Brunker K, and S. Rijal. 2010. Metabolomics to Unveil and Understand Phenotypic Diversity between Pathogen Populations. PLoS Negl. Trop. Dis. 4(11): e904. doi:10.1371/journal.pntd.0000904.

Tullet, S. G., and R. G. Board. 1976. Oxygen flux across the integument of the avian egg during incubation. Br. Poult. Sci. 28: 239-243.

Ulmer-Franco, A. M., G. M. Fasenko, and E. E. O'Dea Christopher. 2010. Hatching egg characteristics, chick quality, and broiler performance at 2 breedr flock ages and from 3 egg weights. Poult. Sci. 89: 2735-2742.

USDA, Long-term Projections, 2007. http://www.ers.usda.gov/publications/oce071/oce20071d.pdf

USDA, Agricultural Projections to 2022. http://www.usda.gov/oce/commodity/projections/USDAAgriculturalProjections2022.pdf

Vieira, S. L., and E. T. Moran. 1998. Eggs and chicks from broiler breeders of extremely different age. J. Appl. Poult. Res. 7: 372-76.

Vieira, S. L., and E. T. Moran. 1999. Effects of egg of origin and chick posthatch nutrition on broiler live performance and meat yields. World's Poult. Sci. J. 55:125–142.

Vinayavekhin N, and A. Saghatelian. 2010. Unit 30.1 Untargeted metabolomics. Curr. Protoc. Mol. Biol. 98:30.1.1-24.

Wang, J., P. Alexander, L. Wu, R. Hammer, O. Cleaver, S. L. McKnight, 2009. Dependence of mouse embryonic stem cells on threonine catabolism. Science. 325: 435-439.

Wangensteen, O. D., and H. Rahn. 1970-1971. Respiratory gas exchange by the avian embryo. Res. Physiol. 11: 31-45.

Weatherup, S. T. C., and W. H. Foster. 1980. A description of the curve relating egg weight and age of hen. Br. Poult. Sci. 21 (6): 511-519.

Weir, G. C., P. C. Goltsos, E. P. Steinberg, and Y. C. Pate. 1976. High concentration of somatostatin immunoreactivity in chicken pancreas. Diabetologia. 12: 129-132.

Williams, T. D. 1994. Intraspecific variation in egg size and egg composition in birds: effects on offspring fitness. Biol. Rev. 69: 35-59.

Wise, P. M., and Frye, B. E. 1973. Functional development of the hypothalamo-hypophyseal-adrenal cortex axis in the chick embryo, *Gallus Domesticus*. J. Exp. Zool., 185: 277-292.

Wishart, D. S. 2007. Current progress in computational metabolomics. 8: 279-293.

Woods, A., I. Salt, J. Scott, D. G. Hardie, and D. Carling. 1996. The α1 and α2 isoforms of the AMP-activated protein kinase have similar activities in rat liver but exhibit differences in substrate specificity in vitro. FEBS. 397: 347-351.

Wykes, L., F. Jahoor and P. J. Reeds. 1998. Gluconeogenesis measured with [U-^{13}C] glucose and mass isotopomer analysis with apoB-100 amino acids in pigs. Am. J. Physiol. (Endocrinol. Metab., 37), 274: E365-376.

Xiao, B., R. Heath, P. Saiu, F.C. Leiper, P. Leone, C. Jing, P. A. Walker, L. Haire, J.F. Eccleston, C.T. Davis. 2007. Structural basis for AMP binding to mammalian AMP-activated protein kinase. Nature. 449: 496-500.

Yadgary, L., A. Cahaner, O. Kedar, and Z. Uni. 2010. Yolk sac nutrient composition and fat uptake in late-term embryos in eggs from young and old broiler breeder hens. Poult. Sci. 89: 2441-2452.

Yafei, N., and R. C. Noble. 1990. Further observations on the association between lipid metabolism and low embryo hatchability in eggs from young broiler birds. J. Exp. Zool. 253: 325-329.

Yang, J., S. C. Kalhan, and R. W. Hanson. 2009. What is the metabolic role of phosphoenolpyruvate Carboxykinase? J. Biol. Chem. 284: 27025-27029.